



2019

## VISUALIZING BARRIER DUNE TOPOGRAPHIC STATE SPACE AND INFERENCE OF RESILIENCE PROPERTIES

Li-Chih Hsu

*University of Kentucky*, [geolchsu@gmail.com](mailto:geolchsu@gmail.com)

Digital Object Identifier: <https://doi.org/10.13023/etd.2019.357>

[Right click to open a feedback form in a new tab to let us know how this document benefits you.](#)

---

### Recommended Citation

Hsu, Li-Chih, "VISUALIZING BARRIER DUNE TOPOGRAPHIC STATE SPACE AND INFERENCE OF RESILIENCE PROPERTIES" (2019). *Theses and Dissertations--Geography*. 63.

[https://uknowledge.uky.edu/geography\\_etds/63](https://uknowledge.uky.edu/geography_etds/63)

This Doctoral Dissertation is brought to you for free and open access by the Geography at UKnowledge. It has been accepted for inclusion in Theses and Dissertations--Geography by an authorized administrator of UKnowledge. For more information, please contact [UKnowledge@lsv.uky.edu](mailto:UKnowledge@lsv.uky.edu).

## **STUDENT AGREEMENT:**

I represent that my thesis or dissertation and abstract are my original work. Proper attribution has been given to all outside sources. I understand that I am solely responsible for obtaining any needed copyright permissions. I have obtained needed written permission statement(s) from the owner(s) of each third-party copyrighted matter to be included in my work, allowing electronic distribution (if such use is not permitted by the fair use doctrine) which will be submitted to UKnowledge as Additional File.

I hereby grant to The University of Kentucky and its agents the irrevocable, non-exclusive, and royalty-free license to archive and make accessible my work in whole or in part in all forms of media, now or hereafter known. I agree that the document mentioned above may be made available immediately for worldwide access unless an embargo applies.

I retain all other ownership rights to the copyright of my work. I also retain the right to use in future works (such as articles or books) all or part of my work. I understand that I am free to register the copyright to my work.

## **REVIEW, APPROVAL AND ACCEPTANCE**

The document mentioned above has been reviewed and accepted by the student's advisor, on behalf of the advisory committee, and by the Director of Graduate Studies (DGS), on behalf of the program; we verify that this is the final, approved version of the student's thesis including all changes required by the advisory committee. The undersigned agree to abide by the statements above.

Li-Chih Hsu, Student

Dr. Jon Anthony Stallins, Major Professor

Dr. Tad Mutersbaugh, Director of Graduate Studies

VISUALIZING BARRIER DUNE TOPOGRAPHIC STATE SPACE AND  
INFERENCE OF RESILIENCE PROPERTIES

---

DISSERTATION

---

A dissertation submitted in partial fulfillment of the  
requirements for the degree of Doctor of Philosophy in the  
College of Arts and Sciences  
at the University of Kentucky

By

Li-Chih Hsu

Lexington, Kentucky

Director: Dr. Jon Anthony Stallins, Professor of Geography

Lexington, Kentucky

2019

Copyright © Li-Chih Hsu 2019

## ABSTRACT OF DISSERTATION

### VISUALIZING BARRIER DUNE TOPOGRAPHIC STATE SPACE AND INFERENCE OF RESILIENCE PROPERTIES

The linkage between barrier island morphologies and dune topographies, vegetation, and biogeomorphic feedbacks, has been examined. The two-fold stability domain (i.e., overwash-resisting and overwash-reinforcing stability domains) model from case studies in a couple of islands along the Georgia Bight and Virginia coast has been proposed to examine the resilience properties in the barrier dune systems. Thus, there is a need to examine geographic variations in the dune topography among and within islands. Meanwhile, previous studies just analyzed and compared dune topographies based on transect-based point elevations or dune crest elevations; therefore, it is necessary to further examine dune topography in terms of multiple patterns and processes across scales.

In this dissertation, I develop and deploy a cross-scale data model developed from resilience theory to represent and compare dune topographies across twelve islands over approximately 2,050 kilometers of the US southeastern Atlantic coast. Three sets of topographic variables were employed to summarize the cross-scale structure of topography (elevational statistics, patch indices, and the continuous surface properties). These metrics differed in their degree of spatial explicitness, their level of measurement, and association with patch or gradient paradigms. Topographic metrics were derived from digital elevation models (DEMs) of dune topographies constructed from airborne Light Detection and Ranging (LiDAR). These topographic metrics were used to construct dune topographic state space to investigate and visualize the cross-scale structure of dune topography.

This study investigated (1) dune topography and landscape similarity among barrier islands in different barrier island morphologic contexts, (2) the differences in barrier island dune topographies and their resilience properties across large geographic extents, and (3) how geomorphic and biogeomorphic processes are related to resilience prosperities.

The findings are summarized below. First, dune topography varies according to island morphologies of the Virginia coast; however, local controls (such as human modification of the shore or shoreline accretion and erosion) also play an important role in shaping dune topographies. Compared with tide-dominated islands, wave-dominated islands exhibited more convergence in dune topographies. Second, the dune landscapes of the Virginia Barrier Islands have a poorly consistent spatial structure, along with strong collinearity among elevational variables and landscape indices, which reflects the rapid retreat and erosion along the coast. The dune landscapes of the Georgia Bight have a more consistent spatial structure and a greater dimensionality in state space. Thus, the weaker multicollinearity and higher dimensionality in the dataset reflect their potential for

resilience. Last, islands of different elevations may have similar dune topography characteristics due to the difference in resistance and resilience. Notwithstanding the geographic variability in geomorphic and biogeomorphic processes, convergence in dune topography exists, which is evidenced by the response curves of the topographic metrics that are correlated with both axes.

This work demonstrates the usefulness of different representations of dune topography by cross-scale data modeling. Also, the two existing models of barrier island dune states were integrated to form a conceptual model that illuminates different, but complementary, resilience properties in the barrier dune system. The differences in dune topographies and resilience properties were detected in state space, and this information offers guidance for future study's field site selections.

KEYWORDS: Barrier islands, Biogeomorphology, Cross-scale structure, Dunes, State space, Resilience

Li-Chih Hsu

---

07/25/2019

---

Date

VISUALIZING BARRIER DUNE TOPOGRAPHIC STATE SPACE AND  
INFERENCE OF RESILIENCE PROPERTIES

By  
Li-Chih Hsu

Dr. Jon Anthony Stallins  
\_\_\_\_\_  
Director of Dissertation

Dr. Tad Mutersbaugh  
\_\_\_\_\_  
Director of Graduate Studies

07/25/2019  
\_\_\_\_\_  
Date

## ACKNOWLEDGEMENTS

It has been a very long journey. Now, as I approach the completion of my degree and dissertation, I am arriving at the ultimate destination. Here, I would like to and need to say “thank you” to all of you who helped me to grow as a scholar, an educator, and a professional physical geographer.

First, I would like to thank my advisors, Dr. Jon Anthony Stallins and Dr. Daehyun Kim, and committee members, Dr. Jonathan Phillips and Dr. Ole Wendroth, for their support throughout my dissertation process. I look forward to their continuing mentorship throughout my career, and I am grateful for their collective mentorship, patience, and guidance over these past years. In particular, I am grateful to Dr. Stallins for his dedicated efforts to help me improve and become successful in my studies. Dr. Phillips, I can never thank you enough for always reminding me of the value of my work and for all the ways in which you inspired me to keep going.

In addition, I am grateful for the multiple opportunities I received to work with Dr. Liang Liang as a teaching assistant in his classes over the past few years. Through this experience, I learned so much, and I hope to utilize the teaching skills I gained from this experience throughout my career. Still further, I would like to express my appreciation for Dr. Lynn Phillips’s patience and willingness to listen to me every time I stopped by her office to chat. Also, thank you to Lori Tyndall and Jeff Levy for helping me with administrative tasks over the past several years. Thank you to my graduate student colleagues, especially Dr. Linsay Shade, Dr. Priyanka Ghosh, Dr. Malene Jacobsen, Megan White, Jackie Monge, Robby Hardesty, Guetchine Gaspard, Leif Johnson, Edward Lo, and Jonghee Lee, for your encouragement and perspective.

Moreover, I am thankful to have met numerous, wonderful people (including Dean Brian Jackson, Dean Patricia Bond, Dean Cleo Price, Maureen Barker, Director Elizabeth Leibach, Director Karen Slaymaker, and so on) from different offices on the University of Kentucky's campus who cared about me and worked hard to help me overcome various challenges and difficulties along the way. Furthermore, my experience with the Robert E. Hemenway Writing Center has been fantastic, and I am deeply appreciative for the individuals who offered me guidance and helped me to learn many writing skills. To start, I would like to thank the graduate writing consultants I worked with over the years: Jillian Winter, Kelly Wright, Leslie Davis, Logan West, Tess Given, and Nathan Petrie. To finish, I would like to express my extreme gratitude to the most vital member of the Writing Center: Director Judith Gatton Prats. As Director of the Writing Center, Director Prats organized and led one of my most unforgettable memories at UK: the International Conversation Hour. Through this weekly event, I learned more about American culture and I was privileged to meet other students and individuals from different cultures. Director Prats, thank you for always making me feel welcome and heard.

Last but not least, I would like to thank my parents, Bi-Chih Hsu and Bi-Lian Wang, for encouraging my dream. They sacrificed a lot and have done whatever they could to help me fulfill my dream. Without their support, I never would have gained a graduate education. Their emphasis on the importance of and consistent valuing of education was and is a crucial factor that facilitated my success throughout my academic career. Thank you both for everything.



## TABLE OF CONTENTS

|  |      |
|--|------|
| ACKNOWLEDGEMENTS .....   | iii  |
| LIST OF TABLES .....   | vii  |
| LIST OF FIGURES .....  | viii |
| Chapter 1. Introduction.....   | 1    |
| 1.1 Introduction.....  | 1    |
| 1.2 Background.....  | 4    |
| 1.2.1 Barrier island morphology .....  | 4    |
| 1.2.2 Biogeomorphic stability domains in barrier dune systems .....  | 5    |
| 1.2.3 Visualizing cross-scale structure in state space .....   | 7    |
| 1.2.4 Defining resilience and resistance .....   | 8    |
| 1.3 Structure of the dissertation .....  | 11   |
| Chapter 2. Dune topographic variability along the U.S. Virginia coast: how landscape mosaics complicate existing biogeomorphic models of barrier island responses to storm disturbance ..... | 13   |
| 2.1 Introduction.....  | 14   |
| 2.2 Background.....  | 15   |
| 2.3 Methods.....   | 21   |
| 2.3.1 Study area.....  | 21   |
| 2.3.2 Plot selection.....  | 25   |
| 2.3.3 LiDAR methods .....  | 26   |
| 2.3.4 Characterization of topography.....  | 26   |
| 2.4 Results.....   | 31   |
| 2.5 Discussion.....  | 35   |
| 2.6 Conclusion .....   | 39   |
| Chapter 3. Barrier island dune resistance and resilience inferred from topographic state space: a cross-scale data modeling approach.....  | 54   |
| 3.1 Introduction.....  | 55   |
| 3.2 Background.....  | 60   |
| 3.2.1 Cross-scale structure .....  | 60   |
| 3.3 Methods.....   | 65   |
| 3.3.1 Study area and sampling design.....  | 65   |
| 3.3.2 LiDAR data.....  | 67   |

|            |  |     |
|------------|--|-----|
| 3.3.3      | Topographic metrics .....  | 68  |
| 3.3.4      | Statistical analysis .....   | 70  |
| 3.3.5      | Hypotheses .....   | 71  |
| 3.4        | Results .....  | 73  |
| 3.4.1      | Georgia Bight topographic state space .....  | 73  |
| 3.4.2      | Virginia dune topographic state space .....  | 74  |
| 3.4.3      | Combined dataset .....   | 75  |
| 3.5        | Discussion .....   | 76  |
| 3.5.1      | Individual state spaces .....  | 76  |
| 3.5.2      | Combined state space .....   | 77  |
| 3.5.3      | Island morphology and resilience properties .....  | 79  |
| 3.6        | Conclusion .....   | 81  |
|            |  |     |
| Chapter 4. | Delineation of geomorphic and biogeomorphic resistance and resilience in barrier island dunes using cross-scale modeling and state space visualization ..... | 101 |
| 4.1        | Introduction .....   | 102 |
| 4.2        | Background .....   | 104 |
| 4.2.1      | Cross-scale structure in resilience theory .....   | 104 |
| 4.2.2      | Dune biogeomorphic resistance and resilience .....   | 108 |
| 4.3        | Methods .....  | 110 |
| 4.3.1      | Selection of cross-scalar variables .....  | 110 |
| 4.3.2      | Exploratory hypotheses .....   | 113 |
| 4.3.3      | Sampling and data .....  | 114 |
| 4.4        | Results .....  | 118 |
| 4.5        | Discussion .....   | 122 |
| 4.6        | Conclusion .....   | 125 |
|            |  |     |
| Chapter 5. | Conclusion .....   | 146 |
| 5.1        | Dune topography and island morphologies along the Virginia coast .....   | 147 |
| 5.2        | Comparing topography and resilience across two barrier coast regions .....   | 148 |
| 5.2.1      | Topographic differences between Virginia and the Georgia Bight .....   | 149 |
| 5.2.2      | Resilience properties and the compatibility of existing dune dynamical models .....  | 151 |
| 5.3        | Using response curves to delineate resistance and resilience .....   | 153 |
| 5.4        | Broader implications .....   | 155 |
|            |  |     |
|            | Bibliography .....   | 157 |
|            |  |     |
|            | VITA .....   | 169 |

LIST OF TABLES

Table 2. 1 Island morphologies..... 41  
Table 2. 2 MRPP tests of group difference for cluster groups..... 42  
Table 2. 3 Annual shoreline movement rate for each island (1990-2014) from graphical results Haluska (2017) ..... 43

Table 3. 1 Dimensionality, stress, and variance extracted for each state space visualization ..... 84  
Table 3. 2 Pearson's correlation coefficients for plot NMDS axis coordinates and topographic metrics for the Georgia Bight ..... 85  
Table 3. 3 Pearson's correlation coefficients for plot NMDS axis coordinates and topographic metrics for Virginia Barrier Islands ..... 87  
Table 3. 4 Pearson's correlation coefficients for plot NMDS axis coordinates and topographic metrics for the combined data set ..... 89  
Table 3. 5 MRPP tests of group difference for each cluster solution ..... 91

Table 4. 1 Cross-scale data ontologies and levels of measurement ..... 128  
Table 4. 2 Summary of FRAGSTATS landscape indices utilized in the study ..... 129  
Table 4. 3 Pearson's correlation coefficients for NMDS axis position and original variables ..... 130

## LIST OF FIGURES

|   |     |
|---|-----|
| Figure 2. 1 Study area with its four island morphological compartments .....  | 45  |
| Figure 2. 2 Study plots on Assateague Island .....  | 46  |
| Figure 2. 3 Study plots .....   | 47  |
| Figure 2. 4 Boxplots of elevation in 1-m cells for each plot.....   | 48  |
| Figure 2. 5 Plot DEMs scaled to local minimum and maximum elevation .....   | 49  |
| Figure 2. 6 PCoA scatterplot showing variability in the directional correlograms of island plots.....   | 50  |
| Figure 2. 7 NMDS scatterplot of plot topographies grouped by island identity (i.e., specific to their local nearshore context and island morphology)..... | 51  |
| Figure 2. 8 NMDS scatterplots of dune topography for 2, 3 and 4 cluster group solutions .....   | 52  |
| Figure 2. 9 NMDS scatterplots of dune topography for 5, 6 and 7 cluster group solutions .....   | 53  |
|   |     |
| Figure 3. 1 Regional map of coastline of the southeastern USA .....   | 92  |
| Figure 3. 2 Map of coastline, spanning from Maryland to the Delaware Peninsula.....   | 93  |
| Figure 3. 3 DEMs for study plots along the Georgia Bight, scaled to local minimum and maximum elevations .....  | 94  |
| Figure 3. 4 PCoA scatterplot of directional spatial autocorrelation structure for the Georgia Bight plots .....   | 95  |
| Figure 3. 5 NMDS topographic state space for Georgia Bight DEM plots.....   | 95  |
| Figure 3. 6 DEMs of Virginia study plots, scaled to local minimum and maximum elevations .....  | 96  |
| Figure 3. 7 PCoA scatterplot of directional spatial autocorrelation structure for Virginia plots.....   | 97  |
| Figure 3. 8 NMDS topographic state space for Virginia DEM plots .....   | 97  |
| Figure 3. 9 PCoA scatterplot of directional spatial autocorrelation structure for the combined dataset.....   | 98  |
| Figure 3. 10 NMDS topographic state space for the combined dataset.....   | 99  |
| Figure 3. 11 NMDS topographic state space for the combined data set based on island centroids .....   | 100 |
| Figure 3. 12 Summary of resilience properties in barrier island dune topographic state space .....  | 100 |

|  |     |
|--|-----|
| Figure 4. 1 Examples of state space in other studies .....   | 131 |
| Figure 4. 2 How patch structure is derived from a more continuous elevational surface from Wu et al. (2017).....   | 132 |
| Figure 4. 3 DEMs illustrating the contrasts in landscape indices of patch elevational structure among island sites .....   | 134 |
| Figure 4. 4 Six Moran's <i>I</i> values were sampled from the directional correlograms and ordinated using PCoA to distill spatial autocorrelation structure into individual metrics ..... | 135 |
| Figure 4. 5 Topographic state space. Cross symbols represent centroids for all the plots of an individual island. ....   | 136 |
| Figure 4. 6 Island centroids and response surfaces for mean elevation, AI, LPI, SHAPE_AM, and SIDI.....  | 139 |
| Figure 4. 7 Island centroids and response surfaces for kurtosis, skewness, spatial autocorrelation structure, and size. ....   | 141 |
| Figure 4. 8 PCoA scatterplot for the combined dataset, showing variability in the directional spatial autocorrelation structure among island plots.....                                    | 142 |
| Figure 4. 9 Directional correlograms for each site plotted in NMDS state space. ....   | 142 |
| Figure 4. 10 Island centroids and response surfaces for CONTAG, LSI, and maximum elevation.....  | 144 |
| Figure 4. 11 Gray scale convex hulls.....  | 145 |

## **Chapter 1. Introduction**

### **1.1 Introduction**

Barrier islands are coastal landforms that can protect the mainland from the full impacts of tropical and extratropical storms (Temmerman et al. 2013; Spalding et al. 2014). The processes shaping the morphology of the barrier islands are closely associated with the evolution of smaller and superimposed features, including sand dunes (Plant et al. 2014). Dune landscapes on barrier islands are environmentally complex and reflect an interaction among topography, dune vegetation, steep abiotic gradients of salt spray and sand burial, and disturbances from overwash events and blowing sand (Godfrey 1977; Everard et al. 2010; Feagin et al. 2010; Miller et al. 2010).

Two basic morphological categories of barrier islands are recognized, each originating from relative differences in tidal range and wave height (Hayes 1979; Davis and Hayes 1984; Hayes 1994). The low tidal range and high wave energy settings of microtidal, wave-dominated coasts result in narrow, elongated barrier island morphologies; the high tidal range and low wave energy settings of mesotidal, mixed-energy coasts lead to wide, drumstick-shaped barrier island morphologies. Within the boundary conditions set up by larger oceanic, climatic, and geologic controls on islands, feedbacks between prevailing patterns of sediment mobility, dune vegetation, and topography can potentially canalize local process-response behaviors to high water events, giving rise to distinctive landscape dynamics and topography on each island morphology (Stallins 2005).

Specifically, the dune topographies and vegetation of these two morphologies each exhibit positive feedbacks that modify movements of sediment and water during high water

events. On microtidal barrier islands, a low flat topography is maintained through the interaction of dune grasses with prevailing patterns of sediment mobility. More infrequent storm-forced overwash on mesotidal barrier islands can lead to greater topographic roughness and more extensive ridge-and-swale landforms. These barrier dune topographies can either reinforce or resist overwash events, respectively, promoting the vegetation that in turn facilitates the maintenance of topography. A number of studies have proposed to further validate these two biogeomorphic models (i.e., overwash-resisting and overwash-reinforcing feedbacks) (Godfrey and Godfrey 1976; Godfrey 1977; Stallins 2005; Wolner et al. 2013; Brantley et al. 2014). They each demonstrated the linkage between the two morphological types of barrier islands and their relative frequency of exposure to meteorological or tidal events capable of forcing overwash, the type of topography, and vegetation type. However, like the initial research to develop these models, most of subsequent work has focused on topographic and vegetation patterns on one or two islands. Moreover, these two biogeomorphic models, as alternative stable states or stability domains, were associated with entire islands. Considerable topographic and biogeographic variability can develop within even a single island.

The goal of this dissertation is to investigate the generalizability of linking barrier island morphologies to specific type of dune topographies. To what extent are there potential geographic variations in biogeomorphic feedbacks within and among barrier islands, as expressed through dune topography? Several researchers have suggested how dune topographies may not neatly correspond to one or the other of these two stability domain models (Monge and Stallins 2016; Zinnert et al. 2017). A broader geographic sampling is needed. This would allow for a more nuanced comparison of the spatial

patterns of topography among many different nearshore island contexts that influence island morphology and the relief expressed in the dune landscape.

However, making comparisons of topography among and within many different barrier islands is not a straightforward process. Dune topography reflects landscape-extent processes. Topography is polygenic, a range of factors operating at different spatial and temporal extents contribute to its expression. In this dissertation, I develop and deploy a cross-scale data model developed from scholars in resilience theory to represent and compare the pattern-process facets of dune topography. This methodology accounts for the nested, or hierarchical geomorphic and ecological processes that manifest across scales. It also accounts for the different paradigms to account for patterns and process. In addition, a method is needed to analyze the spatial patterns embedded in this data modeling of topography. This dissertation employs the concept of state space (Prager and Reiners 2009) to compare patterns and the processes they reflect through their cross-scalar structure. Specifically, this study will visualize dune topographic state space across multiple islands along a stretch of coast from south Florida to Virginia, by means of three sets of topographic variables. They metrics are derived from digital elevation models (DEMs) constructed from airborne Light Detection and Ranging (LiDAR) data. The following three research questions are proposed. (1) To what extent does island morphology track dune topography? (2) How do barrier islands of two distinctive coastal regions, Virginia and the Georgia Bight, differ in topography and in their resilience properties? (3) Under what conditions can biogeomorphic domain dynamics be expected to develop? Although vegetation is not sampled in this study, topography at the resolutions examined is strongly influenced by vegetation. On barrier islands topography and vegetation are highly



correlated. Maximum elevations are often a function of vegetative processes (Duran and Moore 2013), implying that the size of dunes and sediment storages in a coastal dune system are controlled by dune-building species.

## **1.2 Background**

### **1.2.1 Barrier island morphology**

Barrier islands form and develop along the coastlines of the trailing edges of continental plates with abundant sediment and generally low gradients. Along with wind, wave and tidal energy are major controls on barrier island formation and later morphologic development (Davis 1994). Historically, the first classifications of barrier island process-form morphologies were based on wave and tidal energy (Hayes 1979; Davis and Hayes 1984; Hayes 1994). The low tidal range and high wave energy settings of microtidal, wave-dominated coasts lead to narrow, elongated barrier islands as island widths are primarily limited by overwash processes. The high tidal range and low wave energy of mesotidal, mixed-energy coasts generate wide, drumstick-shaped barrier islands as tidal energy limits island length by inlet formation and increases island width through the welding of sediments at tidal inlets. Generally, mesotidal barrier islands are viewed as high, overwash-resisting islands; microtidal barrier island morphologies are viewed as low, overwash-reinforcing islands.

However, barrier islands are complicated, heterogeneous landforms, rather than the distinctive categories that Davis and Hayes (1984) theorized. Along mesotidal, mixed-energy coasts, there can be a broad spectrum of island morphologies with very little difference in tide and wave parameters (Anthony and Orford 2002). In this way, strict

cutoff values for wave and tidal energy have some limits in how they are correlated with island morphology. In the past few decades, more barrier morphologies were examined, and there is no universal validity to distinguish the different barrier types merely based on wave and tidal energy (Stutz and Pilkey 2011). Later studies have also found a wide variety of morphological variability within the broad classificatory scheme used to categorize island morphology (Mulhern et al. 2017). Thus, the question arises as to the extent to which dune topography and domain dynamics correspond to island morphology. Biogeomorphic models of how dunes respond to high water events were initially based on generalizations of island morphology to its underlying dune topography.

### 1.2.2 Biogeomorphic stability domains in barrier dune systems

The two-fold stability domain model (Stallins 2005; Wolner et al. 2013; Brantley et al. 2014; Durán and Moore 2015; Goldstein and Moore 2016) also originates out of the idea that distinctive dune topographies, vegetation, and biogeomorphic feedbacks generate resilience properties. Although this resilience was initially generalized to the two main categories of barrier island morphology, what was central was that the feedbacks conferred a stability and persistence of topography and vegetation that reflects the local overwash disturbance regime (Stallins and Corenblit 2018). However, biogeomorphic feedbacks are likely to vary within an individual island and among adjacent islands given the topographic variability present within an individual island (Stallins 2005; Zinnert et al. 2017). Durán and Moore (2015) even suggest that at intermediate elevations, bistability may develop. In this case, either the overwash-resisting or overwash-reinforcing stability domain can develop. In these perspectives on the original domain models, domain states and the resilience that they confer can potentially manifest along the coastline of a single barrier

island. Not only are studies needed that question how valid it is to generalize island morphology to dune topography, insights into how resilience properties vary between and within islands are also needed. By examining topography over a wide range of islands, in different nearshore conditions having similar island morphologies, it may be possible to infer more of the geographically-variable relationships between island morphology, dune topography, and resilience properties.

Most of the evidence for the overwash disturbance-resisting and overwash disturbance-reinforcing domains has come from geographically-limited field work and from modeling. These geographically-restricted studies as well as the simulation-based approaches have relied on transect-based point elevation, dune crest elevations, and highly generalized parameterizations of topography. A different approach is needed to compare the spatial patterns of topography, particularly when working at the landscape extents that the two-domain model has been postulated to operate across. Different data representations may be necessary to capture the complexity of earth surface patterns (McGarigal and Cushman 2002; Lausch et al. 2015). Thus, this study will compare spatial patterns of dune topography in more detail than prior studies, in addition to sampling dune topographies from a much larger geographic area. Monge and Stallins (2016) employed a similar approach, although the older barrier island dune studies had a much larger geographic extent at which they deployed their ideas (Godfrey et al. 1979; Zaremba and Leatherman 1986.). However, these earlier studies did not have the theoretical and methodological basis to perform detailed comparisons of topography in a robust quantitative fashion.

### 1.2.3 Visualizing cross-scale structure in state space

The concept of cross-scale structure is used in this dissertation to make comparisons of topographic patterns and to link them to process. Cross-scale structure is the theoretical base for resilience properties in geomorphic and ecological systems (Sundstrom et al. 2014, 2016; Nash et al. 2014). These ideas developed in ecology with Holling (1996). Although formally defined with adaptive cycles and panarchies, the working units of resilience theory, cross-scale structure provides a way to parse variables into different hierarchical levels and to relate this structure to resilience properties. It has long been recognized in ecology that ecological and geomorphic processes which operate at one scale can propagate across multiple scales on barrier islands (Odum et al. 1987; Zinnert et al. 2017). However, formal cross-scale structure from resilience theory provides a methodological basis for characterizing and comparing this hierarchical structure (Stallins and Corenblit 2018). The scalar extents and resolutions bound to a cross scale data model for dunes vary from cycles of sediment accumulation and individual plant growth to the feedbacks with overwash and sediment transport at the extent of a landscape.

Unique to a cross-scale data structure approach is that it allows for multiple explanatory paradigms to be integrated, each with their own particular methods of representing patterns. Geomorphologists and ecologists often delineate and segregate patterns and processes operating at different spatial and temporal scales. As a compromise, comparing patterns across scales has been approached through more scale-condensing techniques such as spatial autocorrelation, hierarchical modeling, fractals, and wavelets. Modeling dunes using the cross-scale structuring of resilience theory has several advantages to these methods. It allows for multiple types of pattern and different

conceptual paradigms, like patch and gradient perspectives, to be integrated. It allows for a multivariate comparison of pattern that integrates across scalar extents and also incorporates a mechanism to account for resilience properties.

Cross-scale data requires a method of visualization that can retain the data's underlying structure yet simplify its interpretation. State space visualization of cross-scaled topographic data is employed in this dissertation. State space specifically refers to Poincaréan ecological topologies, in which phenomena are mapped in an abstracted field space (Prager and Reiners 2009). There are typically axes, in a Cartesian coordinate system, that give shape to state space. The state space of a dynamical system defines the set of all possible states that the system can take. Uses of state space similar to those employed in this study can be found in ecology and geomorphology (e.g., Baas and Nield 2010; Donohue et al. 2013; Chartier et al. 2014; Barros et al. 2016; Inkpen and Hall 2016; Stevens and Tello 2018). In the approach used in this dissertation, state space is constructed via dimensionality reduction using ordination. Cross-scale data is designed to be nested and exhibit multicollinearity. Using ordination, the variance structure of cross-scales data can be visualized. In this reduction of the dimensions of the data, the axes of state space represent resistance and resilience. These state space approaches to resilience properties are frequently employed in ecology (Donohue et al. 2013, 2016; Laughlin 2014).

#### 1.2.4 Defining resilience and resistance

Resilience theory was developed through theoretical discussions about the relationship between diversity and stability (MacArthur 1955). From case studies in population ecology, Holling (1973) proposed concepts of stability and resilience that were later used to develop the terminology of engineering resilience and ecological resilience.

Although there are many definitions that vary slightly, engineering resilience (i.e., resistance) is the structural and functional attributes that resist disturbance; ecological resilience is the magnitude of disturbance that a system can absorb before the system changes its structure.

Resilience concepts have long been recognized by geomorphologists (Brunsdon and Thornes 1979; Schumm 1979; Thomas 2001; Brunsden 2001; Phillips 2006, 2009a). For example, landscape sensitivity discusses how landforms respond to perturbations and includes the probability or propensity for change as well as the ability of the system to recover from disturbance (Downs and Gregory 1995; Fryirs 2017). Several aspects in landscape sensitivity were proposed by Phillips (2009a) and Philips and Van Dyke (2016) to assess resilience properties in geomorphic systems. Within geomorphic systems, resistance is the intrinsic property that resists geomorphic perturbations from floods, wind or gravity, while resilience is the ability of a geomorphic system to recover from disturbances and the degrees of freedom to absorb or adjust to disturbances.

An important distinction about resilience properties is that there is an underlying structure that can be visualized and interpreted through dimensionality in state space. Resilience is not a matter of absence or presence, but a multidimensional concept (Gunderson 2000). It includes the underlying dimension of resistance, as well as how resistance and resilience interact with each other. Dimensionality and position in state space is as an approach to compare topographic patterns but it can also be used to gauge the resistance and resilience of observations (Donohue et al. 2013, 2016; Stevens and Tello 2014, 2018). Donohue et al. (2013) elaborates on how resilience properties can be explicitly represented as dimensionality in state space. Following Donohue et al. (2013,

2016), as well as Stallins and Coreblit (2018), the first axis in a multidimensional volume can represent resistance, and the second axis and higher dimensionalities represent the resilience that emerges out of the underlying property of resistance. In the context of barrier island dune systems, resistance is the stabilization of topography such a foundation that exists for biogeomorphic interactions to emerge and promote resilience through more spatial, landscape-extent interactions between topography and vegetation.

However, in order to compare topographic patterns and to examine how they reflect different relative levels of resistance and resilience within and between barrier islands, metrics have to be designed to reflect a cross-scalar structure. Three basic types of topographic metrics were used. Implicitly spatial descriptive statistics for elevation comprise the resistance variables. The landscape patterns of elevational patches, as based on FRAGSTATS measures of patch structure derived from interval groupings of elevation, comprised the middle dimension variables. These reflect more spatial attributes of dune topography, but do not capture the continuous, gradient structure of topography. The highest dimensional variables were chosen to be the spatial autocorrelation structure of topography, along with the extent or size of a particular DEM study site. Skewness and kurtosis of the point elevations that comprise the DEMs were also designated as high dimensional properties, as they are reflect the boundary constraints upon which landscape-extent topographic patterns could be expressed. Low dimensional resistance metrics set the boundary conditions for the emergence and expression of higher dimension resilience metrics.

### **1.3 Structure of the dissertation**

The dissertation is composed of five subsequent chapters. Chapter 1 has summarized the basic theoretical background necessary for an understanding of barrier dune systems and cross-scale resilience. In Chapter 2, the dune topography of barrier islands of Virginia will be assessed in terms of how variable their topographies are in relation to their island morphology. Like the Georgia Bight, island morphology has been well-studied along the Virginia coast. This chapter will assess how well dune topographies correspond to the older morphological classifications of the Virginia Barrier Islands. It also relies on the recent observations of Virginia Barrier Island shoreline trends in erosion and accretion to assess this linkage between island nearshore context and dune topography. More precisely, given that topography was assessed at multiple locations along each island, to what extent do all of the sites on an island retain an affinity for its particular nearshore morphological context? To what extent are topographies within an individual island more similar to those in different island morphological contexts? Understanding the degree to which topography varies across different morphological contexts provides insight into the potential limits of the existing biogeomorphic stability domain model with its generalization that island morphology determines topography and biogeomorphic interactions.

In Chapter 3, the focus will be on expanding the geographic extent of dune topographic comparisons. Dune topographies of the Virginia Barrier Islands are compared to those of several islands in the Georgia Bight, which spans from Florida to North Carolina. Specifically, how do dune topographies of these two stretches of the U.S. southeastern Atlantic coast compare given that some of the same island morphologies are



expressed in each? Are the interpretations of their individual state spaces logical based on the known characteristics of these two stretches of coast? The Virginia Barrier Islands are undergoing rapid retreat and erosion when compared with much of the US Atlantic coast. Do island morphologies shared by both regions exhibit similar topography given these differences in erosion and island retreat? By examining where sites from barrier islands from both regions plot in a combined state space, comparisons will be made not only of the topographic affinities, but also in relation to the relative levels of resistance and resilience.

In Chapter 4, the last analytical chapter, the topographic state space formed by the analysis of sites from Virginia and the Georgia Bight will be assessed in more detail. The goal was to describe how aspects of state space axis dimensionality and the loading of topographic metrics on these axes suggests domain dynamics and possibly other types of dynamical behaviors. This chapter will provide a summary as to which islands may be more likely to be overwash-resisting and overwash-reinforcing domains, and where in state space bistability could be expected to develop.

Chapter 5 will synthesize results and discuss the implications of the above analytic chapters.

## **Chapter 2. Dune topographic variability along the U.S. Virginia coast: how landscape mosaics complicate existing biogeomorphic models of barrier island responses to storm disturbance**

### *Abstract*

*Context* How dune topography varies within and among barrier island morphologies has not been examined. Existing models of how barrier dune coasts respond to high water events assume homogeneity in dune topography.

*Objectives* Through thirty plots across seven barrier islands of Virginia (U.S.A), this study quantitatively assessed how dune topographies correspond to barrier island morphologies.

*Methods* For LiDAR-derived DEMs of each plot, topographic attributes were derived from elevational descriptive statistics, landscape indices of elevation patch structure, and the directional autocorrelation structure of elevation. Non-metric multidimensional scaling and hierarchical cluster analysis were used to gauge topographic similarity. Multiple response permutation procedures compared the similarity in dune topography based on island morphology to the similarity identified from clustering of all island plots.

*Results* Topography on mixed energy wave-dominated island morphologies was distinctive from tide-dominated morphologies. However, differences in topography on the much smaller tide-dominated barrier island morphologies were as great as those between wave and tide-dominated island morphologies. Topographic differences were more robust when based on clustering of all plots rather than island identity (i.e., morphology).

*Conclusions* Local controls such as shoreline accretion and erosion fostered larger differences in topography among tide-dominated islands. Wave-dominated islands exhibited more convergence in dune topographic form. Island morphology is an incomplete

guide for anticipating potential dynamic dune biogeomorphic responses to high water events.

## **2.1 Introduction**

Dunes and beach landscapes are major features of barrier islands, a globally widespread landform that can buffer storm inputs on the mainland. Barrier islands have been classified according to how wave and tidal energy shapes their macro-scale morphology (Hayes 1979; Davis and Hayes 1984). Island morphology has in turn been used to make generalizations about the underlying dune topography and how barrier islands potentially respond to storms and high water events. Wave-dominated mixed energy barrier island morphologies are often associated with reduced topographic roughness and a lower resistance to incursions of overwash. On mixed-energy barrier island morphologies where tidal energy is greater, topographic roughness increases, and overall resistance to overwash disturbance is often assumed to be higher (Godfrey and Godfrey 1976; Stallins and Parker 2003).

However, barrier island morphology can exhibit a considerable amount of variability (Stutz and Pilkey 2011; Mulhern et al. 2017). Dune topography within an individual barrier island is not uniform. Consequently, how barrier island shorelines respond to high water events may be more open-ended than what is assumed by these island morphological models. They oversimplify how sandy barrier coasts respond to high water events by assuming homogeneity in dune topography within tide-dominated versus wave-dominated mixed energy barrier island morphologic types.

In this paper, we documented the relationship between dune topography and barrier island morphology for barrier islands of Virginia (U.S.A), a mixed wave and tidal energy stretch of the U.S. southeastern Atlantic coast. As how to demarcate a dune is a complex question (Wernette et al. 2018b), we utilized a cross-scale data set comprised of a suite of topographic metrics. These metrics spanned different extents and resolutions, and encompassed different geometric attributes of dunes. The intent of these metrics was to capture more of the correlated, nested causal structure of biogeomorphic systems (Corenblit et al. 2015; Stallins and Corenblit 2018). Their usage facilitated the delineation and interpretation of topographic similarity within a multidimensional dune state space. As the stretch of Virginia coast in this study ranges from wave to tide-dominated conditions, we were able to ascertain how variable dune topography was among the different process-form nearshore contexts shaping island morphology. As Phillips (2018) observed, responses to sea level rise may be much more local, with less coherence with models of change in which large sections of contiguous coastline respond uniformly. Coastal responses to sea level should also be assessed based on multiscale, nested environmental gradients and the data that represent them. The topographic metrics employed in this study to make comparisons of topography between and within barrier islands incorporate these recommendations.

## **2.2 Background**

Early classifications of barrier island process-form morphologies were based on wave and tidal energy (Hayes 1979; Davis and Hayes 1984; Hayes 1994). Tidal energy limits island length by inlet formation, and increases island width through the welding of sediments at tidal inlets. This creates the more rounded, drumstick-shaped islands found

on tide-dominated coasts. Conversely, barrier islands on wave-dominated coasts are primarily width-limited by overwash processes. This results in elongate island morphologies, some approaching tens of kilometers in length.

Geographic variability in barrier island dune topography was initially based upon these distinctions in island morphology (Godfrey and Godfrey 1976; Hosier and Cleary 1977). This generalization from island morphology to dune topography arose out of observed geographic generalizations about island sediment budgets, exposures to extratropical and tropical storm tracks, and biogeomorphic feedbacks. Wave-dominated morphologies have low flat overwash topographies that peak in elevation along the fronting dunes. Tide-dominated barrier islands have multiple shore-parallel ridge and swale topography. Each of these two topographies were hypothesized to entrain distinctive storm-driven cycles of sediment erosion and deposition that constrain dune plant functional abundances and topography on each island morphologic type. This perspective has been formalized into a view of dune topography and island morphology as a self-organizing complex system exhibiting process-form feedbacks that propagate across scales (Stallins 2005; Wolner et al. 2013; Brantley et al. 2014; Durán and Moore 2015; Goldstein and Moore 2016). Local, largely geomorphic constraints, like elevation above water level, initiate the potential for interaction of sediment transport processes with vegetation. These culminate in landscape-scale feedbacks among geomorphic and ecological components that can confer ecosystem properties like resistance and resilience (Stallins and Corenblit 2018, Schwarz et al. 2018).

While a wide range of techniques, from field description to mathematical modeling, have been employed to document these complex dynamics, these studies do agree on the

potential for reinforcing biogeomorphic feedbacks to emerge out of nearshore context, storm history, dune vegetation, and topography. These feedbacks shape the expression of overwash-resisting, overwash-reinforcing and bistable dynamical states. Bistability suggests that either the overwash-resisting or the overwash-reinforcing stability domain can develop within intermediate dune elevations. The two end points of these dynamical behaviors still retain an affiliation with island morphology (Stallins and Parker 2003; Wolner et al. 2013; Brantley et al. 2014). Tide-dominated barrier islands are taken to be high, overwash-resisting islands. Wave-dominated barrier island morphologies are taken to be low overwash-reinforcing islands. However, it is to a degree simplistic to link dune characteristics and dynamical states to entire barrier island morphologies. Erosion and accretion can vary considerably along any barrier island. While evidence for overwash-resisting, overwash-reinforcing, and bistable dune landscape dynamics grows, what merits clarification is a basic description of how dune topography varies not only within individual islands, but also among different and geographically continuous barrier island morphologies.

Analogous characterizations of topography in riparian landscapes (e.g., Phillips 1999) have observed that geomorphic processes can lead to increasingly divergent topography over short distances. Conversely, the same topography can be expressed over large geographic extents and be considered invariant or convergent. Comprehending the degree of divergence and convergence in topography within an individual island, and among islands of the same and different barrier island morphologies can inform us of the limits to employing the resisting, reinforcing and bistable models of dune landscape

dynamics. It provides detail about the generalizability of models predicting how sandy barrier island landscapes respond to high water events (Carter 1991).

Along these lines, a recent study by Mulhern et al. (2017) observed that variability in island morphology is more complex than the earlier barrier island classifications (e.g., Hayes 1979; Davis and Hayes 1984). Mulhern et al. (2017) found that mixed-energy tide-dominated barriers and mixed-energy wave-dominated barrier islands have more variable morphologies than previously assumed. This can be in part attributed to the greater contextual dependence upon where and when tidal energy dominates over more unpredictable inputs of wave energy. The way waves and the tides interact on tide-dominated barriers (via mutual muting, modulation, or amplification) can enhance the expression of distinctly local processes of sediment transport and morphological development. Whether this augmented heterogeneity in island morphology extends to the underlying dune topography has not been explicitly examined.

Biogeomorphic processes, rather than island morphology per se, may constrain topographic variability in some contexts, but diversify it in others. For example, Durán and Moore (2015) used mathematical modeling and primary foredune elevations along the Virginia coast to reassert that when the biophysical processes driving dune recovery dominate, islands tend to be high in elevation, and their vulnerability to storms is minimized. In this overwash-resisting state, topography is constrained to have more roughness. Alternatively, when the effects of storm erosion dominate, islands may become trapped in a perpetual state of low elevation and maximum vulnerability to storms, even under mild storm conditions. In this overwash-reinforcing state, topography is constrained to be low and flat. However, for intermediate elevations, either dune topography can be

potentially expressed. This complicates any straightforward linkage of dune topography to barrier island morphological context. At intermediate elevations, different topographies and dynamical properties may develop under the same nearshore conditions and island morphologies. While a low or high island may constrain topography to certain dynamically favorable topographic states, islands with intermediate elevations could exhibit greater turnover in topography over time or across space. As this study by Durán and Moore (2015) also shows, what constitutes a high island may not necessarily be a tide-dominated morphologies, nor are low islands going to be those that are wave-dominated.

Given the relatively unexamined generalizations made between island morphology, dune topography, and the biogeomorphic dynamical states arising out of responses to high water events, greater field-based details as well as additional conceptualizations are warranted. As a form of null model, all possible dune topographies may develop on a single barrier island no matter what its morphological type is. This is because barrier islands are bounded entities that transit from terrestrial to marine habitats. Consequently, a wide range of topography should occur on any one island. For instance, where a barrier island beach reaches its inevitable terminus near a tidal inlet, low flat topography and overwash will inevitably develop, albeit locally. Overwash topography may be limited to this small extent, perhaps only a few tens of meters or less, and driven by minor forcing events. While this implies that the overwash-reinforcing dynamical state can develop on all islands, such a position is of little value to coastal planners who need to work across larger coastal extents. Their work must consider the more dominant types of dune topography across a barrier island landscape. Within these two extremes is the relevant middle ground for documenting dune topographic variability. It is specious to assume a uniform topography



within a category of barrier island morphology. Yet assuming that each island contains all possible dune topographies and the biogeomorphic feedbacks that contribute to them is likewise unproductive if the goal is to better anticipate barrier island coastal responses to high water events. As an investigation of landscape similarity (Niesterowicz and Stepinski 2016), this study documents this middle-range variability in dune topography.

To characterize dune topography, we developed a suite of cross-scaled topographic metrics. Their intent was to account for the variety of topographic features expressed at different scalar extents and to lessen dependence upon any generalized measure of topography such as average point elevation, dune crest height, or two-dimensional cross-sectional elevation profiles. Studies that rely only on point elevations or dune crest height are capturing important aspects of topography. However, how barrier island dune landscapes respond to forcings of high water events is a spatial landscape process (Houser 2013). To compare dune topography between and within island morphologies, we constructed dune topographic state space. State space is a demarcation of the range of conditions under which a dynamic phenomenon is expressed, from those that are favored, and more likely, to those that are less persistent and unlikely to occur (Baas and Nield 2010; Inkpen and Hall 2016). The dimensionality and data structure of topographic state space provided the explanatory framework for how individual topographic metrics contributed to topographic differences. We hypothesized that within the dune topographic state space for the sampled barrier islands, dune topographies for any specific island would not be in perfect accord with its morphology. While the position of some within-island topographies were expected to have a propensity to track with island morphology, we

expected to encounter exceptions reflective of the limits to assuming a tit-for-tat relationship between island morphology and underlying topography.

Island morphology was based on qualitative and quantitative classifications of the nearshore process-form contexts of the Virginia coast. These earlier descriptive classifications are in general agreement with the later quantitative classifications, which incorporated measures of wave and tidal energy, historical hurricane strikes, as well as island length and width (Williams and Leatherman 1993; Monge 2014). Geological framework and sediment exchange with nearshore components contribute to the morphology of islands, beaches and dunes. These factors are also critical to how barrier coasts respond to high water events. However, we consider that these processes are folded into the geographic location of each island and as such are subsumed into their current nearshore process-form island morphology.

## **2.3 Methods**

### **2.3.1 Study area**

Dune topography was characterized on seven largely undeveloped mixed-energy barrier islands of Virginia (Figure 2. 1). All of these islands are experiencing rapid rates of relative sea level rise. These rates are among some of the highest on the US Atlantic coast (Sallenger et al. 2012). Landward retreat rates for barrier islands along this coast vary depending upon the time frame examined (Leatherman 1982; Haluska 2017; Deaton et al. 2017). Long-term trends (1851 to 2010) are approximately 1-6 m/year. Short-term retreat rates (1980-2010) for the entire coast are approximately 7 m/year. This is leading to erosion, reduction in the backbarrier area, and narrowing of the islands. Abundant

washover fans and marsh clumps on the islands attest to the importance of retreat processes along this stretch of the mid-Atlantic coast. Net longshore transport of sediment is to the south. Virginia Barrier Islands differ in their shape, size, and sediment processes, but they are all responding to sea level rise through a few mechanisms including parallel retreat, rotational instability, rollover, and drowning (e.g., Lorenzo-Trueba and Ashton 2014; Deaton et al. 2017). Rotational instability is non-parallel retreat that gives the appearance of island rotation caused by one part of the island retreating faster than another.

Following Leatherman (1982), Rice and Leatherman (1983), and Oertel and Kraft (1994), islands of this stretch of coast have been classified into coastal compartments based on the geomorphic influences shaping island morphology (Figure 2. 1). Although this entire stretch of coast experiences wave and tidal energy inputs, wave energy dominates in the most northern compartment. Tidal energy increases in importance to the south. These more southerly tidally-influenced island morphologies have been segmented into three contiguous geomorphic groups based on whether island morphologies reflect parallel or non-parallel retreat. Retreat for some of these islands have shifted from parallel to non-parallel and vice versa over time (Kochel et al. 1983; Nebel et al. 2012; Deaton et al. 2017; Haluska 2017).

The northernmost island, Assateague (Table 2. 1), exhibits the long, linear barrier island morphology characteristic of mixed-energy, wave-dominated coasts. Assateague is undergoing parallel retreat (Haluska 2017). It is prone to breaching with numerous ephemeral and long-lived tidal inlets that have formed during extratropical and tropical storms (Seminack and McBride 2015). Anthropogenic modifications of the inlet above Assateague and on Wallops island just below it include sediment dredging. Consequently,

downdrift locations on Assateague and islands immediately south experience greater erosion and higher retreat rates (Roman and Nordstrom 1988; Psuty and Silveira 2011).

South of Assateague are the increasingly tide-dominated barriers of Metompkin Island and Cedar Island. These islands have simple topographies and low elevations that result in frequent overwash even during mild extratropical and tropical storms (Brantley et al. 2014). Their coastlines experience significant sediment starvation and erosion due to altered sediment dynamics on Wallops and Assateague islands. Metompkin is undergoing pervasive rapid retreat. The northern half of Metompkin is retreating faster than the southern half, causing a counter-clockwise rotation (Haluska 2017). Because of shoreline retreat, Cedar Island is decreasing in overall area and losing vegetation cover at the expense of bare sand (Zinnert et al. 2016b). It is retreating at high rates for the entire mid-Atlantic shoreline (Nebel et al. 2012). Cedar Island has more parallel beach retreat for the period 1990-2014, although there is evidence it has alternated between parallel and rotational motion in the past.

Parramore Island and Hog Island comprise the next morphological compartment to the south. These islands have relatively high relief (>6m) and exhibit the distinctive drumstick shape where morphology is strongly influenced by tidal energy. On Parramore extensive erosion is associated with scarping as the island migrates rapidly landward. The north-central stretch of Parramore is characterized by the truncation of high-profile, tree-lined beach ridges as the island retreats and rolls over into upland forest. Parramore Island's previous clockwise rotational pattern documented by Leatherman (1982) has evolved into a sustained rapid parallel retreat (Haluska 2017). Parramore has been described as a low island that tends to reinforce overwash exposure and remain in a low elevation state

through biogeomorphic feedbacks. Like Parramore, Hog Island exhibits mostly parallel retreat. However, it has lower shoreline retreat rates. Accretion and dune ridge-swale landforms dominate on the northern half of the island, while erosion dominates on the southern half. Hog and Parramore exhibit ‘pimple’ topography in which erosion during high water events leaves behind circular topographic highs (Hayden et al. 1995). Hog Island differs from the other islands in that it has increased in woody vegetation over the last 40 years (Zinnert et al. 2016b). It is designated as one of the high, overwash-resisting islands along the Virginia coast (Wolner et al. 2013; Brantley et al. 2014).

The most southern compartment of the mixed-energy tide-dominated barrier islands of Virginia consists of Ship Shoal Island and Wreck Island. Their diminishment of wave energy is evident in sands that are finer than those to the north (Fenster et al. 2016). Both islands are exhibiting non-parallel shore retreat. Ship Shoal and Wreck also have greater longshore variability in shoreline changes than the larger islands to the north (Fenster et al. 2016; Haluka 2017). Wreck is retreating faster on its northern part, with the southern end exhibiting shoreline advance seaward. Both islands have had the greatest maximum shoreline retreat of all the Virginia Barrier Islands (Haluska 2017).

The quantitative classifications of barrier island morphology partition this gradient of wave and tidal energy into a northern wave-dominated compartment (Assateague) and three southerly tide-dominated compartments. Williams and Leatherman’s (1993) classification assigned Assateague Island to class of wave-dominated islands with long, linear morphologies. Parramore Island was assigned to the widest-island class. Metompkin, Cedar, and Hog islands were assigned to the outlier class, which Kochel et al. (1983) described as islands lacking “geomorphic organization.” Wreck and Ship Shoal islands

were classified into the shortest-island class, typifying tide-dominated island morphologies strongly influenced by antecedent topography. Monge (2014) classified barrier island morphologies using variables similar to those in Williams and Leatherman (1993) and found a similar compartmentalization. Assateague Island was classified into its own group. The remaining six barrier islands formed three morphological groupings that were more geographically contiguous, and comprise Metompkin and Cedar, Hog and Parramore, and Wreck and Ship Shoal.

### 2.3.2 Plot selection

Within each of the seven islands, locations to characterize dune topography were determined by visually identifying from air photos the distinctive, predominant stretches of dune and beach topography. Criteria to identify these locations included beach width, the width of the dune field, linearity of the dunes, and type of habitat behind dunes. Areas of pervasive human impact and locations directly on tidal inlets were avoided. Four to five distinctive stretches of topography were required for each island (Figure 2. 2 and Figure 2. 3). To sample dune topography within these stretches of predominant alongshore relief, we employed a natural sampling technique (Bissonette 2017). In this technique, the phenomena under study defines the observational windows and the site dimensions. Square plots were randomly located within each distinctive stretch of barrier island dune shoreline so that they initiated at the mean high water mark datum (MHW) and extended inland to where salt marsh or significant stabilized woody vegetation developed. So instead of standardizing plot size, size became a spatial characteristic of the sampled topographies and was retained as an explanatory variable.

### 2.3.3 LiDAR methods

To capture small extent and fine grain patterns of dune topography, as well as those that are larger in extent and coarser in grain, we utilized Light Detection and Ranging (LiDAR) data derived from airborne surveys of the Virginia coast. Digital elevation models were constructed for each plot from LiDAR ground elevation data available online from the NOAA's Coastal Services Center. A post-Hurricane 2014 data-set collected by the NOAA National Geodetic Survey was used for all seven islands. Vertical (horizontal) accuracy was 6.2 cm (100 cm) and nominal point space was 0.3 m. In each of the plots, LiDAR point elevations were resampled to a resolution of 1 m and then interpolated using inverse distance weighing to fill any gaps. LiDAR processing was performed in ArcGIS using LAStools. The MHW shoreline was defined as the 0.7m contour line relative to the NAVD 88 datum (Rogers et al. 2015). The plots were then clipped along the edge coinciding with the MHW mark elevation of zero, clipped again to be square, and rotated to a common orientation.

### 2.3.4 Characterization of topography

#### *Cross-scale topographic metrics*

To avoid reliance on a few synthetic metrics to capture topography, we derived a suite of cross-scale metrics from the high resolution, broad extent coverage of the airborne LiDAR data. These metrics captured longitudinal (along-island; Houser 2013; Sherman et al. 2013), transverse (cross-island) and vertical (elevational) aspects of topography. Because controls on topography interact across scales, these metrics are intended to be nested and collinear. Such cross-scale data structure is intrinsic to dynamical systems (Nash

et al. 2014; Sundstrom et al. 2014). Cross-scale approaches have been deployed in dune studies using wavelet analysis (Houser et al. 2018; Wernette et al. 2018a). These studies also aimed to capture how dune topography reflects interactions across scales and how this in turn shapes barrier island responses to high water events.

These plot-level topographic metrics ranged from spatially-implicit to more spatially-explicit measures. For example, elevation is very informative property of dune topography, particularly when measured at the dune crest or along the high water mark datum (Long et al. 2014; Yousefi Lalimi et al. 2017). However, the actual elevation value at a point or along a line, or as calculated as a mean for an area and then assigned to a centroid, can be similar to average values derived from dune landscapes with very different arrangements of dune landforms. Thus, more spatially explicit measurement of alongshore and cross-island topographic variability, and not just elevation per se, are important properties of dune topography to include. To capture the geometry of elevations, we employed landscape patch metrics expressed as FRAGSTATS indices as well as gradient representations of landscape structure summarized through spatial correlograms. Both patch and gradient representations were employed because neither paradigm can fully capture landscape structure and process on its own (McGarigal et al. 2009; Lausch et al. 2015; Kedron et al. 2018). No single method for representing observations is entirely free of scale dependency (Wu et al. 2000). Thus, our approach is to model topography by taking an intensive set of observations (LiDAR) and reassembling it through metrics having different measurement levels (absolute versus relative), different degrees of spatial explicitness, and association with different conceptual paradigms and their data representations.



Through this strategy, we avoided dichotomizing variables as strictly local or landscape (Heisler et al. 2017). It also lessened the propensity to associate observations with a few arbitrarily defined levels (Jackson and Fahrig 2015). High resolution broad extent datasets like LiDAR facilitate the development and integration of multiple metrics, thereby accounting for different ontological representations (i.e., patch versus gradient) to account for pattern and process. Through these metrics, we examined similarity in dune topography with more accounting for its cross-scale, polygenetic (i.e., derived from a large number of attributes) nature and for the different conceptual paradigms that inform their detection and interpretation.

#### *Low and middle dimensional metrics*

The intrinsic dimensionality of these topographic metrics and their position along these dimensions, or axes, was used to infer the similarity in dune topography among the different island plots. Lower dimensional metrics were those expected to form the greatest source of variance in the data set. Spatially-implicit values of absolute elevation, as expressed in descriptive statistics (mean, 25<sup>th</sup>, 50<sup>th</sup>, and 75<sup>th</sup> percentiles) comprised these low dimensional variables. They were obtained from the 1-m interpolated plot surface using GS+ software (Robertson 2000).

Landscape metrics defined our midrange dimensional variables. These metrics (patch metrics) quantified the patch pattern of elevations. Because FRAGSTATS is designed to work with categorical observations, raster DEMs were converted into areal representations by reclassifying pixels into elevation intervals. This decreased the number of elevation classes from all the possible centimeter intervals to decimeter intervals (a categorically oriented representation). Wu et al. (2017, p. 56) as well as Ryu and Sherman

(2014) illustrate the logic of how the patch structure of topography can be represented with landscape indices. To avoid derivation of FRAGSTATS descriptors without a process interpretation, we chose landscape patch indices with consistent ecologically meaningful value (Cushman et al. 2008). This set of indices was then constrained to those better-suited for characterizing continuous gradient surfaces like elevation (McGarigal et al. 2009) and for discerning pattern-process relationships associated with foredune building and overwash. These indices were selection: the aggregation index (AI), the landscape shape index (LSI), the area-weighted mean shape index (SHAPE\_AM), the interspersion and juxtaposition index (IJI), the contagion index (CONTAG); the largest patch index (LPI); the Simpson's diversity index (SIDI), and the perimeter-area fractal dimension (PAFRAC).

AI increases with greater aggregation of patches into a single type. SHAPE\_AM increases as patches become more curvilinear. A higher IJI indicates that patch types are equally adjacent to all other patch types and are thus fully interdispersed. This index is based on patch rather than pixel adjacencies. Higher LPI implies higher dominance of a single patch within the plot. Higher SIDI implies higher patch richness and more equitable patch distribution within the plot. Higher PAFRAC implies all patch shapes within a plot tend to be convoluted. CONTAG increases as patches become larger and dominated by a similar elevation. This index is based on pixel rather than patch adjacencies. LSI increases as patch types become larger and more aggregated. It measures patch rather than pixel adjacencies and is similar to AI.

#### *Higher dimensional metrics*

Barrier island dune topography can be spatially variable, ranging from the linear patterns of alongshore ridges to broad, flat uniform overwash sheets. Given their capacity

to summarize elevational distributions for a continuous surface, skewness and kurtosis of point elevation values were defined as higher dimensional variables (continuum metrics). The size of the plots was also selected as a higher dimensional property of elevation. Autocorrelation of elevation values was also a higher dimension topographic metric. Continuous, spatially-explicit summaries of gradient structure in elevation were summarized by directional correlograms assembled in GS+ software (Robertson 2000). Autocorrelation were calculated for each plot-level 1-m DEM and constrained to the cross-shore direction (i.e., perpendicular to the water line).

#### *State space assembly*

A standard approach in landscape similarity is to make comparisons of locations using similarity distances (Niesterowicz and Stepinski 2016). Because our topographic metrics were measured in different units, each of them was first standardized as Z-scores. Similarities among plots was then calculated using Euclidean distances. Characterization of the dimensionality of these data and visualization of the similarity among plots was derived from ordination of topographic metrics with non-metric multidimensional scaling (NMDS) in PC-Ord Version 7 (McCune and Mefford 2016).

The NMDS solution was assessed for significance by comparing the reduction in stress in the actual data with reduction observed with Monte Carlo randomizations of the data. The final solution was also subjected to an orthogonal rotation to maximize variance in the data set along the first and succeeding axes. To infer how the plots from different barrier islands compared to each other, Spearman's nonparametric correlation coefficients were calculated for the NMDS scatterplot coordinates and their original topographic metrics. Six Moran's  $I$  values from the major breaks along each plot's directional

correlogram were ordinated with principal coordinates analysis (PCoA) in order to distill correlogram structure into coordinates that could then be ordinated with the other dune topographic metrics in NMDS. Like NMDS, PCoA is a distance-based, non-parametric ordination method. PCoA reduces the dimensionality of a dataset based on extractions of variance similar to principal components analysis.

To complement interpretation of the similarities in topography in NMDS state space, topographic metrics were clustered using a hierarchical agglomerative algorithm and a flexible beta linkage method with Euclidean distances. Multiresponse permutation procedures (MRPP) were used to test for significant differences among the cluster groups and among groupings of the plots based on their island identity. MRPP compares the average within-group or within-cluster similarity distance to between-cluster similarity distances. The statistical significance of cluster groupings can then be calculated by comparing the observed average within- and between-cluster similarity distances with the distribution of similarity distances obtained from random permutations of cluster membership. When all items are identical within groups, the A value, a measure of effect size, equals 1. If contrasts within groups equal expectation by chance, then the A value approaches 0. The A values between 0.1 and 0.3 are common for environmental data (Peck 2010). PCoA, clustering and MRPP was performed in PC-Ord Version 7 (McCune and Mefford 2016).

## **2.4 Results**

The distribution of pixel-level elevations for island plots was wider and more variable to the north toward Assateague (Figure 2. 4). Lower and less variable point

elevations tended to develop on the southernmost barrier islands of Ship Shoal and Wreck. The lowest spot elevations were observed on Cedar and Metompkin. While the overall variability in the central tendency of elevation among island sites was small, there were notable differences in how these elevational observations were arranged to form landscape-extent dune topography (Figure 2. 5). The geometry of topography varied from uniform to patchy (Cedar E versus Assateague A). Some plots had topographic highs close to the high water mark while others peaked in elevation toward the rear of the plots (Parramore B versus Metompkin C). Topography also differed in the predominance of alongshore versus cross-shore orientations of dune topography (Wreck D versus Assateague B). Some plots exhibited complex combinations of these along-shore and across-shore orientations (Hog C and Ship Shoal C). As captured in FRAGSTATS indices, AI differentiated large, continuous patches of elevation (Cedar A, AI = 91.8) from smaller, less aggregated patches (Assateague C, AI = 53.3). SHAPE\_AM distinguished between curvilinear patch structure (Cedar D, SHAPE\_AM = 5.5) and rectangular patch structure (Hog B, SHAPE\_AM = 2.9). CONTAG varied from more interspersed (Parramore B, CONTAG = 38.4) to less interspersed (Cedar E, CONTAG = 58.0) pixel values for elevation within elevation patches. IJI identified differences in how the elevations defining a patch type were clumped together. Elevation patches varied from clumpy (Ship Shoal C, IJI = 47.8) to uniformly dispersed (Hog B, IJI = 61.5).

The first axis of the PCoA ordination of directional correlograms (Figure 2. 6) captured 54% of the variance in the data set and was statistically significant based on Monte Carlo randomizations ( $n = 999$ ,  $p = 0.001$ ). The second axis did not extract a statistically significant amount of variance. Island plots with low flat overwashed topography

characterized the left (more negative) positions along first PCoA axis. These correlograms exhibited a peak in elevation close to the high water mark and then Moran's  $I$  values became increasingly negative with greater distance lags as elevation became increasingly lower. Plots that maintained more positive to zero correlations among elevation observations at high distance lags loaded to the right (more positive) on the first PCoA axis. These correlations tended to hover around zero as a reflection of their minimal relief and tendency to have peaks in elevation further inland from the MHW.

Two NMDS dimensions (i.e., axes) were optimal for the visualization of topographic state space. Stress reduction for this solution was significantly greater than solutions derived from ordinations of Monte Carlo randomizations of the data ( $p = 0.004$  for both axes,  $n = 249$ ). Final mean stress was 11.5. When island plots were color coded in the scatterplot of topographic state space, Assateague's topography was distinctive from the other islands. More tide-dominated islands had a region of overlapping topographies but also spanned a large area of the total state space (Figure 2. 7).

Elevational descriptive statistics (mean, maximum, 25th, 50th, 75<sup>th</sup> percentiles) had significantly stronger correlations with the first NMDS axis ( $p < 0.01$ ). Mean elevation ( $r_s = -0.87$ ) decreased from left to right along the first axis. Several FRAGSTATS landscape indices had similarly strong statistically significant correlations with the first axis ( $p < 0.01$ ). Elevations became more aggregated (AI) into large uniform patches moving toward the lower elevations to the right of the first axis ( $r_s = 0.80$ ). Conversely, elevations became more disaggregated into small uniform patches of similar elevation moving toward the higher elevations to the left on the first axis. Patch shapes for elevation intervals became more curvilinear (rectangular) as elevation decreased (increased) along the first axis

(SHAPE\_AM;  $r_s = 0.68$ ). Elevations for 1-m grid cells within patch types were more dispersed (less dispersed) at lower (higher) island plots (CONTAG;  $r_s = 0.62$ ). Individual patch types were more clumped (less clumped) at lower (higher) island plots (IJI;  $r_s = 0.71$ ).

Spatial autocorrelation structure had little discriminatory power as reflected in its low correlations with the first as well as the second NMDS axes (Axis 1  $r_s = -0.09$ ; Axis 2  $r_s = -0.24$ ). Correlations for the second NMDS axis were strong and significant for plot size ( $r_s = -0.76$ ) and for skewness of pixel-level elevation values ( $r_s = -0.55$ ). In moving from top to bottom along the second axis of the NMDS scatterplot, plots become larger and had elevational distributions with only a few extreme topographic highs as outliers. Elevation again had a significant but weaker correlation with the second NMDS axis (e.g., mean elevation  $r_s = -0.44$ ). However, this was in part due to high outlier elevations for Assateague plots B and C. Other outlier plots (Ship Shoal D, Assateague C, Hog A) also contributed disproportionately to the weak significance of some FRAGSTATs correlations with the first axis position, notably LPI ( $r_s = 0.67$ ), LSI ( $r_s = -0.56$ ), SIDI ( $r_s = -0.84$ ), and PAFRAC ( $r_s = -0.59$ ). Kurtosis has a weak correlation ( $r_s = 0.65$ ) with the second axis only as a result of outlier plots Cedar E and Hog A and their strongly peaked narrow range of low elevations.

When island plots were symbolized according to hierarchical clustering results, the relevance of island identity was evident in the composition of some clusters, but it was not the overriding control (Figure 2. 8 and Figure 2. 9). Clusters were not homogenous in terms of island plot membership. At the level of two clusters, Assateague formed a heterogeneous group with plots chiefly from Hog and Parramore instead of the islands just south of it, Metompkin and Cedar. The second cluster comprised the plots of the rapidly retreating,

rotating islands of Metompkin and Cedar as well as the low relief plots on Wreck and Ship Shoal. At the three cluster level, two low-elevation outliers (Hog A and Cedar E) formed their own group. With four clusters, topography was organized into a northern wave-dominated cluster dominated by chiefly the plots on Assateague, a less erosional middle cluster in plots from Hog and Parramore were abundant, and a third cluster of very low elevation plots chiefly from Wreck and Cedar. Higher cluster group levels only identified individual island plots as outliers. MRPP detected significant differences in topography for island identity and for cluster groupings (Table 2. 2). However, the robustness of this significance varied. The A values were highest for the three- and four-cluster groupings, indicating the robustness of these groupings of topographic similarity over those based solely on island identity.

## **2.5 Discussion**

Island morphology contributed to how dune topographies were clustered in their state space. Three major topographic clusters emerged (Figure 2. 8). These clusters had a propensity to track with their morphological context: (1) a cluster of higher, positive dune relief on wave-dominated Assateague Island; (2) a cluster of more erosional remnant dune relief dominated by Hog and Parramore islands, and (3) a cluster of very low, flat, topography on Cedar, Metompkin, Ship Shoal, and Wreck (plus two outliers). This clustering of topography reflected island-level morphological coastal compartments identified in prior classifications by Williams and Leatherman (1993) and Monge (2014).

While topography had a degree of affiliation with island morphology, these cluster groups were not homogeneous with respect to their island morphological compartment.



None of the clusters were comprised exclusively of all the individual plots of any one island. Instead, variability of topography in state space was more heterogeneously distributed along the gradient of wave to tide-dominated island morphologies captured by the first axis. Although geographically closer to Assateague Island, some of the plots on Metompkin and Cedar were positioned in state space near those of Wreck and Ship Shoal, the lowest and southernmost islands of the study area. Coastline engineering on Assateague and Wallops Island to the south of it are likely responsible for downdrift sediment starvation and the enhanced erosion and retreat on Metompkin and Cedar. Thus, human shoreline modification generated topographies on Metompkin and Cedar more like those of Wreck and Ship Shoal in the southernmost coastal morphological compartment.

The dune topography of some plots was more similar to topographies found on geographically distant island morphologies. Use of Haluska's (2017) data for shoreline erosion and accretion over time gives further support to the limits of using island morphology and nearshore setting to anticipate dune topography. We paired the geographic position of plots in this investigation with Haluska's (2017) reconstruction of trends in alongshore erosion and accretion for the Virginia Barrier Islands (Table 2. 3). In that study, the locations where our A and B plots on Metompkin occurred were highly erosional while the location where our C and D plots were much less so. In our topographic state space, dune topographies for Metompkin C and D plots were grouped into the cluster group consisting of the less erosional topographies on Hog and Parramore islands. Metompkin A and B plots were clustered with the low relief erosional plots on Ship Shoal and Wreck, as would be expected based on Haluska's measurements.

Based on plot locations in topographic state space, topographic divergence is greater on morphologies where tidal energy dominates over wave energy. Even with their much smaller island dimensions, plots from tide-dominated islands were more widely distributed across clusters. Therefore, assuming island morphology reflects dune topography may be more valid for wave-dominated versus tide-dominated mixed energy barrier island morphologies. The mixed-energy wave-dominated island in this study, Assateague Island, was distinct in state space from more tide-dominated mixed energy barrier coasts. Dune topography of these tide-dominated barrier islands were distributed across a larger region of state space. Hayes (1979) noted that mixed-energy, tide-dominated barriers exhibit rotational retreat behavior more frequently than wave-dominated barrier islands. The switching between rotational- and parallel-shoreline retreat observed on the Virginia Barrier Islands may explain the pronounced variability in topography observed over relatively short geographic distances on the tide-dominated islands.

The greater variability in dune topography on tide-dominated islands of the Virginia coast may also be due to the lack of strong landscape-level biogeomorphic feedbacks. The Virginia Barrier Islands are retreating rapidly and in some cases drowning in place. Consequently, topography may be coupled to the high frequency and intensity of storm surge and overwash events rather than vegetation feedbacks. As noted earlier, negative relief (i.e., pimples) formed by erosion are common on Hog and Parramore islands (Hayden et al. 1995). By examining the Google Earth imagery, these topographic features are to be expected where overwash, inundation, and retreat are frequent and pervasive. Because the generation of positive relief through biogeomorphic feedbacks is less developed, topography on many on the Virginia lots may be less biotically constrained. Consequently,

topography simply takes the form dictated by the storm regime. Biogeomorphic feedbacks may be more operative across the landscape of wave-dominated island morphologies like those of Assateague. This island's relatively higher elevations may facilitate more adaptive responses arising from the interaction of dune vegetation growth, disturbance, and recovery. As a result, island morphology becomes more tightly coupled to dune topography, even over the large dimensions that these wave-dominated barriers take.

The structure of topographic state space also supported this interpretation. Biogeomorphic feedbacks may be weakly developed on the Virginia Barrier Islands because of how topographic metrics loaded on the two axes of state space. The lower dimensional variables (elevation, FRAGSTATS indices) loaded strongly on the first axis. The second axis lacked any higher dimension spatial structuring. Directional autocorrelation in elevation, a variable reflective of more spatially-integrated landscape dynamics, did not have any significant correlations with island plot positions in the state space. In other words, the dune topographies may be controlled by frequent storm and overwash events. The topographies were characterized by low elevation, as evidenced by higher colinearity among the lower dimensional variables on the first axis and poor spatial structuring on the second axis. Storms and overwash may return too frequently on the lowest Virginia Barrier Islands to allow biogeomorphic feedbacks to constrain topography at landscape extents. Small hummocky dunes require storm-free intervals so that they might coalesce into larger continuous landform features that could modulate overwash exposures (Goldstein et al. 2017).

Wave-dominated barrier islands have been assumed to be low, overwash-reinforcing islands. Tide-dominated islands have been assumed to be high, overwash-

resisting islands. However, in this study, the opposite situation existed. The lowest and more frequently overwashed conditions were expressed on tide-dominated barrier island morphologies. These rapidly retreating islands are strongly shaped by adjacent inlet dynamics, shifts between parallel and rotational retreat, and frequent exposure to storm surge and overwash. This may override biogeomorphic feedbacks that could entrain landscape spatial structure and lead to an overwash-reinforcing topography.

## **2.6 Conclusion**

For the stretch of coast examined in this study, the nearshore context shaping island morphology contributed to dune topographic position in state space, but only in the terms of the division between wave- and tide-dominated barrier islands. Local shoreline trends in accretion and erosion were responsible for much of the variability in dune topography among tide-dominated islands. This study suggests that the way in which dune topography varies within and among barrier islands is more complex than existing dynamical models of barrier islands propose. Plotting the Virginia Barrier Islands in a state space spanning barrier islands from a larger geographic range of nearshore conditions and barrier island morphologies is one way to test this interpretation.

Some general rules of thumb can be recommended based on the findings in this study. Wave-dominated barrier islands may exhibit more convergence of dune topographic form. Greater divergence of topography is a characteristic of more tide-dominated mixed energy barrier islands. However, this may be applicable tide-dominated barriers when they are low and highly erosional like on the Virginia coast versus other locations (for example, Georgia and South Carolina). In these locations tide-dominated morphologies are higher

in elevation and may exhibit biogeomorphic feedbacks that constrain topographic variability. Whether tide-dominated barrier islands are high and resisting and wave-dominated barrier islands are low and reinforcing depends upon the local rates of sea level rise and erosion. Tide-dominated island morphologies may lack the landscape scale topographic spatial structure associated with biogeomorphic feedbacks when they are extremely low and erosional, such as is the case for many of the Virginia Barrier Islands.

Through the identification of the topographic similarities between island morphologies as well as within individual islands, the findings in this study echo those from other biogeomorphically dynamic systems that argue for a mosaic approach to the classification of landforms (Lane et al. 2017). Spatially explicit mosaics may create threshold and transitions dynamics that are more complex and unpredictable (Génin et al. 2018) than those currently articulated for overwash-resisting, overwash-reinforcing, and bistable models of barrier island dune dynamics. Field investigations to identify the ecological mechanisms underlying these dynamics should consider within-island location as much as general island morphological setting. Selecting study sites based on their position in state space in order to maximize topographic dissimilarity may be a useful a priori strategy when setting up controlled plots to detect and delineate the specific biogeomorphic and ecological mechanisms underlying how barrier dune coasts respond to high water events (Brown and Zinnert 2018).

**Table 2. 1** Island morphologies.

| Island     | Length (km) <sup>a</sup> | Width (km) <sup>b</sup> | Area (km <sup>2</sup> ) <sup>c</sup> | Retreat rate (m/yr) <sup>d</sup> |
|------------|--------------------------|-------------------------|--------------------------------------|----------------------------------|
| Assateague | 60.0                     | 0.8                     | 49.2                                 | 1.9 ± 0.6                        |
| Metompkin  | 10.4                     | 0.3                     | 2.7                                  | 10.9 ± 1.0                       |
| Cedar      | 9.6                      | 0.4                     | 4.2                                  | 10.8 ± 0.5                       |
| Parramore  | 12.8                     | 0.8                     | 9.6                                  | 12.4 ± 0.3                       |
| Hog        | 11.2                     | 0.9                     | 9.7                                  | -1.3 ± 0.3                       |
| Wreck      | 4.8                      | 0.4                     | 2.1                                  | 4.2 ± 1.0                        |
| Ship Shoal | 2.4                      | 0.4                     | 0.9                                  | 6.0 ± 4.8                        |

<sup>a</sup> Fenster et al. (2016)

<sup>b</sup> Width is summarized as area/length.

<sup>c</sup> Reported by Zinnert et al. (2016b) except for Assateague, Metompkin and Ship Shoal, which were estimated from digitization of aerial photos in Google Earth.

<sup>d</sup> The retreat rate of Assateague island (2005-2010) is from Psuty and Silveira (2011), other islands are from Deaton et al. (2017) for 1980-2010. Positive values indicate retreat (westward shoreline movement). Negative values indicate advance (eastward shoreline movement).

**Table 2. 2** MRPP tests of group difference for cluster groups

| Grouping        | T      | A    | P      |
|-----------------|--------|------|--------|
| 2 Clusters      | -10.88 | 0.12 | <0.001 |
| 3 Clusters      | -10.09 | 0.19 | <0.001 |
| 4 Clusters      | -10.08 | 0.23 | <0.001 |
| Island identity | -4.58  | 0.14 | <0.001 |

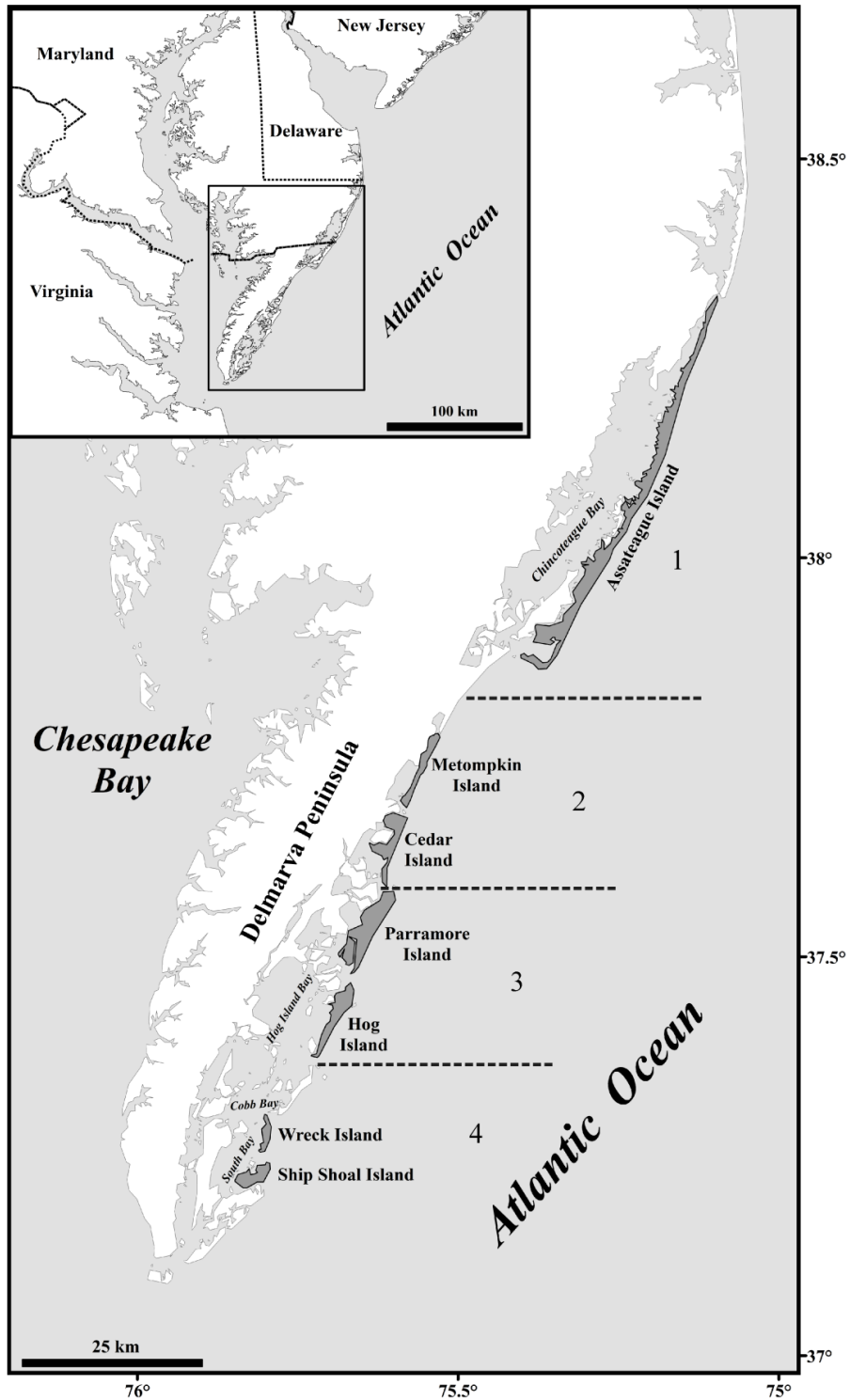
**Table 2. 3** Annual shoreline movement rate for each island (1990-2014) from graphical results Haluska (2017). Distance is the location alongshore in km starting from the southern terminus of each island.

| Island    | Plot | Distance(km) | Shoreline movement rate(m/year) |
|-----------|------|--------------|---------------------------------|
| Metompkin | A    | 8.70         | -10.00                          |
|           | B    | 7.26         | -13.00                          |
|           | C    | 2.86         | -1.00                           |
|           | D    | 1.43         | 2.00                            |
| Cedar     | A    | 10.64        | -22.00                          |
|           | B    | 8.65         | -15.00                          |
|           | C    | 6.43         | -10.00                          |
|           | D    | 3.86         | -15.00                          |
|           | E    | 2.34         | -18.00                          |
| Parramore | A    | 11.11        | -10.00                          |
|           | B    | 9.46         | -12.00                          |
|           | C    | 7.04         | -10.00                          |
|           | D    | 3.74         | -15.00                          |
|           | E    | 0.99         | -20.00                          |
| Hog       | A    | 11.15        | 7.00                            |
|           | B    | 6.79         | -1.00                           |
|           | C    | 2.71         | 2.00                            |
|           | D    | 0.68         | 5.00                            |
| Wreck     | A    | 3.94         | -10.00                          |
|           | B    | 3.36         | -5.00                           |

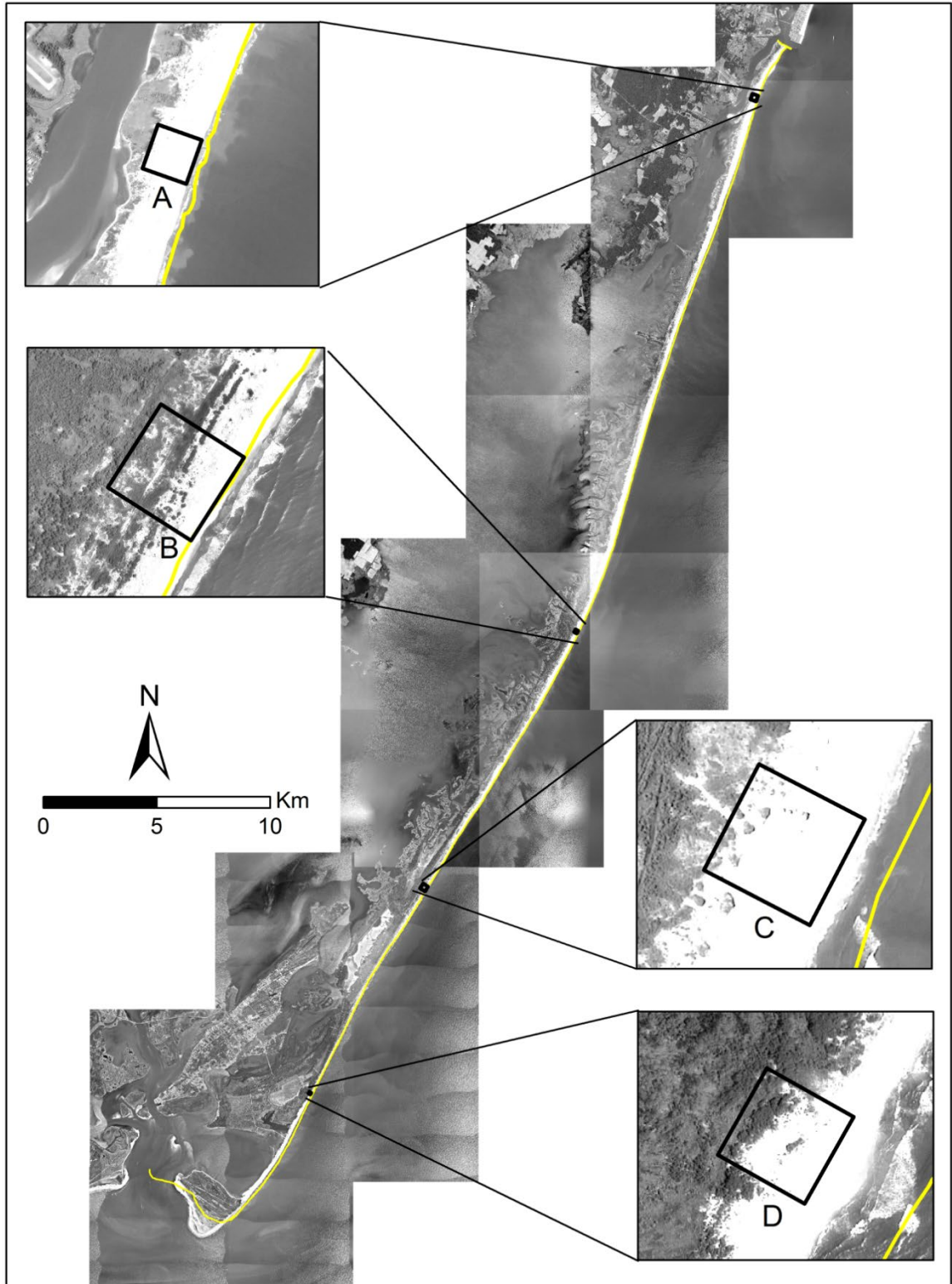


Table 2. 3 (Continued)

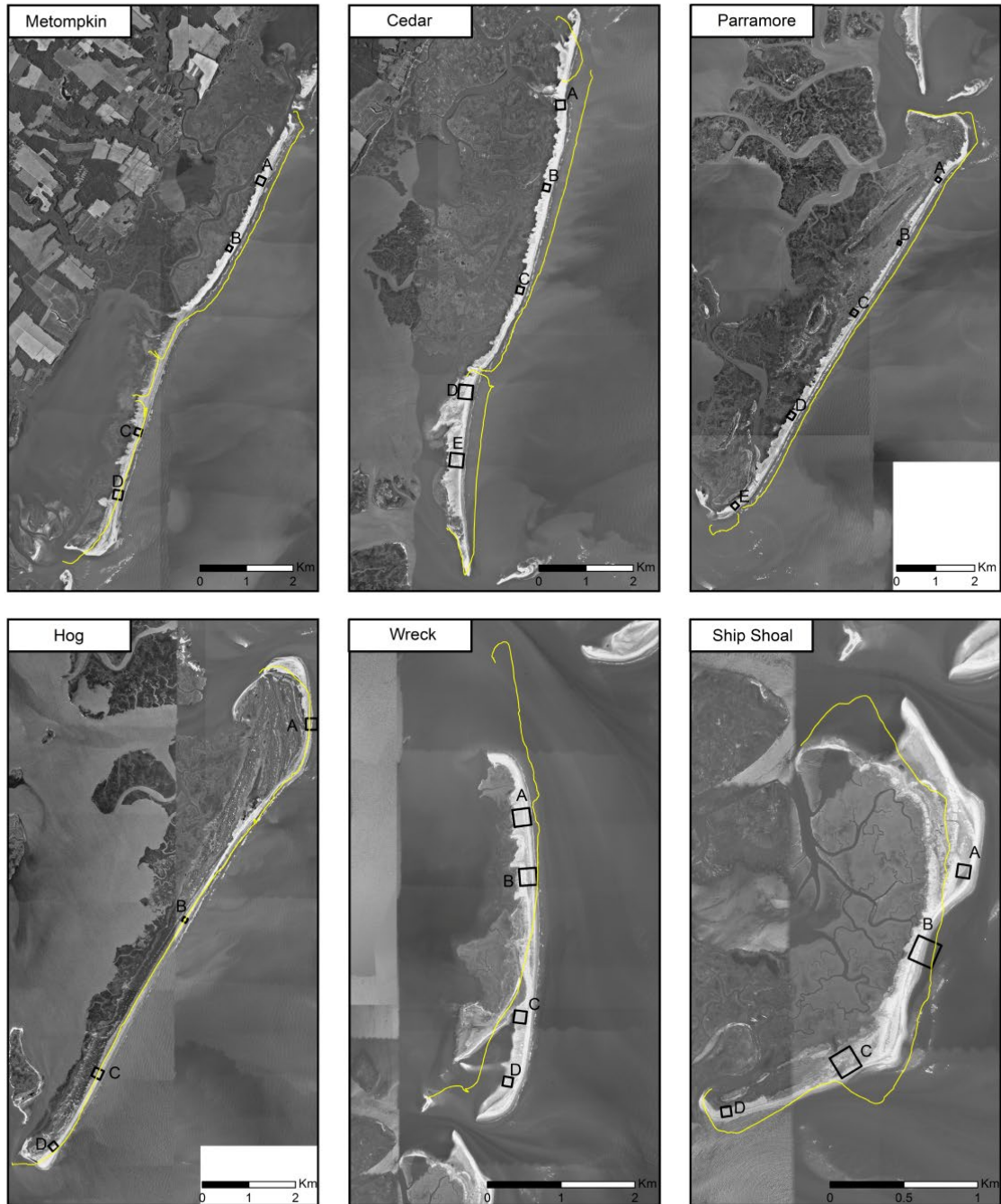
| Island     | Plot | Distance(km) | Shoreline movement rate(m/year) |
|------------|------|--------------|---------------------------------|
| Wreck      | C    | 0.87         | 28.00                           |
|            | D    | 0.29         | 45.00                           |
| Ship Shoal | A    | 2.03         | 8.00                            |
|            | B    | 1.45         | -2.50                           |
|            | C    | 0.58         | -6.00                           |
|            | D    | 0.08         | -8.00                           |



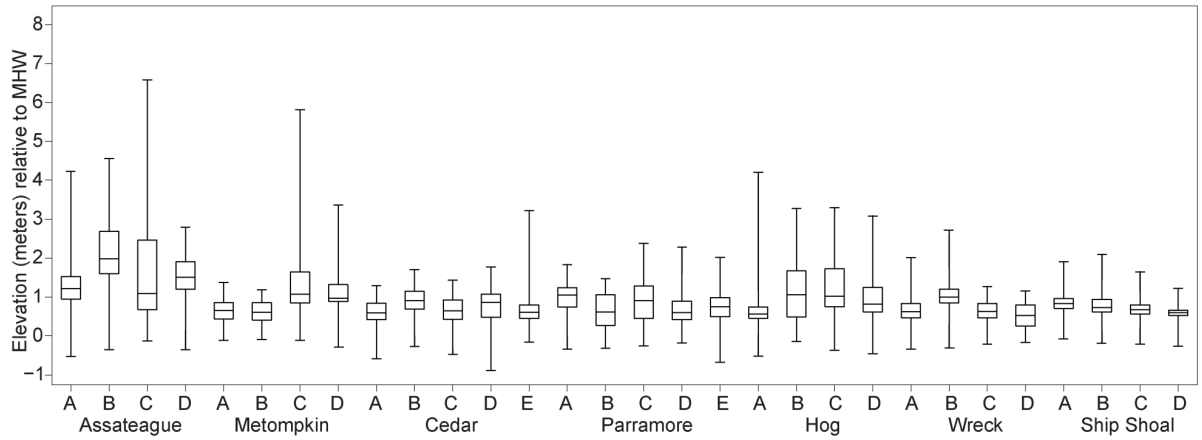
**Figure 2.** 1 Study area with its four island morphological compartments. Northernmost compartment 1 is wave-dominated, the southernmost compartment 4 is more tide-dominated.



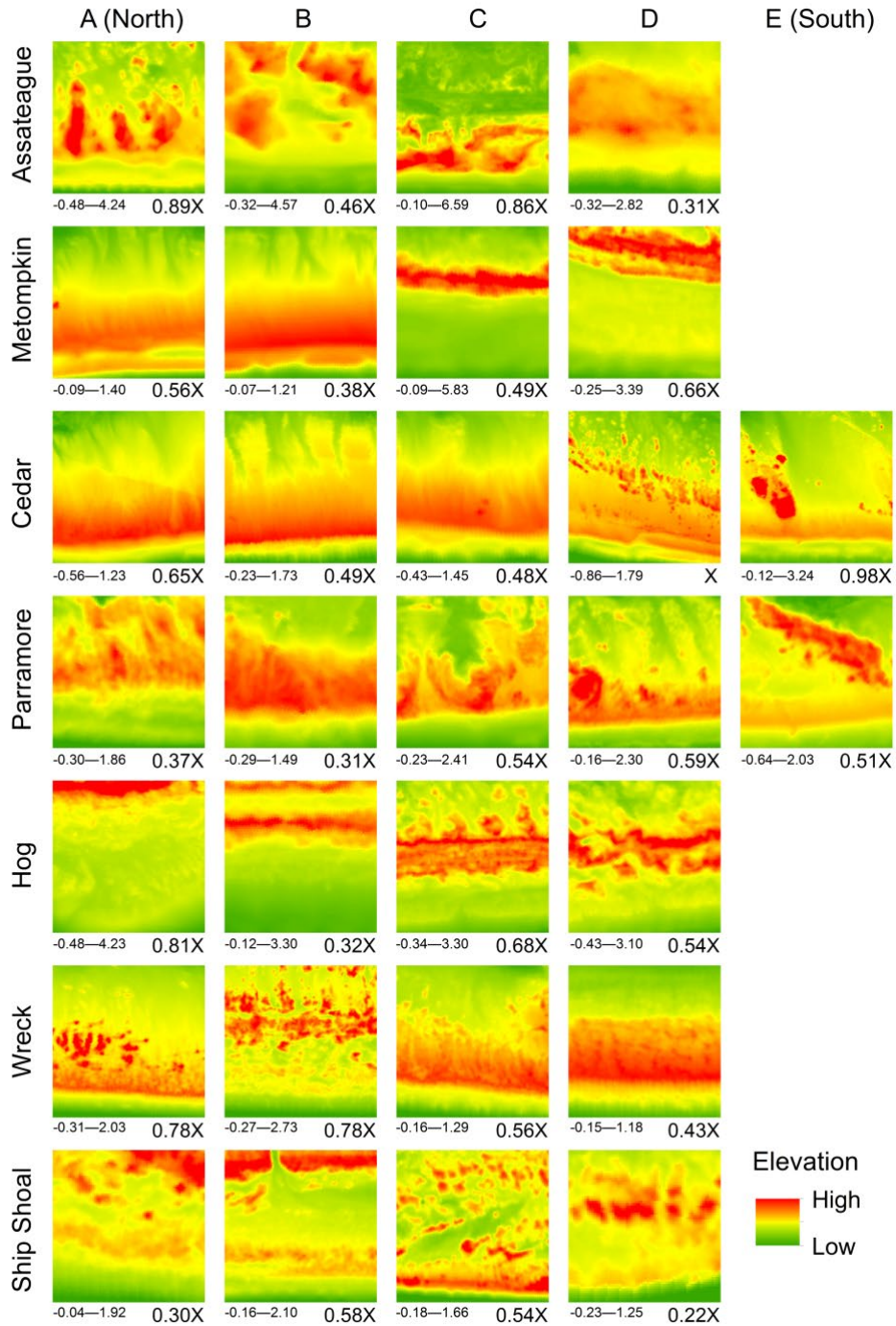
**Figure 2. 2** Study plots on Assateague Island. Letters indicate position along island, from A (northernmost) to E (southernmost).



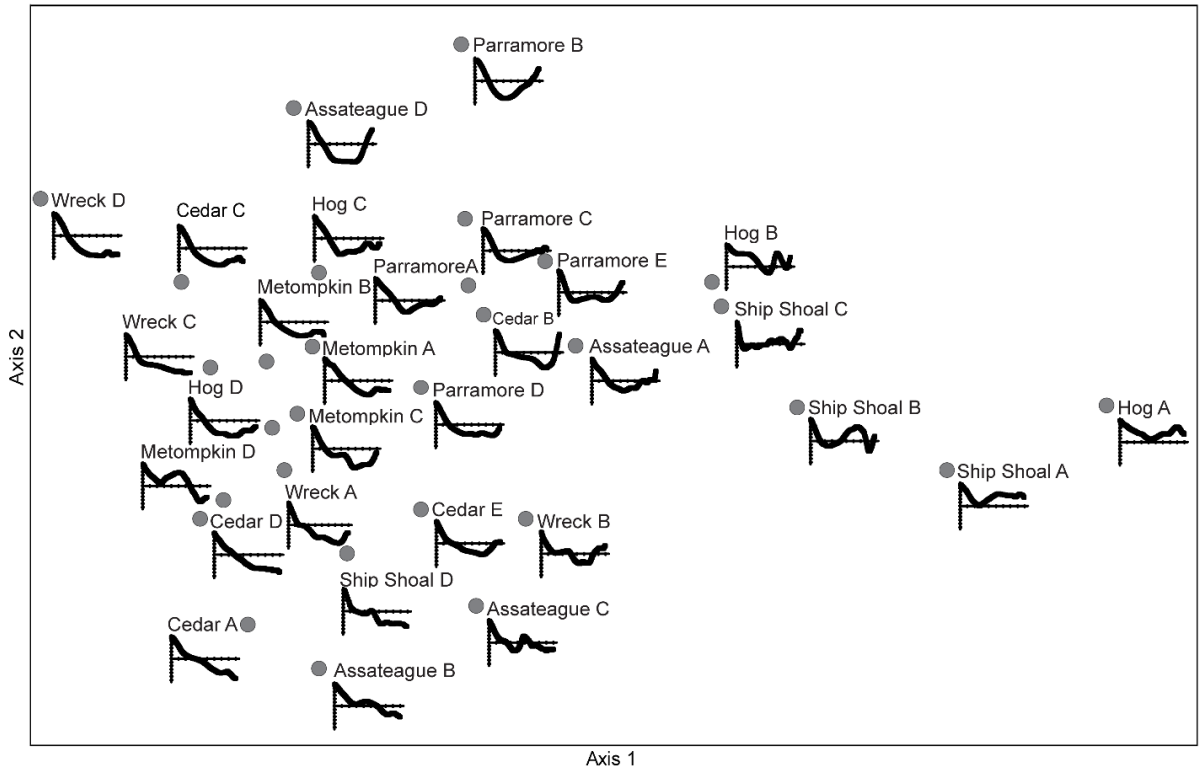
**Figure 2. 3** Study plots. Wave energy decreases as tide energy increases from Metompkin to Ship Shoal. The yellow line is the approximate shoreline in 1994 based on the location of the high water mark for each island derived from Google Earth Imagery. Aerial photos taken in 2011 are from the National Agriculture Imagery Program.



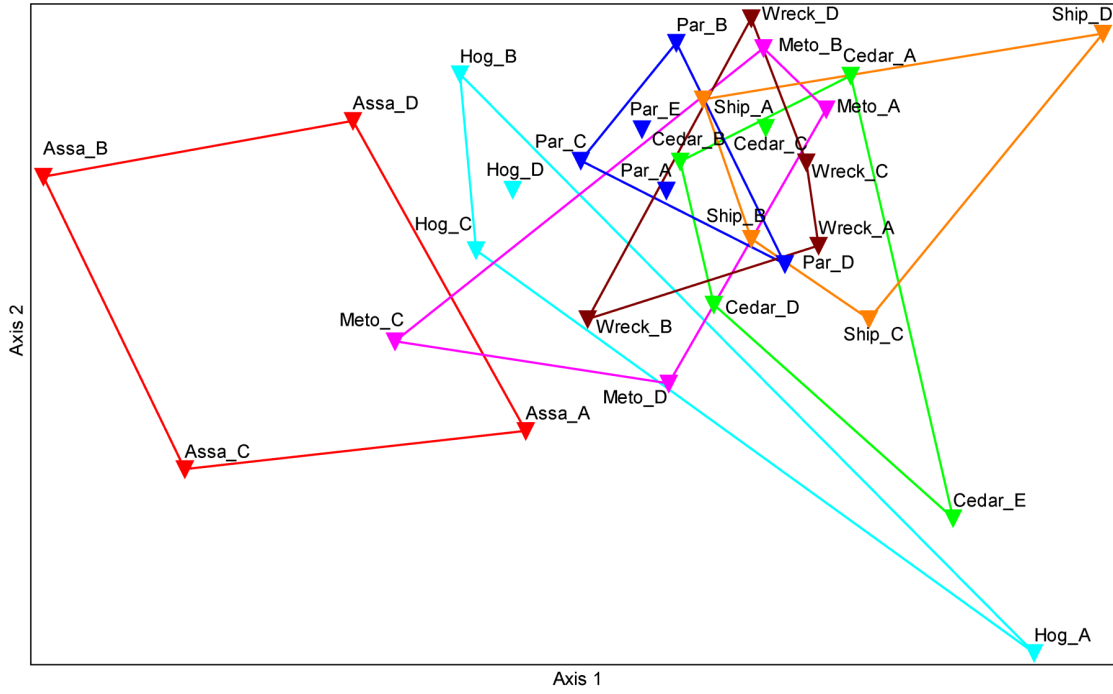
**Figure 2. 4** Boxplots of elevation in 1-m cells for each plot. The central mark indicates the median, and the bottom and top edges of the box indicate the 25th and 75th percentiles, respectively. The whiskers extend to the maximum and minimum values.



**Figure 2. 5** Plot DEMs scaled to local minimum and maximum elevation. Letters indicate position along island, from A (northernmost) to E (southernmost). Island plots differed in size although scaled to be the same here. Conversion factors below each raster can be used to derive their plot size relative to the largest island plot, Cedar D (295 x 295 m). For example, the actual dimensions of Assateague plot A are 262 x 262 m ( $0.89 \times 295 = 262$  m).



**Figure 2. 6** PCoA scatterplot showing variability in the directional correlograms of island plots. Moran's  $I$  is represented on the vertical axis of each correlogram. The horizontal line represents a Moran's  $I$  value of zero.



**Figure 2. 7** NMDS scatterplot of plot topographies grouped by island identity (i.e., specific to their local nearshore context and island morphology).



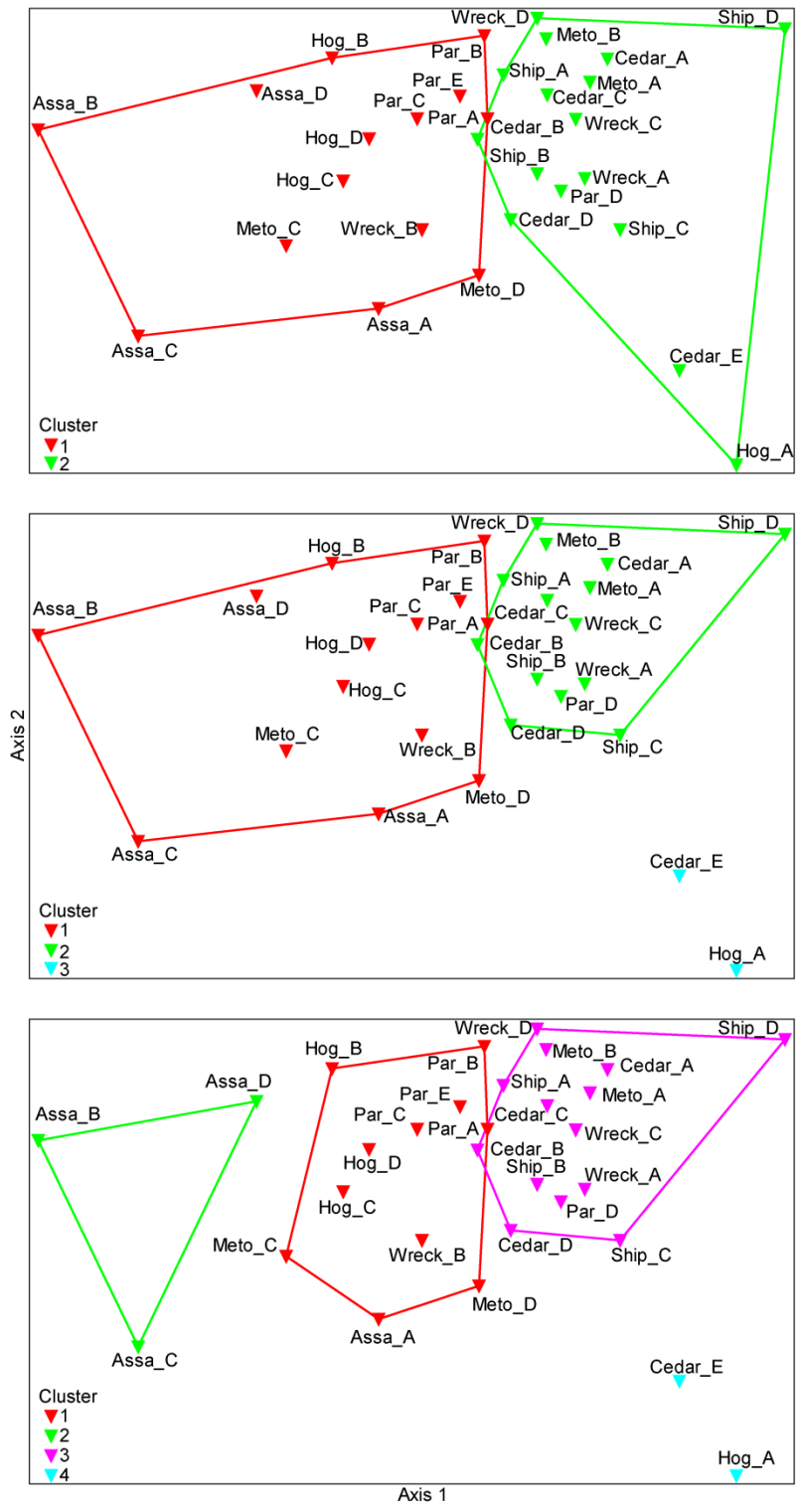


Figure 2. 8 NMDS scatterplots of dune topography for 2, 3 and 4 cluster group solutions.

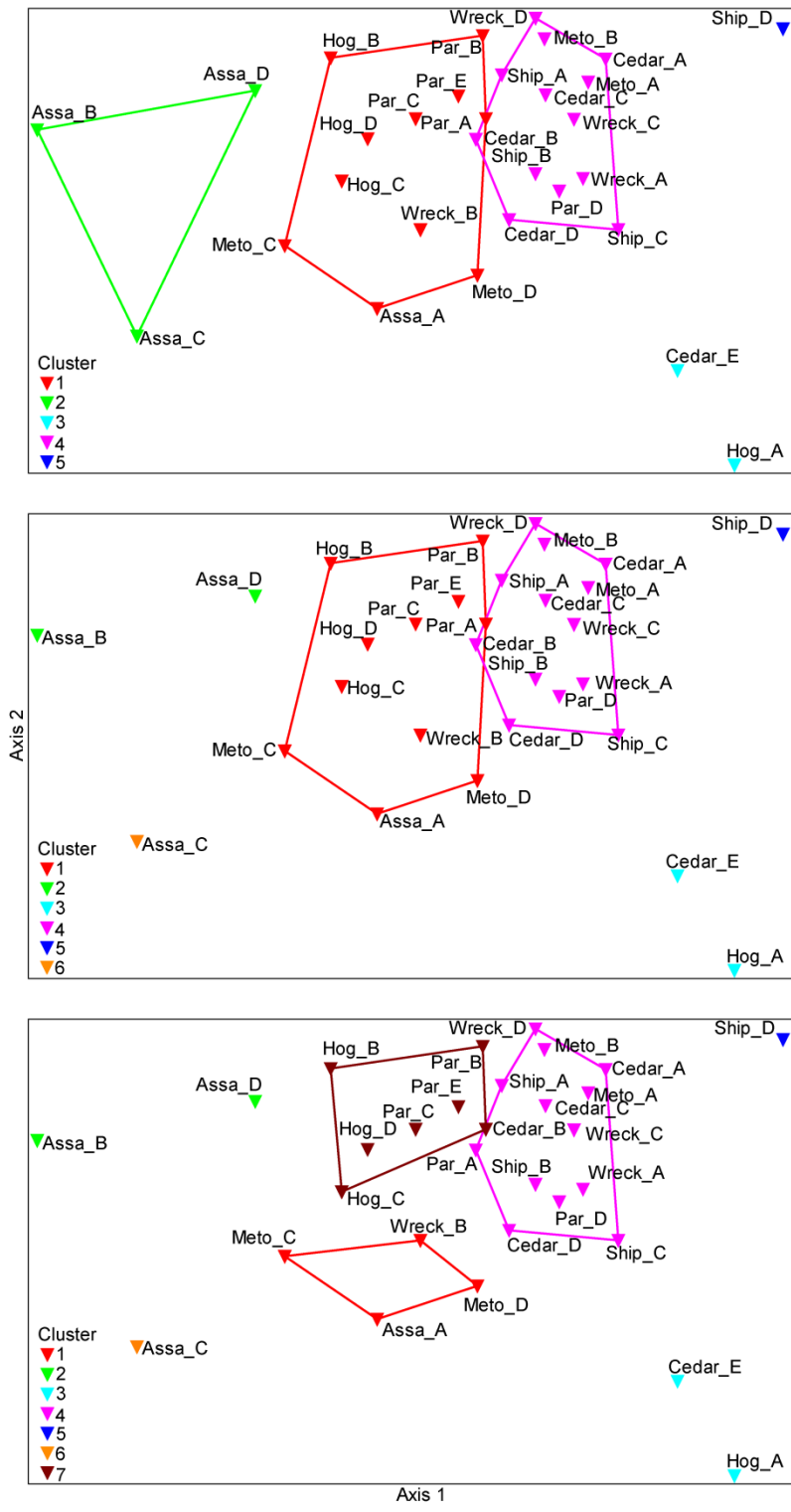


Figure 2. 9 NMDS scatterplots of dune topography for 5, 6 and 7 cluster group solutions.

### **Chapter 3. Barrier island dune resistance and resilience inferred from topographic state space: a cross-scale data modeling approach**

#### Abstract

Dune topography contributes to differences in how barrier coasts respond to and recover from high water events. To test ideas about barrier dune resilience, we deployed a cross-scale data modeling approach to compare dune topographic patterns among sites on selected barrier islands of the U.S. Virginia coast and the Georgia Bight. Hierarchically-nested dune topographic metrics constructed from airborne LiDAR were combined into a data model of cross-scale resilience that was subsequently visualized as a multidimensional state space. Similarity in topographic pattern in this state space was gauged through a site's position along low-dimension axes representing geomorphic resistance and high-dimension axes representing the spatial landscape properties of biogeomorphic resilience. Dimensionality and the loading of topographic metrics on these axes in state space were utilized to assess resilience prosperities. Topographic state space for Virginia islands had lower dimensionality, reflective of their erosional, rapidly retreating status. Elevation properties were collinear with weakly expressed landscape metrics, suggesting that dune landscape structure here equates more to the direct geomorphic impacts of frequent storms and process like overwash that homogenize topography. Georgia Bight topographies had greater dimensionality, and stronger separation of geomorphic and biogeomorphic landscape metrics among axes. Based on a visualization of both data sets simultaneously, resilience developed in only a small region of state space occupied chiefly by locations from the Georgia Bight. Because of reduced geomorphic resistance for the Virginia barrier island sites, resilience that emerges out of feedbacks between vegetation and topography

may be more weakly expressed. Stabilizing biogeomorphic feedbacks that promote resilience in barrier dunes may be more contingently expressed than previously hypothesized and linked secondarily to island morphology.

### **3.1 Introduction**

Comparing spatial patterns is a fundamental mode of geographic inquiry, one that has taken on new urgency in light of ongoing anthropogenic environmental change. For physical geographers, spatial pattern comparison has been augmented by availability of data collected at high resolution and large spatial extents. These data have increased interest in how to compare the spatial attributes of landforms in new and more subtle ways (Jasiewicz et al. 2014; Long and Robertson 2018; Praskiewicz 2018). This is particularly true for coastal regions (Zinnert et al. 2017). With rising sea levels, sandy barrier islands are where pronounced environmental changes are anticipated, if not well underway. Although questions about the stability and persistence of barrier islands motivated scholars in the 1970s and 1980s (Leatherman 1982), how these landforms respond to sea level rise and storm surges during hurricane landfall has reemerged with a new urgency as a consequence of human-caused climate change.

To add to our understanding of how barrier coasts respond to and recover from high water events, we compared dune topographies expressed at sites across six barrier islands of the Georgia Bight, from Florida to North Carolina (Figure 3. 1), to sites expressed across seven islands of the Virginia barrier coast (Figure 3. 2). Topography reflects the dynamical properties of barrier island beaches and dunes, whether applied in simple mathematical models (Bruun 1988), conceptual descriptions (Godfrey 1977), or complex simulations

(Gutierrez et al. 2015). The stability and persistence of barrier islands has been attributed in part to feedbacks among dune topography, dune vegetation, and overwash disturbance (Godfrey et al. 1979; Stallins 2005; Durán and Moore 2015; Zinnert et al. 2016a; Goldstein and Moore 2016). In the earlier versions of this biogeomorphic perspective, mixed-energy wave-dominated barrier island morphologies were hypothesized to maintain components of dune landscape structure through the reinforcement of overwash exposure and plant-sediment feedbacks that maintain a low relief topography. Mixed-energy tide-dominated barrier island morphologies were postulated to maintain aspects of their structure through biogeomorphic feedbacks that enhance topographic roughness and limit overwash exposure.

The topographies of these two island-level ‘stability domains’ (Gunderson 2000) were defined as indicators of their resilience (Stallins 2005). This resilience arises through the way in which biogeomorphic feedbacks resist or reinforce overwash disturbances and promote the persistence of landforms and vegetation in a positive feedback. In short, high resilience is related to the two stability domains because their resilience is generated through biogeomorphic feedbacks. In each domain, stability is linked to specific dune topographies and vegetation types that are maintained by biogeomorphic feedbacks to resist or reinforce overwash disturbance. However, while these two island morphological types manifest in the two coastal strands compared in this study, they occur in different nearshore contexts, with variable local sediment budgets, wave and tidal energy regimes, and rates of sea level rise. Stability domain properties have been assigned to barrier islands in both regions, but with limited empirical basis using designations of topography. One of the main reasons for this is the fundamental challenge of making spatial pattern

comparisons. Patterns have a variety of components and can be represented in various ways (Lastochkin et al. 2018). For example, dune responses to storm events and recovery afterwards can be predicated upon single summary measures of topography like maximum or mean elevation. However, maximum or mean elevation in and of itself says very little about the spatial patterns the contributing elevations might take. Elevation, as a topographic pattern, can be represented as a point, or a line or area. Taking it further, areal patterns are amenable to representation as discontinuous patches or more continuously as a gradient (Kedron et al. 2018). The outcome of any comparison of spatial patterns also depends upon the level of spatial explicitness employed and at what scalar grain or resolution it was measured. Measurement levels can also shape pattern comparisons. Absolute measures like mean elevation may be similar for two sites, but relativized values, such as the spatial autocorrelation of elevation observations, may differ. As these examples illustrate, independent or singular facets of elevation may be useful, but they are also incomplete descriptions of pattern.

Complicating this issue of comparing spatial pattern is that contrasting ways of representing pattern are often linked to different conceptual paradigms, each preferring certain representational forms. Raster and vector paradigms and their representative ontologies are well known examples. Yet as long recognized in GIScience, taking both paradigms into account can more fully describe the underlying spatial pattern. To make robust comparisons of barrier island dune topography across the geographic regions in this study, we developed methods to characterize dunes in terms of patch and gradient explanatory paradigms. It was designed to integrate and analyze different dune topographic metrics, each capturing a different ontology of pattern. Yet even with this recognition of

the value of integrating multiple representations of spatial patterns in order to compare them, what still remains a constraint is the old problem of insuring that pattern reflects process. Given the mandate of insuring that pattern and process are linked, a larger explanatory framework was needed in this study to guide what data are selected and how they were combined to compare spatial patterns (Praskievicz 2018).

We relied upon the ecological concept of cross-scale resilience as the overarching framework to guide the integration of our representations of dune spatial patterns and to insure that they link to process. As deployed in resilience theory (Nash et al. 2014), cross-scale structure postulates how variability in pattern and process within and across scalar extents links together to shape dynamic properties. Although it borrows from hierarchy theory, cross-scale structure accounts for more of the adaptive and evolving nature of scalar interactions. Through feedback processes, cross-scale structure accounts for the emergence of resistance and resilience. By judiciously selecting geomorphic and biogeomorphic topographic metrics to reflect cross-scale structure, topographic patterns as well as the resilience properties arising from them can be compared (Sundstrom et al. 2014, 2018).

Resistance and resilience have varying definitions in the ecological and geomorphological literatures (Grimm and Wissel 1997; Phillips and Van Dyke 2016). We employ the following definitions. Resistance refers to intrinsic properties that directly counter expressions of power from disturbance. Resilience is the ability of a system to recover from disturbance and the degrees of freedom to absorb or adjust to disturbance. Resilience, then, is a measure of how feedbacks coupled to extrinsic disturbance maintain an organizational structure and function until some threshold is reached and the system can exhibit a change in state. Resistance is more of a static property, a measure of the magnitude

of change related to a response to disturbance. Resilience invokes adaptation and the emergence of stabilizing feedbacks, while resistance does not. While tempting to conceive of these two types of resilience as independent, ecological systems have both resilience properties simultaneously (Gunderson 2000; Donohue et al. 2013). Resilience exhibits a dependency on resistance. In our cross-scale model of dune topography, too much resistance to disturbance or too little will inhibit the development of the adaptive sorting and landform-vegetation feedbacks that can lead to the emergence of ecological resilience.

Two questions guided our comparisons of topography. First, is the cross-scale data structure for these two coastal stretches logically distinct? We expect that their structure should reflect known geomorphic and nearshore contrasts between the Georgia Bight and the Virginia coast. Second, to what extent does the Virginia topographic data fit within the bounds of the Georgia Bight data? Overlap over some range of elevation could be expected, but how do landscape topographic properties vary? These two questions intend to shed light on the degree of general applicability of the two-domain model of biogeomorphic dynamical states. The concept of barrier island stability domains originated from studies in the Georgia Bight. The stability domain concept was then extrapolated to the much smaller stretch of barrier island coast of Virginia. But how similar are these topographies when a more nuanced comparison of spatial pattern is made? The cross-scale data modeling approach developed in this study provides a basis to compare topographies, but it also fits topographies along dimensions or axes representing resistance and resilience so that linked processes can be compared as well. Given the propensity for biogeomorphic feedbacks to constrain topography, one could expect some convergence in relief and therefore in dynamical properties among sites in the Georgia Bight and the Virginia data set. On the



other hand, there may be limits to this convergence of topographic form and in resistance and resilience. The island morphologies of the Georgia Bight and the Virginia coast differ strongly in their rates of relative sea level rise and geologic context. Variability in topography along individual islands may also weaken the association of island morphology with its topography and resilience properties (Zinnert et al. 2016a). More detailed comparisons of the dune topographies of barrier islands in the Georgia Bight and the Virginia coast would permit an assessment of the degree of generalizability of this two-domain model and the properties of resilience associated with it.

## **3.2 Background**

### 3.2.1 Cross-scale structure

Topography, like any spatial pattern, is the outcome of multiple and interacting processes. Hierarchy theory summarizes how nested processes operate at different scalar extents to shape pattern and process. However, study of the integration of these hierarchical levels is challenging because different conceptual frameworks are often invoked at different spatial and temporal scales (Bauer et al. 1999; Harrison 2001; Fonstad and Marcus 2010). For example, process geomorphology has historically focused on small scalar extents and fine grains. Form-based geomorphology has had a propensity to be applied at large extents and coarser grains. Ecologists work with a similar dichotomy, between the local extents in which mechanism can be investigated via controlled experiment and the extents of macroecology. Consequently, approaches to compare landforms and coupled abiotic-biotic processes have often been deployed in a segregated fashion. Process-oriented scalar extents and grains are not readily comparable to the scalar extents and grains of

form-based geomorphology. Comparing measurements from different scales has come to be perceived as reflective of an inherent and unwavering incommensurability.

While conceptual frameworks do have specific scalar extents and data resolutions in which they work better, picking one over the other as more important does not imply that other conceptual frameworks are not relevant and their representational entities of little use. By underfitting our comparisons, that is, relying only on a single paradigm and its ontological standard of representation to derive the data for assessing similarity, important information may be left out (Fonstad and Marcus 2010). Overfitting, as an implicit strategy of model of cross-scale resilience, works around some of the incommensurabilities of pattern comparison imposed by having to choose one best conceptual framework and its particular scalar domain. Given a high resolution dataset collected simultaneously over a broad area, observations can be partitioned into different, but not necessarily uncorrelated representational entities, each with their own particular scalar extents and resolutions affiliated with their conceptual underpinnings. In this overfitting approach that we develop here, multiple data representations and their conceptual paradigms can then be integrated and compared.

If the goal is to make spatial pattern comparisons using this this bottom-up assembly of data, a framework is needed to guide what data are selected and combined to insure that pattern and process are meaningfully integrated (Praskievicz 2018). In ecology, resilience theory, and a lineage of it, discontinuity theory, postulate a hierarchical, cross-scale structure of patterns and processes. Although not necessary to describe here, cross-scale structure incorporates the linkage of adaptive cycles into panarchies, the working units of resilience theory. What is useful for this study is that this cross-scale structure not only

provides a mechanism to integrate different ontologies of pattern across scales, but that it also provides a mechanism to account for the emergence of resilience properties. Cross scale ecological structure has been used to conceptualize the resilience properties of terrestrial and marine landscapes (Nash et al. 2014) as well as dunes (Stallins and Corenblit 2018, p. 85).

Cross-scale structure is formalized as an integration of specifically chosen variables, or metrics, of pattern. It reflects a parsimonious integration of local, individualistic variables with community and landscape processes over time and space (Feagin et al. 2005; Feagin and Wu 2007). Often, the term cross-scale is employed sloppily, as an unspecified quality that does nothing more than reflect the truism that pattern and process are linked across scales. In resilience theory, however, it is more formally mechanistic, and organized around compartmentalized but linked cycles of patterns and processes across scalar grains and extents. For coastal dunes, cross-scale structure initiates with cycles of deposition and erosion of sediment. Its expression as elevation at any particular point is a function of wind and wave energy as well as sediment availability. Geomorphic processes and instantaneous variables are applicable at this scale. With stabilization of sediments by plants, geomorphic processes and forms begin to change over larger extents. Biogeomorphic feedbacks between sediment accumulation and dune plant growth can lead to topographic modification and alteration of sediment transport over increasingly extensive areas. Cycles of plant population expansion and disturbance operate at this extent. The potential then exists for the development of a landscape in which geomorphic processes and ecological interactions are spatially integrated and reinforce one another in a positive feedback

indicative of domain dynamics. At this extent, landscape paradigms invoking spatially explicit patches, gradients, and geometry or configuration have more relevance.

Broad extent-high resolution data are well-suited for the derivation of cross-scaled data sets. LiDAR observations of ground elevation, for example, can cover kilometers at very high vertical and horizontal resolutions. These point data can then be aggregated, zoned, and summarized into various representational entities at the scalar extents associated with their particular conceptual paradigm. In this form of data modeling, multiple representations of topography, at different scalar extents, becomes a desired strategy rather than a practice to avoid. Formally, the lowest level in this cross-scale data structure for dunes is the relatively aspatial compositional measure of topography, elevation. For barrier islands, elevation captures the resistance to exposure to storm surge. Whether dunes are overtopped and storm surge penetrates inland is related to some threshold value of elevation. But mean elevation, as noted earlier, cannot fully represent landscape properties shaping the potential diffusion of overwash in back barrier habitats or the alteration of topographic roughness due to biogeomorphic feedbacks. Thus, it becomes necessary to represent spatial pattern as the size and shape of patches of specific ranges of elevation or the way in which elevation changes along a continuous gradient surface. These geometries of elevation expressed at larger extents, and the extent they form shore parallel features or more discontinuous features, are an aspect of barrier island dune topography that would be overlooked when only elevational statistics are used. Embedded in these landscape dune geometries is the potential development of biogeomorphic feedbacks linked to resilience properties. Through this scalar nestedness, domain-model dynamics

may develop that modulate resistance to overwash and promote the persistence of landforms and vegetation in a positive feedback.

Still, to compare cross-scale data from one location to another requires a technique that can distill the information embedded in cross-scale structure and simplify its interpretation. Given that the multiple metrics derived from LiDAR for a cross-scale data set are designed to be nested, they will have a degree of multicollinearity. We propose that through dimensionality reduction, the variance within this multicollinearity can be partitioned across different dimensions, or axes, in order to visualize how these metrics vary from location to location. We employed dimensionality reduction by ordination to compare topographies. Given that cross-scale structure also reflects the dynamic properties of topography, the visual results of ordination are a snapshot of state space (Inkpen and Petley 2001; Phillips 2009b; Baas and Nield 2010; Inkpen and Hall 2016). State space refers to Poincaréan ecological topologies, in which phenomena are mapped in an abstracted field space (Prager and Reiners 2009). These are typically plotted axes of a Cartesian coordinate system in order to give shape to state space. Conceptually, any single landscape should be capable of being located within a larger state space derived from multiple landscapes, or else expand the boundaries of this state space if it has not been encountered before. Our construction of topographic state space reflect the possible configurations of dune geomorphic and biogeomorphic phenomena. Of particular utility, however, is that the dimensionality of cross-scale data in state space is a means of comprehending resilience properties (Donohue et al. 2013, 2016; Stevens and Tello 2014, 2018; Stallins and Corenblit 2018). Lower dimensional axes represents geomorphic resistance. Higher dimensional axes represent formal resilience. Resilience, as a higher

dimensional property, emerges out of the resistance imparted at lower dimensions. Thus, where locations plot in topographic state space provides specific information not only about their topographic differences, but also about how their resistance and resilience prosperities differ.

### **3.3 Methods**

#### **3.3.1 Study area and sampling design**

The barrier island morphologies of the Georgia Bight are comprised of mixed-energy tide-dominated barrier islands toward its center and wave-dominated barrier islands along its outlying limbs in Florida and North Carolina. For these outlying coastlines, where tidal range is at a minimum and wave heights are high, most barrier islands are long and narrow. Toward the center of the Bight, where tidal range increases and wave heights diminish, barrier islands tend to be shorter and drumstick-shaped. Hayes (1994) compartmentalized the Georgia Bight islands into the wave-dominated barrier islands of the Outer Banks of North Carolina, the mixed tidal and wave energy barrier islands of South Carolina, the tide-dominated estuarine ‘sea islands’ of Georgia, and the more mixed-energy to wave-dominated barrier islands along the east coast of Florida. Many of the Georgia and South Carolina sea islands consist of fringing Holocene sediments that have welded to the Pleistocene core of the island under long-term conditions of sea-level rise. Dune topography was characterized on five islands: Cape Canaveral (Florida), Sapelo Island (Georgia), Bull Island (South Carolina), Kiawah Island (South Carolina), and South Core Banks (North Carolina). An additional island, Parramore Island (Virginia) was

sampled twice, as part of the Georgia Bight data and for the Virginia data set. Having two independent characterizations of topography provided a replicate to assess our methods.

The barrier island morphologies of Virginia and southern Maryland comprise the southern limb of the Atlantic Bight. The Atlantic Bight extends from the northern islands of North Carolina to Massachusetts. The Virginia Barrier Islands are a part of the Delmarva Peninsula. Sediments for Assateague Island in the north, a mixed-energy, wave-dominated barrier island, and for the mixed-energy, tide-dominated barrier islands to the south are derived from headland erosion at the northern extent of the peninsula (Oertel and Kraft 1994). Rates of relative sea level rise from New Jersey to North Carolina include some the highest along the US Atlantic coast (Gutierrez et al. 2007; Sallenger et al. 2012; Piecuch et al. 2018). Many of the Virginia islands have experienced pronounced reductions in barrier island upland area as a consequence of ongoing sea level rise (Zinnert et al. 2016b). The tide-dominated islands of Virginia are also smaller than their counterparts on the Georgia and South Carolina sea island coast. They are susceptible to back barrier areal loss and shoreline retreat (Deaton et al. 2017). Dune topography was characterized for seven islands and include, from north to south: Assateague Island, Metompkin Island, Cedar Island, Hog Island, Parramore Island, Wreck Island, and Ship Shoal Island.

Within each of these twelve islands, locations to characterize dune topography were determined by visually identifying from air photos in Google Earth the distinctive, predominant stretches of dune and beach topography. These stretches of coast are analogous to the fluvial unit of the river reach (Wohl 2018). Criteria to delineate locations included beach width, the width of the dune field, linearity of the dunes, and type of habitat behind dunes. Areas of pervasive human impact and locations directly on tidal inlets were

avoided. Three to five distinctive stretches of topography were required for each island. To sample dune topography within these stretches of predominant alongshore relief, we employed a natural sampling technique (Bissonette 2017). In this technique, the phenomena under study defined sampling extent. A square plot were randomly located within each distinctive reach of barrier island dune shoreline so that it initiated at the mean high water mark datum (MHW) and extended inland to where salt marsh or significant stabilized woody vegetation developed. Plot size was retained as an explanatory variable.

### 3.3.2 LiDAR data

Digital elevation models (DEMs) were constructed for sites along each island using LiDAR ground elevations available online from the NOAA's Coastal Services Center. Dune topographic metrics for islands in the Georgia Bight regional dataset were derived in an earlier study, Monge and Stallins (2016). These metrics utilized a 2010 LiDAR dataset collected by the United States Army Corps of Engineers for four of the islands. Vertical (horizontal) accuracy was 15 cm (75 cm) and nominal point space was 2 m. Due to small gaps in this 2010 dataset, topographic metrics for South Core Banks and Parramore Island were constructed from post-Hurricane Sandy LiDAR datasets collected by the U.S. Geological Survey in 2012. For these data, vertical (horizontal) accuracy was 7.5 cm (19.4 cm) and nominal point space was 1 m. A post-Hurricane Sandy 2014 data-set collected by the NOAA National Geodetic Survey was used to construct digital elevation model (DEM) plots for sites on the Virginia islands. Vertical (horizontal) accuracy was 6.2 cm (100 cm) and nominal point space was 0.3 m. LiDAR point elevations were resampled to a resolution of 1 m and then interpolated using inverse distance weighing to fill any gaps. LiDAR processing was performed in ArcGIS using LAStools (Isenburg 2014). The Virginia MHW



shoreline was defined as the 0.7 m contour line relative to the NAVD 88 datum following Rogers et al. (2015). The islands in the Georgia Bight and the replicate plots on Parramore were referenced to the MHW mark using VDatum (National Oceanic and Atmospheric Administration and National Ocean Service 2012). All of these DEM plots were then clipped along the edge coinciding with the MHW mark elevation of zero and rotated to a common orientation.

### 3.3.3 Topographic metrics

Three sets of topographic metrics were deployed to capture the cross-scale attributes of topography: elevational descriptive statistics, landscape patch indices, and spatially explicit metrics. These sets of metrics differed systematically in their degree of spatial explicitness, level of measurement, and association with patch or gradient paradigms. The first set of metrics, elevational descriptive statistics, were recorded as absolute values for vertical measurements summarized across the DEM for each island plot (mean, maximum, median, 25th percentile and 75th percentile elevations). Elevational statistics were defined as low dimensional metrics in our cross-scale data model. Elevation reflects the baseline geomorphic resistance of any point alongshore. It has a large influence on the extent of exposure or protection from high water events.

The second set of metrics, patch metrics, consisted of landscape indices produced from FRAGSTATS software (McGarigal et al. 2012). These higher dimensional metrics capture the initiation of spatially-organized structure arising from cyclical interactions between sediment mobility and vegetation. Because FRAGSTATS are designed to work with categorical observations, raster DEMs were converted into areal representation by reclassifying pixels into elevation intervals. Wu et al. (2017, p. 56) as well as Ryu and

Sherman (2014) illustrate the logic of how the patch structure of topography can be generated and measured with landscape indices. In these approaches, a patch is defined as an interval of elevations. To avoid derivation of FRAGSTATS descriptors without a process interpretation (Kupfer 2012), landscape indices with consistent ecologically meaningful value were prioritized, as identified by Cushman et al. (2008). This set of indices was then constrained to those well suited for discerning pattern- process relationships associated with foredune building and overwash. These indices were selected: the perimeter-area fractal dimension (PAFRAC), the area-weighted mean shape index (SHAPE\_AM), the aggregation index (AI), the landscape shape index (LSI), the largest patch index (LPI), the contagion index (CONTAG), the interspersion and juxtaposition index (IJI), and the Simpson's diversity index (SIDI).

AI increases with greater aggregation of patches. SHAPE\_AM increases as patches become more curvilinear. A higher IJI indicates that patch types are equally adjacent to all other patch types and are thus fully interdispersed. Higher LPI implies higher dominance of a single patch type within a dune plot. Higher SIDI implies higher patch richness and more equitable patch distribution within the plot. Higher PAFRAC implies all patch shapes within a plot tend to be convoluted. CONTAG increases as patches become larger and dominated by a similar elevation.

The third set of metrics, continuum metrics, summarized aspects of continuous spatial structure. As the highest dimensional metrics, these shape and are shaped by the geomorphic and biogeomorphic patterns represented in lower dimensional metrics. They included the skewness and kurtosis of point elevation values, the spatial autocorrelation structure of elevation, and plot size. Skewness and kurtosis of point elevation values

summarize trends in elevation across an entire DEM surface. Spatial autocorrelation was summarized in directional correlograms derived from the 1-m interpolated surface in GS+ software (Robertson 2000). These were constrained to the cross-shore direction (i.e., perpendicular to the water line). Autocorrelation was assessed up to the distance lag representing the width of the plot. Six Moran's  $I$  values from the major breaks along the plot of Moran's  $I$  were taken from each correlogram and ordinated with principal coordinates analysis (PCoA) in order to reduce correlogram structure into scatterplot coordinates that could be combined with the other dune topographic metrics. As a component of spatial pattern, autocorrelation captures the clustering or dispersion of observations rather than summarizing their boundary geometry as with FRAGSTAT indices. Lastly, the size of the plots, expressed as the length of an edge in meters, was included as a metric because this parameter is the constraint within which any topographic pattern would be confined.

#### 3.3.4 Statistical analysis

To construct state space, the cross-scale topographic metrics for the Georgia Bight region and the Virginia coast datasets were ordinated using non-metric multidimensional scaling (NMDS) separately and then as a combined data set. All topographic metrics were relativized as Z-scores. Similarity distances were Euclidean. The final solution was subjected to an orthogonal rotation to maximize variance in the data set along the first and succeeding axes. Monte Carlo randomizations of the observed data were used to gauge the significance of the reduction in stress and final dimensionality of the state space solution. Pearson's correlation coefficients were derived from plot coordinates of island sites along each NMDS axis and the values for the original topographic metrics. Hierarchical cluster

analysis of the final combined dataset was performed using a flexible beta group linkage method ( $\beta = -0.25$ ). Multiresponse permutation procedures (MRPP) quantified the similarities in topography across clustering levels. To complement NMDS, PCoA was also employed to derive a measure of the variance extracted for each state space axis. Ordinations, clustering and MRPP were performed in PC-Ord Version 7 (McCune and Mefford 2016).

### 3.3.5 Hypotheses

We posed the question as to whether the state space for the Virginia coast and for the Georgia Bight islands would exhibit differences in structure logically consistent with their known contrasts in nearshore settings. A comparison of these two well-studied coastal strands through their separately derived topographic state spaces would help gauge how well our cross-scale data modeling and state space methodology performed. However, by combining these two data sets and visualizing this larger topographic state space, more direct inferences could be made as to how topographies differ between these two regions. As a second question, then, we ask how the resilience properties (resistance and resilience) of the Georgia Bight and the Virginia coast might diverge. Given that there are the same types of barrier island morphologies in each of these coastlines, this second question asks how valid it is to assume that resistance and resilience correspond to island morphology.

Two aspects of the cross-scale structure were used to make comparisons of topography: the dimensionality of the ordinated data, and the way in which cross-scaled variables load on ordination axes (i.e., dimensions). The Georgia Bight has more varied nearshore conditions, barrier island morphologies, and dune topographies. Conditions here are not as consistently low and erosional as in Virginia. Consequently, we expected the

state space solution for the Georgia Bight would have a higher dimensionality because the topographic metrics would exhibit less multicollinearity. Higher-dimensional landscape metrics should be less correlated with elevation because of the potentially stronger influence of dune vegetation on the secondary modification of topography (e.g., Durán and Moore 2013). Because the Virginia Barrier Islands are experiencing some of the most rapid rates of retreat and sea level rise on the eastern US coast, there should be less resistance and resilience. Less resilience should translate to a lower state space dimensionality. Without some resistance to storm surge and overwash, biogeomorphic interactions that can promote the secondary modification of topography and confer resilience may not be as well developed. The exposed, low-lying topography of many of the Virginia Barrier Islands would be expected to foster a landscape structure more collinear with elevation derived directly from storm effects and overwash.

The seminal work on dune biogeomorphic feedbacks occurred well before the ascendance of resilience theory. It had a much broader comparative geographic focus (Godfrey 1977; Godfrey et al. 1979) than the more formal translations of resilience theory to barrier island dunes that came later. These were limited to a small set of observations on Sapelo Island, Georgia and South Core Banks, North Carolina (Stallins 2005). Resilience concepts have now been extrapolated to portions of Virginia coast (Brantley et al. 2014; Wolner et al. 2013; Zinnert et al. 2017). In dune topographic state space, the distribution of sampled dune plots from different island morphologies from a much larger geographic area will provide insight into the generalizability of the two-domain model to island morphology. It will also provide information on where we might expect geomorphic and ecological processes to maximize resilience.

### 3.4 Results

#### 3.4.1 Georgia Bight topographic state space

DEMs indicated three dominant topographies (Figure 3. 3): large areas of aggregated, low relief (Parramore Island); shore-parallel dune ridges and intervening swales (Kiawah B, Sapelo A, Canaveral D); and patchy, fragmented topographies (Kiawah A, South Core Banks C; Bull A). Directional correlograms for elevation reduced down to one significant axis through PCoA (Figure 3. 4). Autocorrelation varied from sites that tended to have no correlation at increasing distance lags (Kiawah D, Canaveral C) to sites that developed progressively more negative correlations at large distance lags (Parramore A, Sapelo C, Bull B).

The optimal NMDS solution required three dimensions, as derived from multiple NMDS runs that optimized starting configuration, stress reduction, and dimensionality (Figure 3. 5). Stress on all three axes was lower than that obtained from Monte Carlo randomization of the data (Table 3. 1). Dune topography differed on individual islands to the extent that some within-island topographies were more similar to those on more distant islands (i.e., Sapelo C and Parramore B or Bull A and South Core A). Stronger, robust Pearson's correlations for plot position relative to the first NMDS axis developed for elevational properties, the aggregation index, patch shape, and patch diversity (Table 3. 2). These correlations indicated that to the left of the state space scatterplot, islands become higher, and elevations become less aggregated and tend to vary over relatively shorter distances. Dunes were more rectilinear in shape. Toward the right on the first axis in the scatterplot, plot elevation decreases and becomes less variable over larger areas. Elevation patches become more aggregated and curvilinear in shape. Robust correlations for the

second axis were observed for the interspersion and juxtaposition index, the landscape shape index, spatial autocorrelation, and plot size. This indicated that island plots toward the top of state space are areally small and have smaller patches. No one single, large elevational patch interval dominates over the others. Spatial autocorrelation of elevation for these plots remains near zero at increasing distance lags because of the more variable topography. Plots toward the bottom of state space are bigger and patches are also larger and dominated by a single elevational range. Spatial autocorrelation of elevations becomes increasingly negative at greater distance lags, an indication of low, flat overwash topographies. The third axis exhibited a robust correlation only with skewness, a high dimensional metric.

#### 3.4.2 Virginia dune topographic state space

Virginia DEMs exhibited patchy, fragmented topographies (Assateague B, Wreck A and B; Cedar D. Ship Shoal C) as well as large, aggregated areas of low, flat topographies (Cedar A, Metompkin B, and Wreck D). Shore-parallel rectilinear ridges were weakly expressed and tended to occur as a single feature in the middle or rear of the site (Metompkin C, Hog A and C; Figure 3. 6). Directional autocorrelation of elevation reduced down to one significant axis in PCoA (Figure 3. 7). This axis represented a change from sites that exhibited increasingly negative correlations at higher distance lags (Wreck D, Cedar D) to those in which elevations became slightly positive and near zero with higher distance lags (Ship B, Hog B).

The optimal final NMDS solution required two dimensions (Figure 3. 8; Table 3. 1). The strength of axis correlations were weaker but more uniform across patch and continuous surface metrics than observed in the Georgia Bight dataset. The influence of

outliers in state space (Hog A) was also more pronounced. Robust correlations for the first axis included elevational properties and the aggregation index (Table 3. 3). The second axis tracked changes in plot size and the skewness and kurtosis of elevation. In general, to the left (right) of state space along the first axis islands become higher (lower) and elevations are less (more) aggregated. To the top (bottom) of the scatterplot, plots become smaller (larger), more negatively (positively) skewed, and more negatively (positively) kurtotic. This implies that Wreck D and Parramore B, for example, have a long tail of elevations skewed toward a few low elevations. For island sites like Hog A and Cedar E, the distribution of elevations is strongly peaked or narrow. Low elevations are most numerous and a long tail is in the direction of a few high elevations.

### 3.4.3 Combined dataset

Directional autocorrelation structure of elevation reduced down to one significant axis in PCoA (Figure 3. 9). Sites to the left along this single axis had Moran's  $I$  values that became strongly negative with larger distance lags (Kiawah C, Sapelo B, Wreck D). These topographies were broad and flat but had their peak in elevation near the middle of the plot. To the right of the first PCoA axis, Moran's  $I$  values became more positive or fluctuated around zero at larger distance lags (Bull A, Ship Shoal A, Hog A). These topographies were very poorly structured and had minimal topographic variability.

A two-dimensional NMDS solution was optimal (Figure 3. 10; Table 3. 1). When sites were hierarchically clustered into two groups, only two sites from the Georgia Bight, Kiawah A and Bull B from South Carolina, fell within the group dominated by the Virginia Barrier Islands. Several sites from Virginia were clustered within the Georgia Bight data, including those from Metompink, Hog, Assateague, and Wreck. The topographies for



Parramore Island that were sampled separately plotted close to one another, a validation of the methods employed.

The first axis was structured by trends in elevation and FRAGSTATS indices (Table 3. 4). To the right of the scatterplot, elevations are lower and topographic homogeneity increases. To the left, elevations are higher and topography becomes more rectilinear and variable over small distances on the surface. The second axis correlations were more strongly robust for kurtosis, the landscape shape index, and plot size. Toward the top (bottom) of state space, the extent of the dune landscape become smaller (larger), patches of elevation are less (more) dominated by a single elevation interval, and elevation values have a less (more) less peaked distribution of elevations.

Clustering at the level seven groups (Figure 3. 10) separated dune topographies along the second axis. The variability in topography expressed along the second axis is largely contained within islands of the Georgia Bight. MRPP indicated increasing robustness of statistical significance for topographic clusters from two up to seven groups (Table 3. 5). With higher groups, individual plots comprised clusters and statistical significance could not be assessed.

## **3.5 Discussion**

### **3.5.1 Individual state spaces**

The topographic state space for the Georgia Bight and for the Virginia Barrier Islands had data structures that reflected their nearshore contexts. Fewer dimensions were sufficient to define the state space of the Virginia Barrier Islands. Correlations of the topographic metrics with axis positions were weaker and more uniform, a reflection of the

greater multicollinearity contained within Virginia's two-dimensional solution. Spatial structuring was poorly developed. The aggregation index, the kurtosis or peakedness of elevation observations, and plot size were the only higher dimensional landscape metrics with explanatory relevance for the Virginia Barrier Islands. In contrast, the Georgia Bight dataset had a higher dimensionality. Axis correlations were not as uniformly weak, and they tended to differentiate across the three-dimensional solution. In both data sets, elevational properties comprised the dominant first axis of variability. However, metrics representing spatial structuring at landscape extents were less collinear with elevation for the Georgia Bight topographies. Here, patch and gradient metrics more strongly separated out along higher dimensional axes. On the Virginia Barrier Islands, elevation was mostly collinear with topographic metrics for spatial structure along the first axis.

### 3.5.2 Combined state space

The Virginia dataset occupied a mostly separate area in the combined state space. Tide-dominated island morphologies in Georgia and South Carolina plotted in a region of state space distinct from those in Virginia, indicating that this island morphology has different dune topographies based on location. The rapid rates of sea level rise along the mid-Atlantic barrier islands of Virginia and differences in island size can account for this separation of tide-dominated island morphologies in state space. Tide-dominated barrier islands are more strongly influenced by their adjacent tidal inlets than wave-dominated islands. These inlets are sources and sinks for sediments that shape adjacent shorelines. Compared to the larger sea islands of Georgia and South Carolina, the smaller, rapidly eroding barrier islands of Virginia like Cedar and Ship Shoal may have greater variability in alongshore depositional and erosional conditions as a consequence of the relatively

closer proximity of tidal inlets. The difference in dune topographies among wave-dominated island morphologies was less pronounced. Assateague Island, a wave-dominated barrier island on the Virginia-Maryland shore, had more similarities to the wave-dominated morphologies of the Georgia Bight and plotted closer to South Core Banks in state space.

Because of the variability in topography within islands, centroids derived from the average of an island's plot positions in state space may be a better way to infer resilience properties (Figure 3. 11). Sankaran et al. (2018) argue that this coarsening is necessary to detect resilience properties when spatial properties are assessed. The greater dispersion of island centroids along the first axis suggests that resistance is a more dominant property than resilience. Centroid positions relative to the second axis suggest that domain dynamics may develop at intermediate elevations along the middle of the first axis. Assateague and South Core may exemplify where overwash- reinforcing, biogeomorphic feedbacks and topography can contribute to a high resilience state. Conversely, Sapelo, Kiawah, and Bull Islands may represent state space positions with higher resilience expressed through overwash-resisting topographies. The centroids for the Virginia Barrier Islands were lower in elevation and did not separate out as strongly along the second axis. These Virginia Barrier Islands likely represent locations where resistance is lower and strong biogeomorphic feedbacks over landscape scales would be less likely to develop and persist.

Figure 3. 12 summarizes regions of resistance and resilience in topographic state space relative to island centroids. Under the assumption that resistance and resilience are correlated with each other and covary geographically (Donohue et al. 2013, 2016; Stallins and Corenblit 2018), the first axis spans the high elevations of the Cape Canaveral sites

next to the Florida mainland, to the low elevation Ship Shoal sites in Virginia. Little biogeomorphic resilience may develop at either of these extremes, as overwash and geomorphic disturbance are too frequent (Ship Shoal) or too infrequent (Canaveral) to allow the self-organizing biogeomorphic feedbacks to develop. Only at intermediate elevations along the middle of this first axis do the higher-dimensional properties of resilience emerge along the second axis. Higher resilience is expressed at more negative (overwash-reinforcing) and more positive (overwash-resisting) axis positions. Speculatively the middle region may be dynamically unfavored or a bistable state space region where one or the other high resilience state can develop (Stallins, 2005; Goldstein and Moore 2016). While aspects of this state space model have been postulated (Monge and Stallins 2016; Stallins and Corenblit 2018), here they have been validated from observations of topography over a wide geographic area.

### 3.5.3 Island morphology and resilience properties

The dominant axis of variability in topographic state space was elevational. It did not reflect island morphology. Instead, the two main barrier island morphological types were distributed at varied positions along this first axis based on the specific elevational properties of the within-island sites. Tide-dominated island morphologies were found all along the length of this axis, at different elevations. Insofar as it determines resistance, island morphology may be less important than these measures of elevation along the first axis, as they more directly shape exposure to maritime inputs (e.g., Durán and Moore 2015). The second axis, however, brought out distinctions in island morphology. Topographies distributed along the second axis spanned mixed-energy, tide-dominated barrier islands to wave-dominated barrier dune landscapes. Higher axes and increasing

dimensionality represent increasing resilience. Consequently, island morphology may be important for the potential development of resilience, but it is secondary to elevation. However, state space structure suggested that this resilience was dependent upon resistance. Only at intermediate elevations did the spatial topographic patterns affiliated with each of these two barrier island morphologies become distinct. These two regions of state space, at either end of the second axis at intermediate elevations, may correspond to the high resilience that has been categorically associated with island morphology. Most of these high resilience islands were from the Georgia Bight. Islands in Florida and Virginia may be too high and too low relative to overwash-forcing events, respectively, for island morphology to have any relationship to the emergence of landscape-scale biogeomorphic resilience.

The actual values of the metrics correlated with the second axis at intermediate elevations may be prerequisites for the development of biogeomorphic resilience properties. Overwash-resisting domain dynamics may have a greater propensity to develop on dunes of tide-dominated morphologies that are neither extremely high nor low, and in which the dune landscapes have relatively small areal dimensions and a less peaked distribution of elevations that form small, disaggregate rectilinear patches. This combination of metrics reflects a greater topographic roughness compacted into a small area. Overwash-reinforcing domain dynamics may have a greater propensity to develop on wave-dominated barrier island morphologies with intermediate elevations, particularly when a more peaked distribution of elevations is dispersed over a larger area and elevation patches are also large and aggregated.

Still, these parameters are only a propensity for the development of resilience. Intermediate mean elevations in this study are approximately  $1.2 \pm 0.5$  meters. Such a value should not be taken as an automatic predictor as to whether resilience is high or low at any one particular site. Any conception of an intermediate elevation and exposure to maritime inputs has to be assessed relative to the life history traits of the dune vegetation present at a site. With a shift in the abundance of dominant dune grasses (Harris et al. 2017; Goldstein et al. 2018) resilience properties may change without the external forcings that are often associated with such transitions. Dune ridges, and hence elevation properties, can also form in the absence of changes in external forcings (Moore et al. 2016). Sediment budget and the timing of coastal storms also have a strong influence on stability and persistence of dunes (Psuty and Silveira 2010; Houser et al. 2015). These factors also suggest that resilience properties for barrier dunes may be more dynamic and changing in space than presently theorized (e.g., Génin et al. 2018; Phillips 2018)

### **3.6 Conclusion**

Aeolian and marine, nearshore and terrestrial, geologic and meteorological, historical or present-day – the controls on barrier island dunes are diverse and expressed at multiple interacting scales (Hapke et al. 2016; Moore et al. 2016; Walker et al. 2017; Wernette et al. 2018a). Process-based (e.g., Hesp et al. 2005; Davidson-Arnott et al. 2018) and form-based approaches (e.g., Short and Hesp 1982; Mitasova et al. 2012) for describing and comparing dunes involve different selections of variables, contrasting representations, and preferences for certain measurement levels and degrees of spatial explicitness. Along with numerical modeling, this range of approaches suggests that no stand-alone route to knowledge generation exists. The approach taken in this paper was to assemble the cross-

scale data structure of dune landscape using high resolution broad extent observations of elevation. This data modeling technique fused different pattern-process paradigms and their representational entities. Topographic forms were then compared in state space in order to infer their resilience properties.

Topographic state space for the Virginia and Georgia Bight barrier islands exhibited differences in data structure logically in agreement with their known contrasts in nearshore context. Most of the island sites from Virginia did not fit within the topographic state space of the Georgia Bight islands. Their resilience properties also differed, largely because of the lower elevations and lowered resistance in Virginia. At very low (high) barrier island elevations, resilience may not be not as well developed because storm exposures and overwash may be too frequent (infrequent) to facilitate the persistence of biogeomorphic feedbacks shaping resilience. Resilience may even be relatively uncommon and limited to certain dune locations. It developed only at intermediate elevations in topographic state space. The relatively large size of state space in comparison to where potentially high resilience developed also suggests that these stabilizing biogeomorphic feedbacks may be more contingently expressed. Although earlier studies affiliated resilience with barrier island morphological types, this study has shown that the process-form context of island morphology may be only a secondary factor to the development of resilience.

The findings of this study are limited in that only topography was sampled, and vegetation was not, even though they are highly interactive on coastal dunes. Construction of a state space in terms of the plant functional types and examination of how it correlates with topographic state space would be the next step in affirming these inferences about the geographic distribution of resistance and resilience. To elucidate more about the

mechanisms that shape resilience via plant influences on topography, selecting sites and/or islands based on their intervening distances along the second axis in state space and position relative to intermediate elevations may be an efficient strategy for selecting where to sample in the field and to conduct field-based experiments.



**Table 3. 1** Dimensionality, stress, and variance extracted for each state space visualization. All values significant ( $p < 0.01$ ) based on Monte Carlo permutations of the observed data.

|   | Axis 1 | Axis 2 | Axis 3 | Final stress or variance extracted |
|---|--------|--------|--------|------------------------------------|
| Virginia state space (n = 30 plots)     |        |        |        |                                    |
| Stress                                  | 42.0   | 13.7   |        | 11.5                               |
| Variance                                | 43.7   | 22.2   |        | 65.8                               |
| Georgia Bight state space (n =22 plots) |        |        |        |                                    |
| Stress                                  | 45.6   | 15.5   | 5.1    | 4.5                                |
| Variance                                | 40.6   | 27.9   | 15.0   | 83.5                               |
| Combined state space (n = 52 plots)     |        |        |        |                                    |
| Stress                                  | 41.8   | 12.8   |        | 11.1                               |
| Variance                                | 48.6   | 20.7   |        | 69.3                               |

**Table 3. 2** Pearson's correlation coefficients for plot NMDS axis coordinates and topographic metrics for the Georgia Bight. Correlations deemed important were  $> 0.70$  and not influenced by outliers (shown in bold).

| Topographic metric               | Axis 1       | Axis 2       | Axis 3      |
|----------------------------------|--------------|--------------|-------------|
| Mean elevation                   | <b>-0.89</b> | -0.26        | -0.29       |
| Max elevation                    | -0.56        | -0.22        | 0.19        |
| 25th percentile elevation        | <b>-0.71</b> | -0.62        | -0.23       |
| 50th percentile elevation        | <b>-0.80</b> | -0.33        | -0.45       |
| 75 percentile elevation          | <b>-0.88</b> | -0.02        | -0.37       |
| Aggregation index                | <b>0.89</b>  | -0.17        | -0.35       |
| Contagion                        | 0.59         | -0.66        | 0.05        |
| Interjuxtaposition               | -0.56        | <b>0.74</b>  | 0.11        |
| Large patch index                | 0.57         | 0.52         | 0.05        |
| Landscape shape index            | -0.33        | <b>-0.87</b> | 0.15        |
| Perimeter-area fractal dimension | -0.60        | -0.14        | 0.31        |
| Mean shape index                 | <b>0.78</b>  | -0.39        | -0.34       |
| Patch diversity                  | <b>-0.80</b> | 0.27         | -0.30       |
| Skewness of point elevations     | -0.12        | 0.16         | <b>0.87</b> |
| Kurtosis of point elevations     | -0.03        | -0.66        | 0.68        |

Table 3. 2 (Continued)

| Topographic metric                               | Axis 1 | Axis 2       | Axis 3 |
|--|--------|--------------|--------|
| Directional spatial autocorrelation of elevation | -0.17  | <b>-0.75</b> | 0.59   |
| Plot size  | 0.17   | <b>-0.93</b> | -0.13  |

**Table 3. 3** Pearson's correlation coefficients for plot NMDS axis coordinates and topographic metrics for Virginia Barrier Islands

| Topographic metric               | Axis 1       | Axis 2       |
|----------------------------------|--------------|--------------|
| Mean elevation                   | <b>-0.91</b> | -0.24        |
| Max elevation                    | -0.64        | -0.65        |
| 25th percentile elevation        | <b>-0.70</b> | -0.17        |
| 50th percentile elevation        | <b>-0.85</b> | -0.08        |
| 75 percentile elevation          | <b>-0.95</b> | -0.14        |
| Aggregation index                | <b>0.80</b>  | 0.15         |
| Contagion                        | 0.64         | -0.65        |
| Interjuxtaposition               | -0.66        | 0.33         |
| Large patch index                | 0.63         | -0.02        |
| Landscape shape index            | -0.60        | -0.59        |
| Perimeter-area fractal dimension | -0.62        | -0.15        |
| Mean shape index                 | 0.65         | -0.44        |
| Patch diversity                  | <b>-0.81</b> | -0.04        |
| Skewness of point elevations     | 0.04         | <b>-0.77</b> |
| Kurtosis of point elevations     | 0.39         | <b>-0.74</b> |

Table 3. 3 (Continued)

| Topographic metric                               | Axis 1 | Axis 2       |
|--|--------|--------------|
| Directional spatial autocorrelation of elevation | 0.14   | -0.38        |
| Plot size  | 0.06   | <b>-0.78</b> |

**Table 3. 4** Pearson's correlation coefficients for plot NMDS axis coordinates and topographic metrics for the combined data set

| Topographic metric                  | Axis 1       | Axis 2       |
|-------------------------------------|--------------|--------------|
| Mean elevation                      | <b>-0.89</b> | -0.27        |
| Max elevation                       | -0.67        | -0.58        |
| 25th percentile elevation           | <b>-0.70</b> | -0.40        |
| 50th percentile elevation           | <b>-0.86</b> | -0.19        |
| 75 percentile elevation             | <b>-0.92</b> | -0.14        |
| Aggregation index                   | <b>0.87</b>  | 0.07         |
| Contagion                           | <b>0.80</b>  | -0.50        |
| Interjuxtaposition                  | <b>-0.71</b> | 0.37         |
| Large patch index                   | <b>0.73</b>  | 0.10         |
| Landscape shape index               | -0.49        | <b>-0.70</b> |
| Perimeter-area fractal dimension    | -0.68        | -0.16        |
| Mean shape index                    | <b>0.78</b>  | -0.25        |
| Simpson's index for patch diversity | <b>-0.85</b> | -0.01        |
| Skewness of point elevations        | 0.15         | -0.54        |
| Kurtosis of point elevations        | 0.40         | <b>-0.72</b> |

Table 3. 4 (Continued)

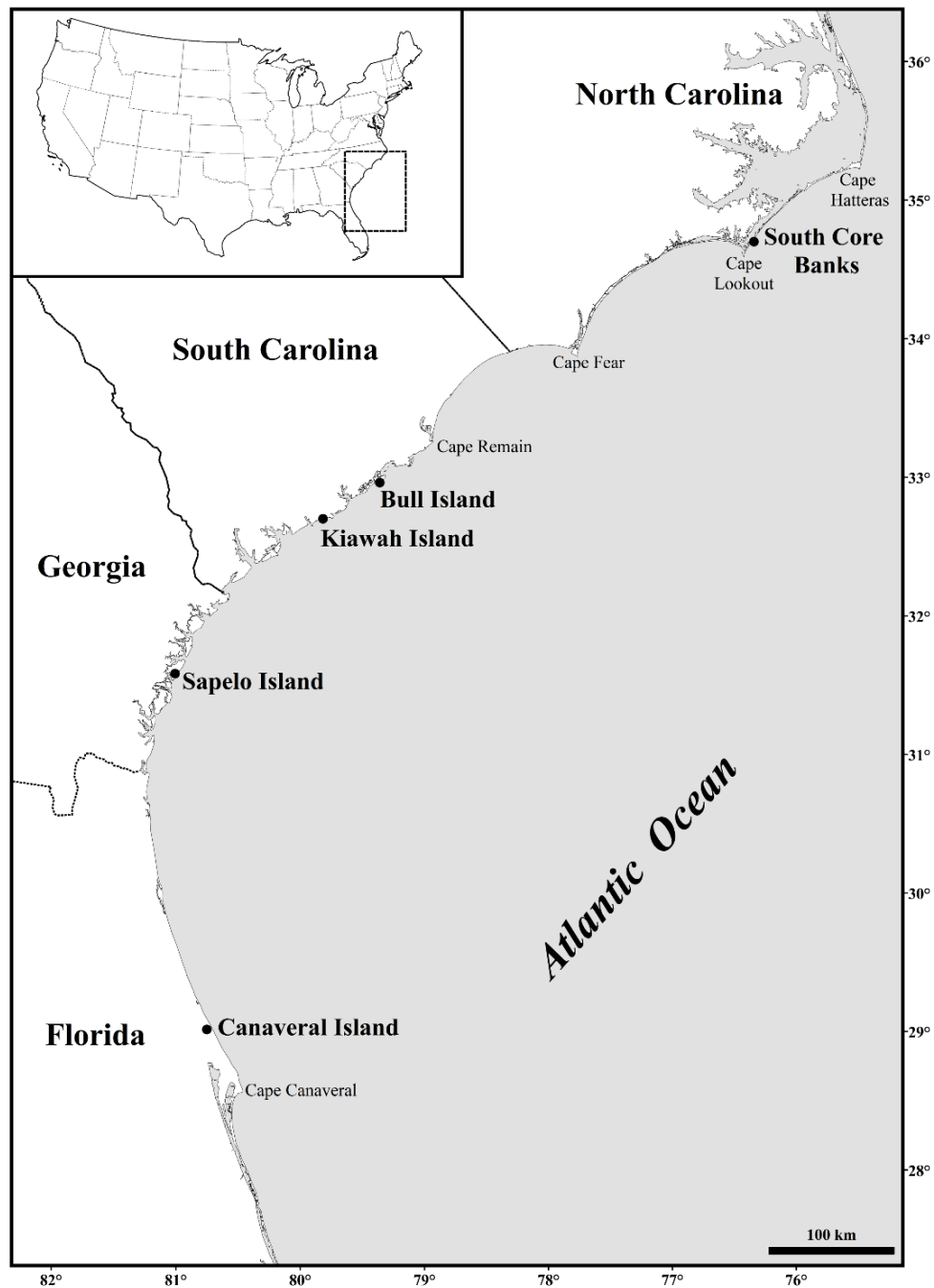
| Topographic metric                               | Axis 1 | Axis 2       |
|--|--------|--------------|
| Directional spatial autocorrelation of elevation | 0.12   | -0.61        |
| Plot size  | 0.32   | <b>-0.74</b> |

**Table 3. 5** MRPP tests of group difference for each cluster solution. All tests significant  $p < 0.01$

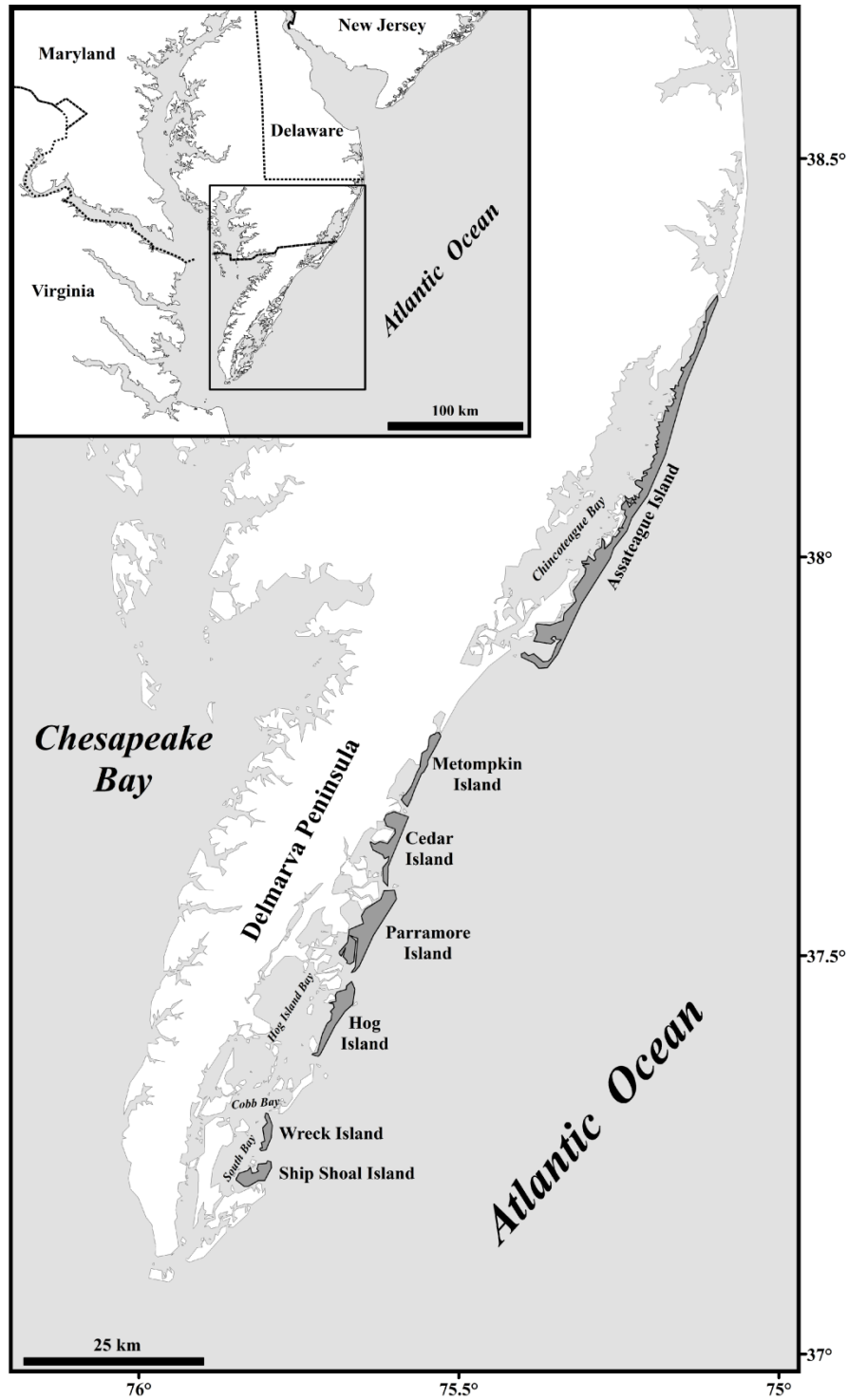
| Grouping   | T      | A    |
|------------|--------|------|
| 2 Clusters | -22.97 | 0.17 |
| 3 Clusters | -17.70 | 0.22 |
| 4 Clusters | -15.44 | 0.25 |
| 5 Clusters | -15.40 | 0.28 |
| 6 Clusters | -16.52 | 0.32 |
| 7 Clusters | -16.98 | 0.36 |

Note: T describes the separation between clusters. Higher A values are indicative of greater confidence in the significance. Values of A closer to zero indicate differences no greater than expected by chance.

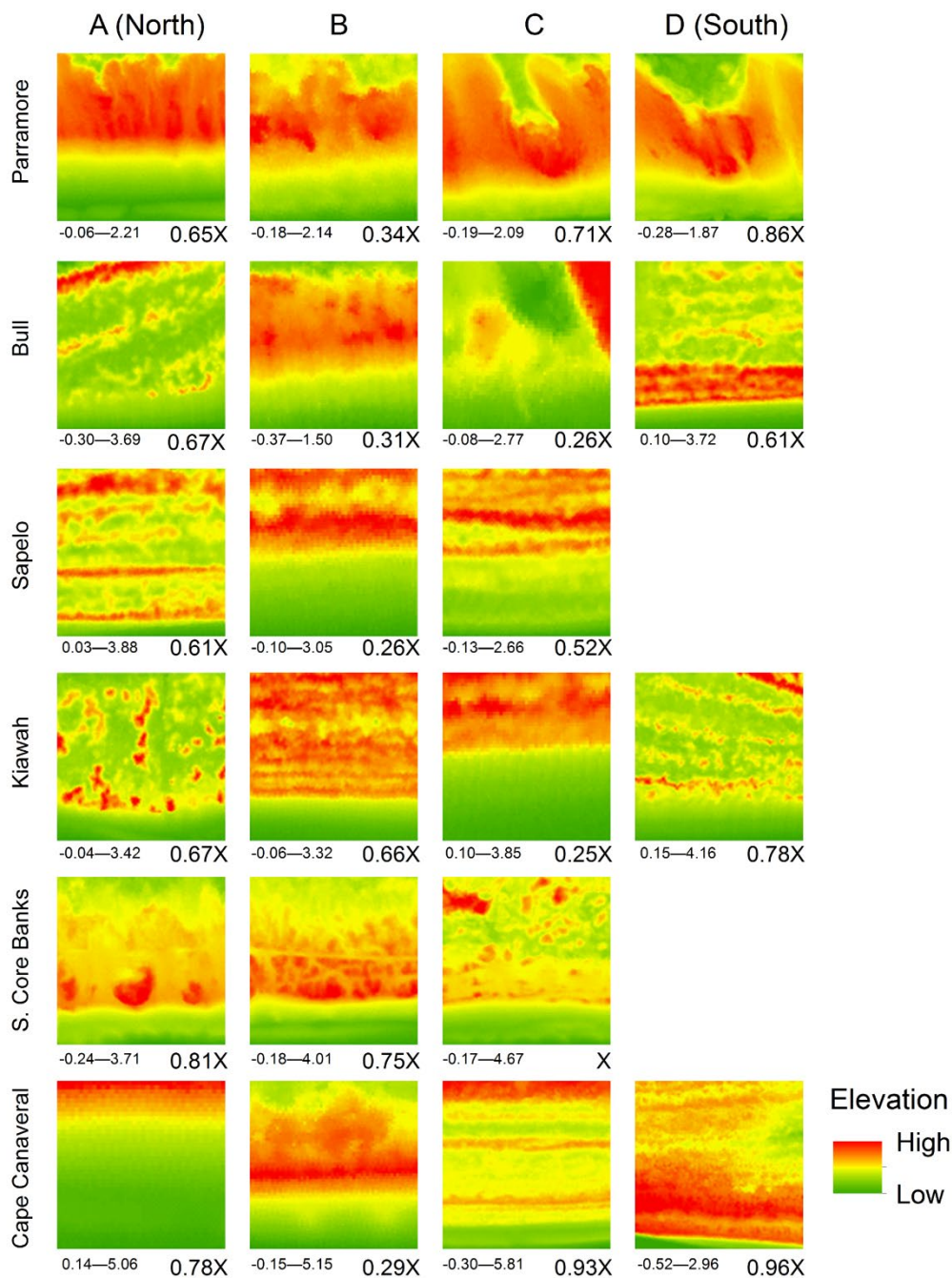




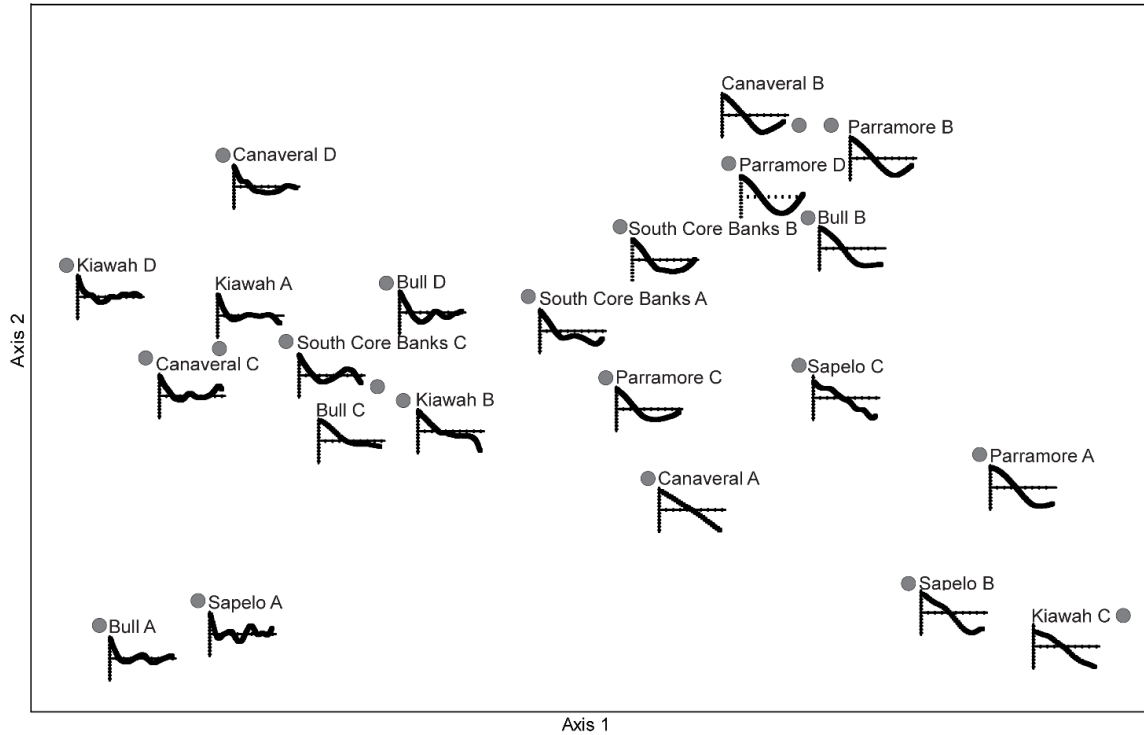
**Figure 3. 1** Regional map of coastline of the southeastern USA. The region covered in this study is located between Cape Hatteras, North Carolina, and Cape Canaveral, Florida (the Georgia Bight). Dune topographies on six islands in this region were selected for examination. These islands are, in order from north to south: South Core Banks, Bull Island, Kiawah Island, Sapelo Island, and Canaveral Island.



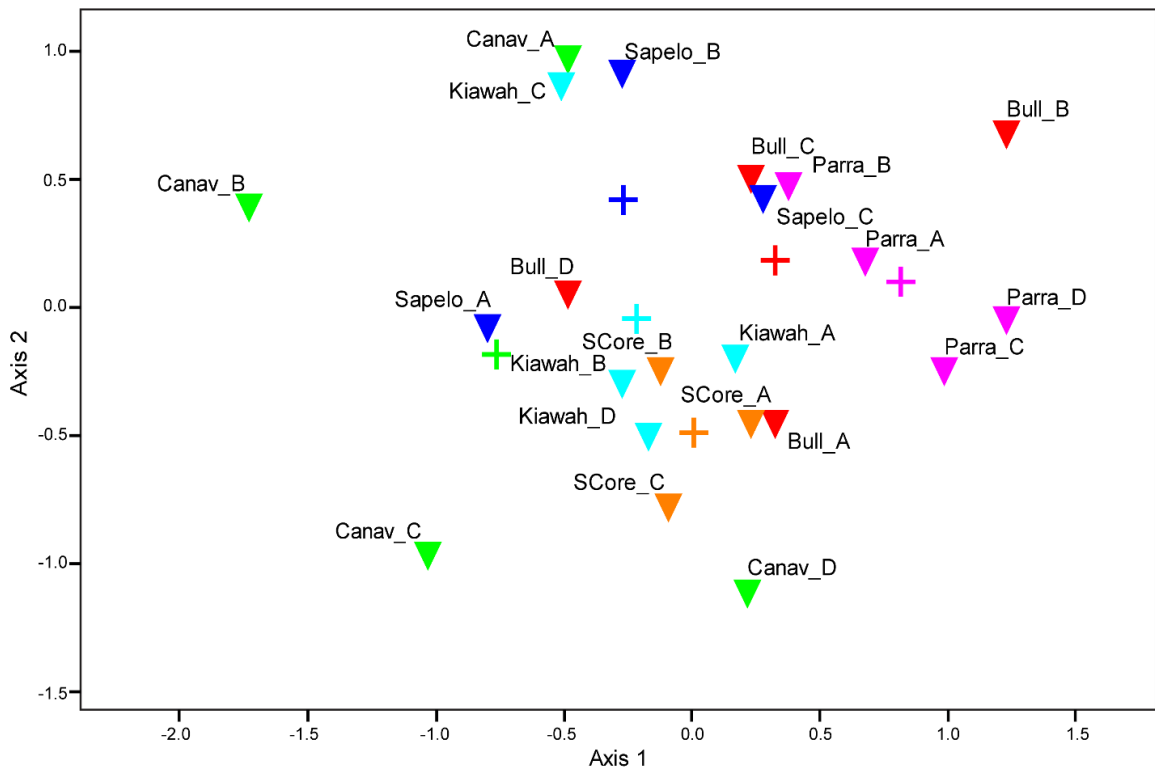
**Figure 3. 2** Map of coastline, spanning from Maryland to the Delaware Peninsula. Dune topographies on seven islands in this area were selected for examination. These islands are, in order from north to south: Assateague Island, Metompkin Island, Cedar Island, Parramore Island, Hog Island, Wreck Island, and Ship Shoal Island.



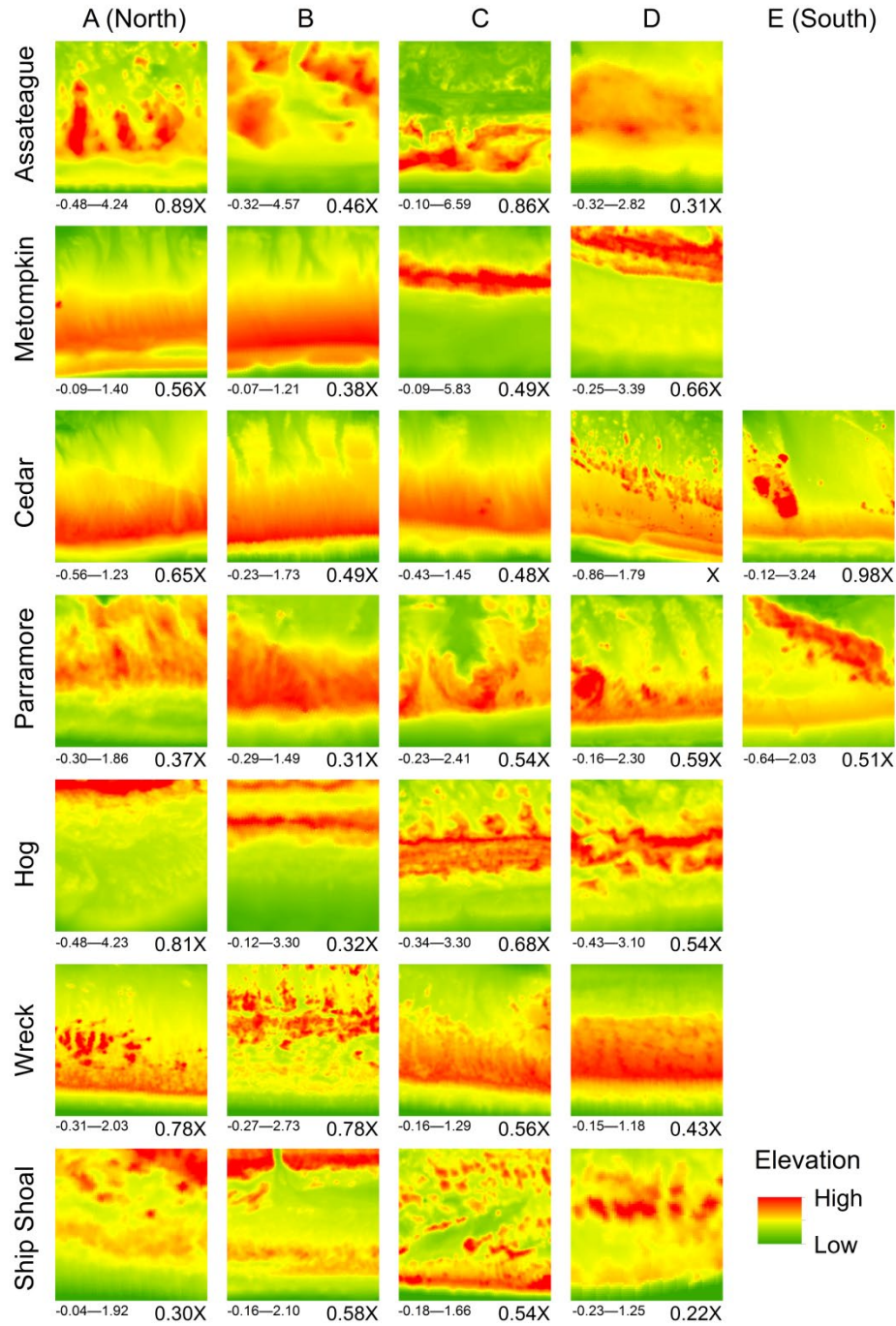
**Figure 3.** 3 DEMs for study plots along the Georgia Bight, scaled to local minimum and maximum elevations. Letters indicate position along the island from A (northernmost) to D (southernmost). Island plots differed in size, although they are scaled to be the same here. The conversion factors below each raster can be used to derive an island’s plot size relative to the largest island plot, South Core Banks C (215 m by 215 m). For example, the actual dimensions of plot C on Sapelo Island are 112 m by 112 m ( $0.52 \times 215 \text{ m} = 111.8 \text{ m}$ ).



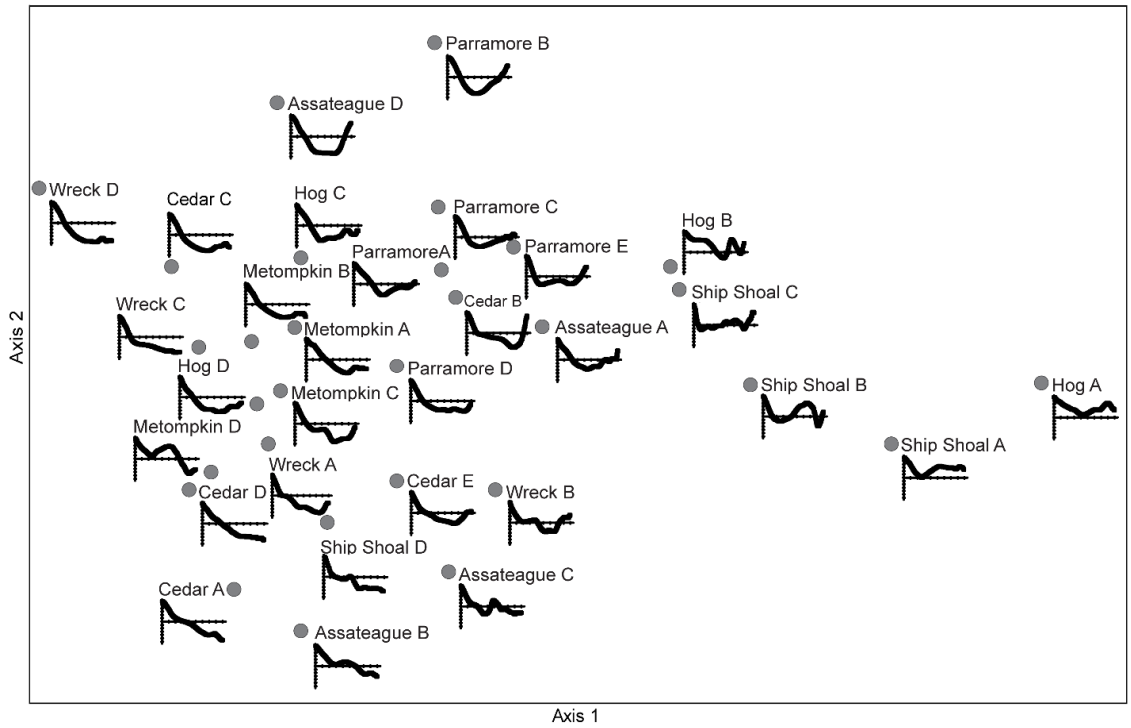
**Figure 3. 4** PCoA scatterplot of directional spatial autocorrelation structure for the Georgia Bight plots.



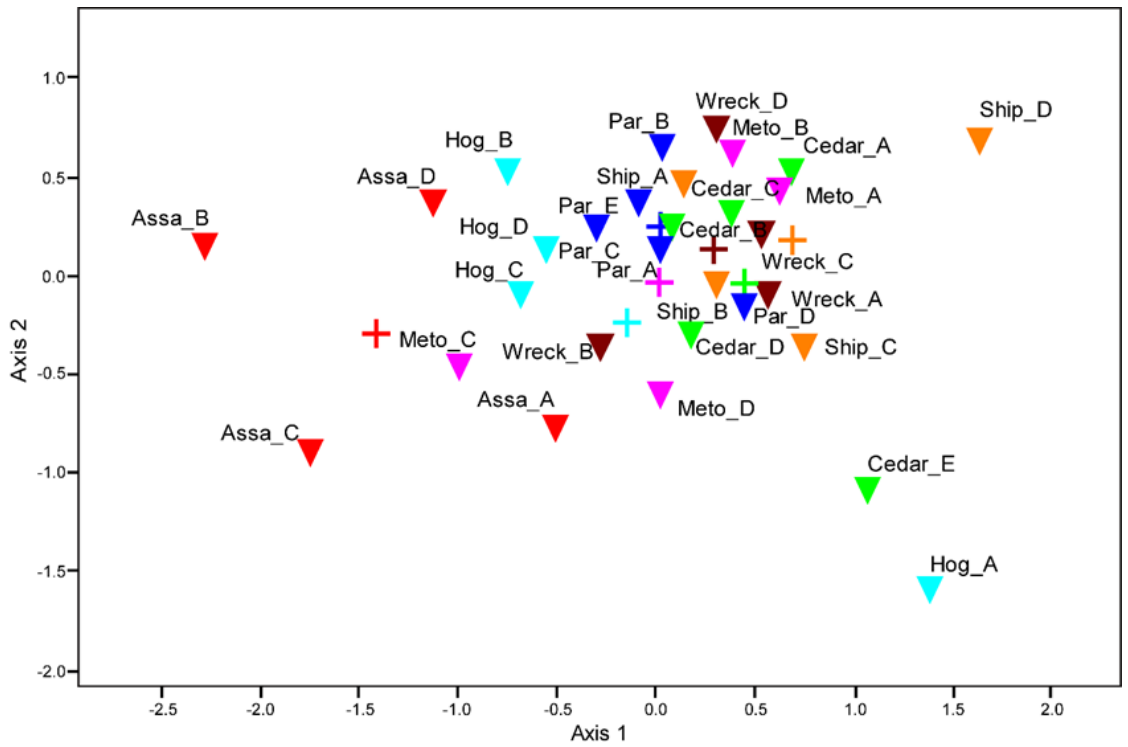
**Figure 3. 5** NMDS topographic state space for Georgia Bight DEM plots.



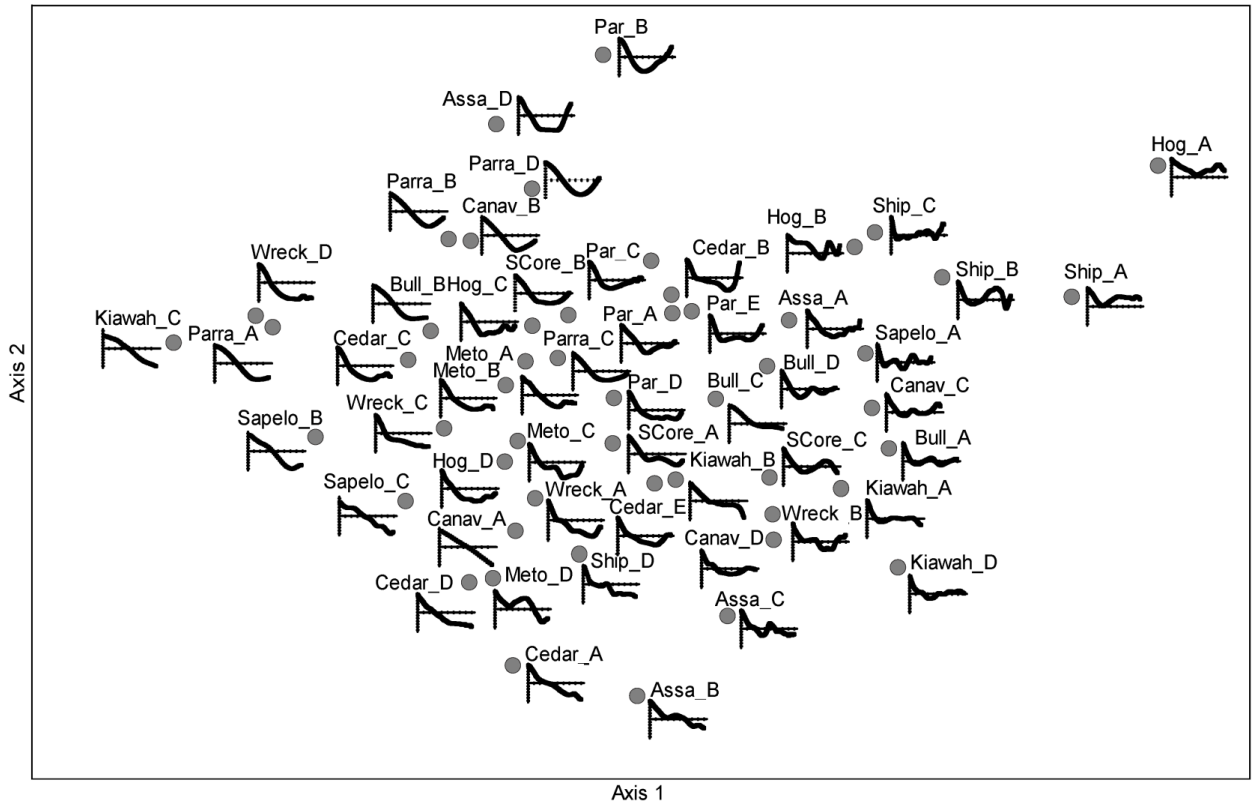
**Figure 3. 6** DEMs of Virginia study plots, scaled to local minimum and maximum elevations. See Figure 3. 5 for explanation. The largest island plot is Cedar D (295 m by 295 m).



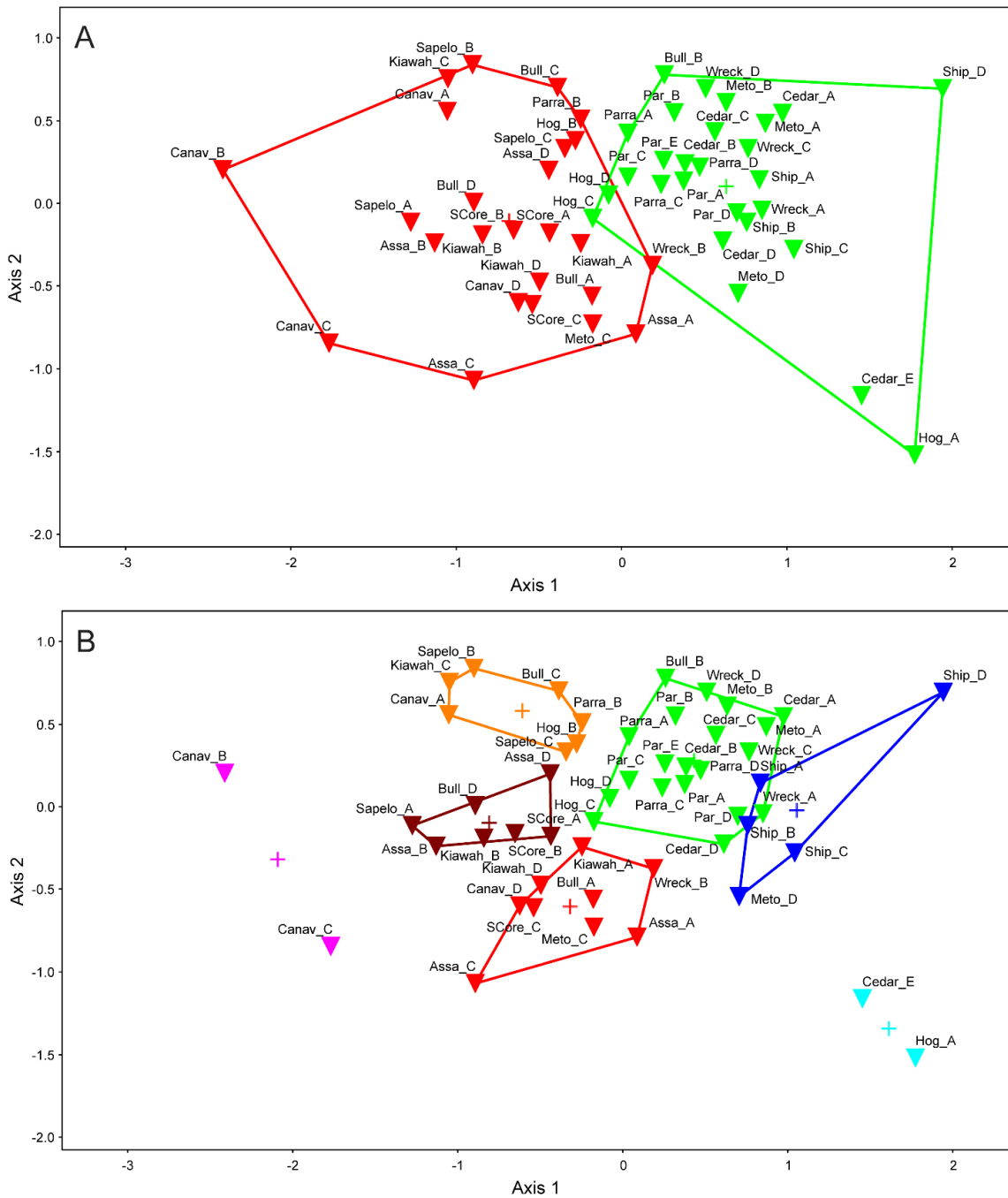
**Figure 3. 7** PCoA scatterplot of directional spatial autocorrelation structure for Virginia plots.



**Figure 3. 8** NMDS topographic state space for Virginia DEM plots.

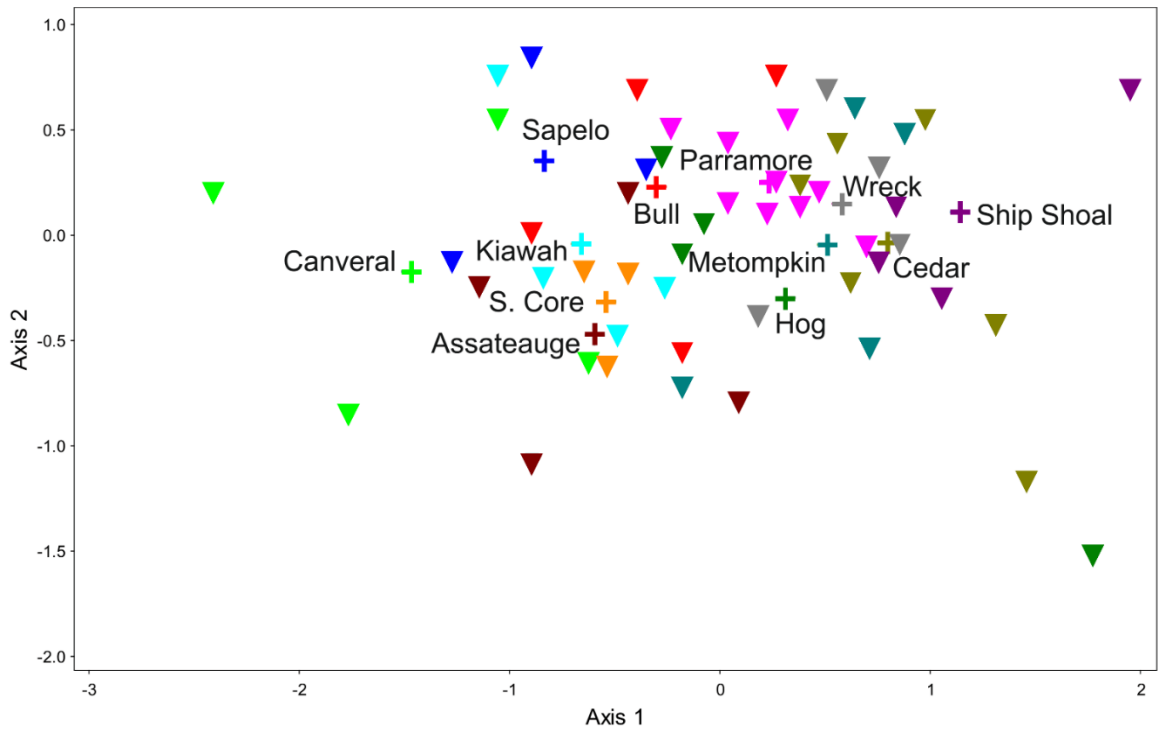


**Figure 3. 9** PCoA scatterplot of directional spatial autocorrelation structure for the combined dataset.

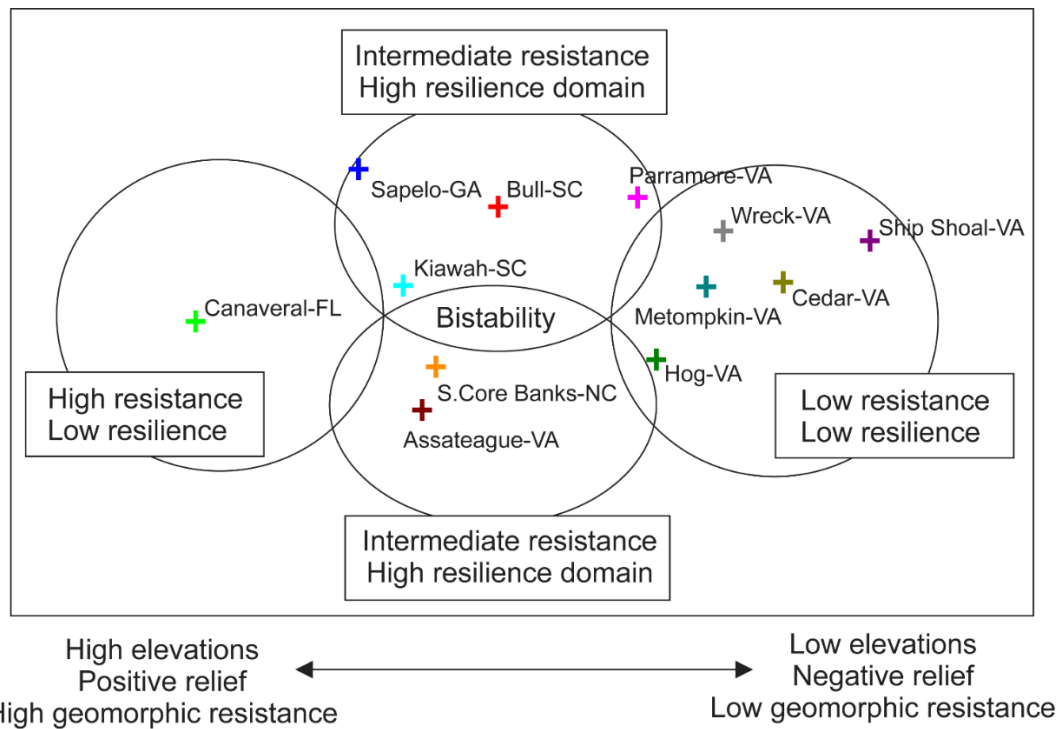


**Figure 3.10** NMDS topographic state space for the combined dataset. A) two-cluster solution, B) seven-cluster solution.





**Figure 3. 11** NMDS topographic state space for the combined data set based on island centroids.



**Figure 3. 12** Summary of resilience properties in barrier island dune topographic state space.

## **Chapter 4. Delineation of geomorphic and biogeomorphic resistance and resilience in barrier island dunes using cross-scale modeling and state space visualization**

### Abstract

Resilience properties have been ascribed to coastal dunes by invoking the idea of stability domains. However, the relative levels of resistance and resilience, and how they vary geographically in light of geomorphic and biogeomorphic controls, has not been fully documented. This study uses cross-scale modeling and state space visualization to delineate the geomorphic and biogeomorphic contributions to resilience properties for dune topographies on twelve barrier islands of the U.S. southeast Atlantic coast. Three sets of dune topographic metrics (elevational statistics, patch indices, and the continuous surface properties) were integrated for fifty-two plots distributed evenly across all of these study islands. Data were selected so that dimensionality reduction through nonmetric multidimensional scaling would produce a solution in which position in this state space reflected topographic similarity among sites as well as the relative importance of resistance, resilience, and the contribution of geomorphic versus biogeomorphic processes. The above resilience properties in this study are measured through variability in topographic metrics that present corresponding adaptive cycles and panarchies in the barrier dune system. The dimensionality of the ordination and loading for each variable on significant axes was used to quantitatively delineate the resilience property distribution in state space. Low-dimensional geomorphic metrics for topography were associated with a gradual transition from high, positive to low, negative relief island sites. At higher dimensions in state space, potentially larger threshold transitions developed between islands that differ in the continuous surface properties of the landscape. Topographic metrics correlated with both

dimensions conveyed how a higher islands can enhance the level of contagion reflected in its landscape topography to that of a low island via biogeomorphic processes. Conversely, metrics spanning both dimensions conveyed how low islands may reduce contagion to that of a higher island by creating greater topographic roughness via vegetation-enhanced dune and swale topography. Greater attention to topographic complexity and adoption of a cross-scaling approach may provide more evidence of multiple kinds of transitions in dunes and how geomorphic and biogeomorphic properties contribute to them.

#### **4.1 Introduction**

Dune plants play a large role in how sandy coastal strands respond to and recover from high water events (Durán and Moore 2013, 2015). While the frequency and intensity of forcing phenomena such as tropical and extratropical storms shape dune responses and recovery (Houser et al. 2015), biogeomorphic processes also play a role. Through their growth forms and adaptations to burial, dune vegetation can modify topography and in turn shape how sediments and water flow across the surface (Feagin and Wu 2007; Feagin et al. 2015, 2019; Zinnert et al. 2017). These biogeomorphic feedbacks can promote topographic conditions and plant functional abundances that may resist or reinforce exposure to overwash disturbance and canalize post-storm development (Stallins 2005; Wolner et al. 2013; Brantley et al. 2014). However, the study of these biogeomorphic feedbacks has been constrained to small stretches of coast or a couple of islands. Moreover, the formal resilience properties that these biogeomorphic interactions promote have not been quantified with variables that represent their spatially-interactive, scalar complexity. Nor has the relative importance of geomorphic and biogeomorphic properties in shaping transitions in dune states been examined in an explicitly geographical manner.

In this study, we delineated geomorphic and biogeomorphic contributions to dune topography on barrier islands from across the U.S. southeast Atlantic coast, a passive continental margin that spans a wide range of nearshore conditions and barrier island types. This was accomplished by modeling topography through a suite of dune topographic metrics designed to reflect the relative importance of geomorphic and biogeomorphic processes, resilience properties, and how changes in structure reflect gradual versus threshold dynamics. A challenge to this task is that geomorphic and biogeomorphic influences are not divorced from one another (Schwarz et al. 2018). Biogeomorphic interactions require a geomorphic template, and biogeomorphic interactions can modify the geomorphic template once they emerge. Then, the relative importance of geomorphic or biogeomorphic processes that shape landforms can also vary in time and space (Parker and Bendix 1996), and consequently in how they contribute to the resistance or resilience of barrier dunes alongshore (Stallins and Corenblit 2018).

To distinguish these properties, we utilized a cross-scale data modeling approach derived from resilience theory (Nash et al. 2014; Sundstrom et al. 2014). Data modeling in the sense employed here is a means of making the phenomena under study and its representation more accessible for analysis. The topographic metrics employed to model topography were selected so that they had a cross-scale structure and a degree of nestedness that captured how geomorphic and biogeomorphic phenomena are integrated. By using ordination as a dimensionality reduction technique, the variance structure of these data could be visualized as topographic state space. State space captures the range of expressed patterns or phenomena. It is a form of statistical mapping employed in many disciplines (Figure 4. 1). Its usefulness in this study is that the modeling is structured so that the axes,

or dimensions of state space, can be associated with not only with geomorphic and biogeomorphic properties, but also with resistance and resilience, the two dominant properties of resilience.

## **4.2 Background**

### **4.2.1 Cross-scale structure in resilience theory**

Typically, inquiries about the relationship between pattern and process confine observations to specific scales in time and space (Schumm and Lichty 1965; Turner and Gardner 2015), perhaps more so for fast systems such as dunes given the dynamism of its highly mobile elements. Scalar extent and resolution are often decomposed as part of the description of problems and the framing of questions and methodologies. Such discreteness in scalar extents and resolutions is often necessary to work within a particular conceptual paradigm or to falsify a specific hypothesis (Fonstad and Marcus 2010). Observations made at the scales affiliated with a particular conceptual paradigm are then statistically examined to determine the relative importance of factors that contribute to a scale-specific pattern. It is inescapable that any observation must inherently begin with the selection of an extent and a resolution that is constrained by human perception and technology. However, the weakness of this mode of sensitivity to scale is that it is an analytical artifact that does not take into account the plurality of conceptual frameworks, with their own particular scalar extents and resolutions as well as unique representational entities. It ignores how information exists continuously across scales out of a need to work within a particular paradigm. It restricts the information to a few levels from which to pose questions and conduct analyses.

Over the past decades, many techniques have been developed to examine pattern and process across scales. Spatial autocorrelation and variograms identify what scale lengths define a pattern-process relationship. They show how pattern and process can vary from place to place in terms of the dominance of a particular distance within which variables are highly correlated. These techniques lead to the identification of key scales that describe a specific property of a habitat or landscape. However, their weakness is that they do not specify how the identified dominant scale of variability propagates from and across scales. Key scales of variability are sublimations of many different scales into a single measure and so are limited in how they can tease apart multivariate relationships existing in different locations. Fractals, wavelets, and power laws also excel in pattern description across scale but they too collapse information and do not provide the variables needed for finer-grain inference of processes across scales and how it vary from place to place.

A common response to these anchorings and collapsings of scale is to forego field measurements and utilize more intensive modeling and simulation as a way to isolate mechanisms that span multiple scales. Modeling, including network approaches, can link mechanisms across scales to derive a tractable, yet simplified set of interactions. While modeling and simulation isolate details about mechanism, they remain approximations of real-world pattern and process. Their results are very often useful and can be compared to field observations to gauge the suitability of the model (Durán and Moore 2015). But such modeling often simplifies geographic variability. Modeling is required to strike a balance between mean-field aggregate and more spatially explicit models (Morozov and Poggiale 2012). Geographic variability and contextual details are often sacrificed in order to gain a

better mechanistic picture through mean-field aggregations of phenomena. These generalizations obscure the causal role of space and the details of spatial patterns.

In this study, a cross-scale data modeling approach is employed as a complement to these strategies. Cross-scale approaches work more simultaneously across scalar extents, resolutions, and the conceptual paradigms that define them. Like hierarchy theory, cross-scale approaches recognize the hierarchical nestedness and stacking of different processes across scales. But in formal cross-scale approaches, the variables account for more of adaptive and contextually variability in their integration. Cross-scaling can better explain differences in the successional development from place to place, and what kind of transitions in state can occur. As a foundation of resilience theory, cross-scale approaches have a long history and an extensive literature beginning more formally with Holling (1992). But of particular relevance is that cross-scale structure is the mechanism postulated to confer resilience properties (Peterson et al. 1998; Allen and Holling 2010). Resilience properties include the underlying dimensions of (1) resistance (engineering resilience), (2) resilience (ecological resilience), as well as (3) the interaction between the above two properties (Gunderson 2000; Donohue et al. 2013; Barros et al. 2016). Resilience, in the context of this study, represents the capacity to maintain a particular organizational configuration of topography before transitioning to a new state. Resistance is what allows resilience to develop. In biogeomorphic systems, resistance is manifested as the stabilization of substrate that facilitates biogeomorphic interactions to emerge and promote resilience.

Although cross-scale approaches have been conceptualized largely around the variable of body mass in animals, they are amendable to multivariate techniques and other

variables so long as they encapsulate key structuring processes (Allen et al. 2005). Variables in a cross-scale model need to be judiciously selected to reflect these key structuring processes and how they link across scales. The variables or metrics chosen should also correlate with each other given that they are nested across different scalar extents. In this study, elevational properties were the foundational topographic metric. Elevation in turn can comprise patches, the areal shapes and geometries taken by elevational observations when categorized into intervals of elevation. These patches in turn nest within continuous surface properties that reflect the connectivity of the entire landscape. When these different data representations and measurement levels are integrated in a cross-scale model, they augment the amount of information available to describe topography. This overcomes some of the loss of information that results from the selection of only a single scalar extent in order to work within a particular pattern-process paradigm. Similar to how raster and vector representations are used in geographic information science, the simultaneous application of different conceptual paradigms such as patch versus gradient and their representations complement the description of pattern (Collins et al. 2018). While it is impossible to escape the necessity to making scale-dependent decisions and observations, the cross-scale approach relies less on restricting scales of analysis and interpretation, and it does not reify any particular scale as more important. It overfits data, rather than relying on a greedy strategy of selecting only variables that correspond to a particular conceptual paradigm or method. Other statistical procedures, like simulated annealing, rely on similar overfitting approaches.

The advent of broad-extent, high-resolution data sets are instrumental for the development of these overfitting strategies that cross-scale data modeling exemplifies



(Fonstad and Marcus 2010). Remote sensors can provide the high resolution data coverage over broad spatial extents. These data can then be partitioned, aggregated, and summarized to reflect different explanatory paradigms and scalar representations of the phenomena of interest. By employing LiDAR data that measures point elevations at sub-meter accuracy over kilometer extents, observations can be simultaneously represented with elevational statistics, patch metrics, and continuous surface properties.

#### 4.2.2 Dune biogeomorphic resistance and resilience

Topographic metrics identified as higher dimension are expected to have stronger correlations with second or higher axes. These variables demarcate biogeomorphic influence and potentially the greater degree of differentiation of dune topographies due to biogeomorphic feedbacks. When dune topography is influenced at a landscape scale by vegetation, it may either reinforce or resist overwash exposure, but not both simultaneously. Too much or too little topographic resistance prohibits the diversity of dune plant types and feedbacks with sediment mobility to biogeomorphically modulate inputs from high water events in a recursive, self-organizing manner. Thus, intermediate elevations (i.e., toward the middle of the elevational boundary conditions) may not be a dynamically favored state. Based on Durán and Moore (2015), we also expect that there will be regions in this state space within intermediate elevations that are bistable. At these bistable regions, neither resisting nor reinforcing biogeomorphic feedbacks dominate. This implies that they can have different biogeomorphic properties and dune landform patterns at the same elevation.

Dune topographic patterns have been linked to resilience properties (Stallins 2005; Durán and Moore 2015; Zinnert et al. 2017). However, topography in these studies is simplified to transect profiles and alongshore point elevations. Fine-resolution spatial structure in three dimensions has not been fully considered. Moreover, these studies link resilience properties to topography but do not adequately consider the multidimensionality of resilience, a phenomena composed of the correlated dimensions of resistance and resilience that can also vary geographically (Donohue et al. 2013; Radchuk et al. 2019). When the idea of cross-scalar structure is invoked, it is in description only and lacks any quantitative or mechanistic basis. However, cross-scale structure has an explicit mechanistic linkage to resilience properties. Adaptive cycles and how they link, break apart, and adapt to new circumstances to form a panarchy that shapes resilience properties and the kinds of transitions in state that can occur. More recently, Sundstrom et al. (2014) and Nash et al. (2014) specified a cross-scale data structure to summarize resilience properties. However, these ecological studies downweight abiotic-biotic interactions like those in biogeomorphology. They favor ecological interactions focusing on body mass over how these ecological interactions shape the habitat template, a perhaps more fundamental key structuring process.

Stallins and Corenblit (2018) conceptualize how cross-scale structure shapes the formation of dune habitat and its resistance and resilience. They proposed a data structure for relating dune topography to the potential expression of biogeomorphic resistance and resilience within and between islands. In this work, the biogeomorphic successional model of Corenblit et al. (2007, 2009) was translated into a geographically-explicit conceptualization of adaptive cycles and panarchies, the fundamental working units of

resilience theory. Stallins and Corenblit (2018) then formalized how multiple representations of dune topographic pattern—each reflecting different scalar extents, resolutions, levels of aggregation and degrees of spatial explicitness—can be integrated and visualized in a multidimensional state space so as to reveal aspects of their resistance and resilience. Their model also postulates as to where overwash-reinforcing and overwash-resisting biogeomorphic stability domains emerge in this state space. In a stability domain, dune plant compositional abundances and landscape topography interact to reinforce one another in a positive feedback that either lowers or increases resistance to overwash exposure. These landscape feedbacks were hypothesized to emerge only at higher dimensions of dune topographic state space and to exhibit threshold dynamics in transitions between them.

In other regions of state space where biogeomorphic interactions are not as integrated into the landscape, gradual transitions may be more common. There is a growing recognition that critical transitions inferred from spatial patterns may be more complex than those detected through time (Bel et al. 2012; Génin et al. 2018). Much of the literature on critical transitions has shifted from simplicity to more complex dynamics as the spatial properties of resilience are acknowledged (Cumming 2011; Allen et al. 2016; Cumming et al. 2017).

## **4.3 Methods**

### **4.3.1 Selection of cross-scalar variables**

Quantification of the conceptual cross-scale model proposed by Stallins and Corenblit (2018) requires topographic data representations that capture the key structuring

processes and linkages in the developmental sequence from bare mobile substrate to vegetated, biogeomorphically interactive dune landscapes. Most of the underlying variability in topography should be related to geomorphic variables, like elevation, that determine relative position of the terrestrial surface above the high water mark and the presence-absence of a barrier island. In this sense, elevation is the lowest dimensional variable to describe dune topography. Through absolute measures of elevation, resistance to storm inputs and high water events for a location can vary from high to low, from infrequently overwashed to frequently inundated.

Elevation alone does not determine the resistance to high water events. As small vegetated dunes develop, they augment resistance by binding sediment in place. But as these dunes begin to shape the movement of sediment and storm surge, the emergence of resilience at larger landscape extents may become possible. Higher dimensional metrics that reflect the growing spatial organization of the landscape can capture this change. Measures of dune landform configuration and abundance inferred from the boundaries and area of elevational patches can be used to identify the growing importance of biogeomorphic processes and the resilience they contribute. The highest dimension metrics reflect the formation of the continuous spatial structure arising from biogeomorphic feedbacks that operate across a landscape. They emerge out of lower dimensional properties summarized by elevation and measures of patch structure. These summarize dune landscape connectivity through metrics like habitat extent, the distributional properties of elevation (skewness and kurtosis), and spatial autocorrelation of elevation.

Habitat extent in this study is considered to be a spatially-structured continuous surface processes, rather than simply a value to standardize observations. A biome, for

example, has an extent that reflects the spatial processes that shape it. While not as explicitly spatial, skewness and kurtosis summarize a distributional property of the entire continuous elevational surface. Moreover, changes in skewness and kurtosis of a key structuring variable are often associated with transitions in state, along with measures of autocorrelation (Guttal and Jayakaprakash 2008, 2009; Scheffer et al. 2015) From a process perspective, spatial autocorrelation is important because it summarizes variations across-scales that can point to local processes of importance.

Through these metrics and their correlations with each other in state space, resilience properties can be identified and compared. However, a variance partitioning technique is needed to reduce the dimensionality of the data and distill its parsimonious structure (e.g., Kim and Zheng 2011; Kim et al. 2012). The working assumption for this cross-scale data modeling is that lower dimension axes represent resistance and higher dimension axes represent resilience. Two to three dimensional solutions are expected, based on ordination of cross-scaled data in other studies (Monge and Stallins 2016). However, an issue with dimensionality reduction is that the derived axes do not always correspond directly to the properties attributed to them. Some topographic metrics can be expected to correlate well with a single axis, others may be correlated with more than one axis. The exploratory hypotheses below formalize these aspects of dimensionality reduction and their relationships to resistance and resilience. While correlation is not causation, it is an indication of a causal relationship that merits explanation (Laland et al. 2011).

### 4.3.2 Exploratory hypotheses

#### *Lowest-dimension topographic metrics*

Island sites distributed along the lowest dimensions, or axes, of state space represent the variability in resistance as expressed through metrics with a strong geomorphic component. In other words, the lowest dimension of the state space is hypothesized to capture the variance associated with the resistance properties through several topographic metrics that characterize lower adaptive cycles (Stallins and Corenblit 2018). These sites represent the boundary conditions under which a barrier island is possible, from highest to lowest elevations.

#### *Highest-dimension topographic metrics*

Topographic metrics correlated with the highest dimension are expected to reflect landscape-extent biogeomorphic properties. Islands distributed along the highest dimensions may express stability domain dynamics, a high resilience overwash-resisting topography or a high resilience overwash-reinforcing topography. The correlation of topographic metrics with the highest dimension axis is expected to occur at an intermediate level of resistance. Too much or too little topographic resistance may prohibit the development of the abundances of dune plant types and feedbacks with sediment mobility and landforms to biogeomorphically modulate inputs from high water events in the recursive, self-organizing manner attributed to stability domains. Thus, intermediate elevations (i.e., toward the middle of the elevational range spanned along the first axis) are expected to be where stability domains and high resilience are positioned in state space. In their modeling and field-based study, Durán and Moore (2015) observed that transitions

along the coast between high and low domain states similar to stability domains occurred near intermediate elevations. They designated these transitions as bistability, in which either a high or low-island dynamical state can develop at an intermediate elevation.

#### *Dual correlation topographic metrics*

Metrics correlated with a low and a high axis reflect the conjoint influence of geomorphic and biogeomorphic feedbacks on topographic structure. These metrics should provide insight into how islands differ in the relative importance of geomorphic and biogeomorphic processes.

#### 4.3.3 Sampling and data

To examine these hypotheses, a cross-scale data set characterizing dune topography on 52 sites across 12 barrier islands was assembled. This data set spanned barrier islands from Virginia to South Florida. These islands represent a range of island morphologies, from long-linear, wave-dominated to drumstick-shaped, tide-dominated barrier islands. LiDAR data was used to generate a 1-m resolution digital elevation model (DEM) for each dune plot from which elevational statistics, landscape patch indices, and continuous or gradient surface properties were derived (Table 4. 1).

Dune topographic metrics for islands in the Georgia Bight regional dataset were derived in an earlier study, Monge and Stallins (2016). These metrics utilized a 2010 LiDAR dataset collected by the United States Army Corps of Engineers for four of the islands. Vertical (horizontal) accuracy was 15 cm (75 cm) and nominal point space was 2 m. Due to small gaps in this 2010 dataset, topographic metrics for South Core Banks and Parramore Island were constructed from post-Sandy LiDAR datasets collected by the U.S.

Geological Survey in 2012. For these data, vertical (horizontal) accuracy was 7.5 cm (19.4 cm) and nominal point space was 1 m. A post-Hurricane Sandy 2014 data-set collected by the NOAA National Geodetic Survey was used to construct digital elevation model (DEM) plots for sites on the Virginia islands. Vertical (horizontal) accuracy was 6.2 cm (100 cm) and nominal point space was 0.3 m. LiDAR point elevations were resampled to a resolution of 1 m and then interpolated using inverse distance weighing to fill any gaps. LiDAR processing was performed in ArcGIS using LAStools (Isenburg 2014).

Mean, maximum, and percentile elevation observations (25<sup>th</sup>, 50<sup>th</sup>, and 75<sup>th</sup>) were absolute measures relative to the mean high-water mark (MHW) datum. The Virginia MHW shoreline was defined as the 0.7 m contour line relative to the NAVD 88 datum following Rogers et al. (2015). The islands in the Georgia Bight and the replicate plots on Parramore were referenced to the MHW mark using VDatum (National Oceanic and Atmospheric Administration and National Ocean Service 2012). These elevational variables were converted to Z-score standardized elevations before analysis.

Landscape index values were calculated in FRAGSTATS software Version 4.2 (McGarigal 2015). Elevation is represented as patches, where a patch is an interval of elevation. Each patch is composed of pixels that can vary within the defined interval for a patch. FRAGSTATS indices quantify the patch pattern of elevations within a predefined interval. Because FRAGSTATS is designed to work with categorical observations, raster DEMs were converted into areal representation by reclassifying pixels into elevation intervals. This decreased the number of elevation classes from all the possible centimeter intervals (essentially a continuous surface representation), to one based approximately on decimeter intervals (a categorically oriented representation). Figure 4. 2 illustrates the logic



of this conversion, as explained in Wu et al. (2017, p. 56). To minimize derivation of FRAGSTATS descriptors without a process interpretation (Kupfer 2012), this study chose landscape indices with consistent, ecologically meaningful values, identified by Cushman et al. (2008). This set of indices was then constrained to those well-suited for characterizing continuous surfaces like elevation (McGarigal et al. 2009) and for discerning pattern-process relationships associated with foredune building and overwash. This study selected these indices (Table 4. 2): the perimeter-area fractal dimension (PAFRAC), the area-weighted mean shape index (SHAPE\_AM), the aggregation index (AI), the landscape shape index (LSI), the largest patch index (LPI), the contagion index (CONTAG), the interspersion and juxtaposition index (IJI), and the Simpson's diversity index (SIDI). DEMs of representative plots were used to demonstrate the contrasts among the landscape indices (Figure 4. 3).

Continuous surface properties were described by the skewness and kurtosis of elevations derived from the point observations of each pixel in a plot. Habitat extent, expressed as plot size, was defined as the distance in meters of one side of the square study site. The last continuous variable, spatial autocorrelation, was summarized in directional correlograms. These correlograms captured the way in which elevations varied in the cross-shore direction at different distance lags from zero to their plot size. To make the directional correlograms comparable to the other topographic metrics, six Moran's *I* values along correlograms were selected and then reduced to a pair of coordinates using principal coordinates analysis PCoA (Figure 4. 4).

Non-metric multidimensional scaling (NMDS) in PC-Ord Version 7 (McCune and Mefford 2016) was used to construct state space. All topographic metrics were

standardized to Z-scores and analyzed in NMDS as Euclidean distances. Site-level ( $n = 52$ ) data were too noisy to interpret when plotted in the final NMDS scatterplot. Coordinates for these site positions were averaged to obtain each island's centroid in dune topographic state space. Pearson's correlation coefficients were used to infer how these variables correlated with each axis or dimension. These correlations represented the trends of site position along each axis with the original topographic metrics.

Response surfaces were calculated for each topographic metric to enhance interpretation of how they vary across state space. They provide a more quantitative and visual method for the interpretation of state space. To fit the contours of this response surface, nonparametric multiplicative regression (NMPR) was performed against the two ordination axes for each individual topographic metric. The NMPR model was implemented with a local mean estimator and Gaussian kernel (McCune 2006). A leave-one-out cross-validated  $R^2$  ( $xR^2$ ) was calculated based on the differences between the estimated and the observed  $y$  values, where the estimate for a point is calculated without including that point in the model fitting. The response surface was then interpolated by calculating estimates for a finely divided grid for  $x^2$  and  $xR^2$ . The smoothing parameter was optimized such that  $xR^2$  was maximal. The response surface was then drawn through the local mean of the points. Standard deviation was set at zero so that the surface represents the local mean of the overlay variable. Response surfaces were constructed in PC-Ord Version 7 (McCune and Mefford 2016).

#### 4.4 Results

A two dimensional NMDS solution was optimal based on statistically significant reductions in stress compared to Monte Carlo randomizations of the data ( $n = 249$ ;  $p < 0.01$ ). Final stress was 11.1. Stress values less than twelve are considered useful, although stress less than twenty may also be an informative solution (McCune and Grace 2002). Centroids provided a more interpretable state space to gauge response surfaces trends (Figure 4. 5). Topographic metrics were assigned to three groups based on the strength of their Pearson correlation with the first and second axes (Table 4. 3). The first or low dimension axis was correlated more strongly with mean and percentile elevation properties, AI, LPI, SHAPE\_AM, SIDI, IJI, and PAFRAC. The second and highest dimension axis was more strongly correlated with kurtosis, size, skewness, and spatial autocorrelation. CONTAG, LSI, and maximum elevation had more evenly balanced correlations with both axes.

As hypothesized, elevation was the dominant source of variability along the lowest dimension or axis of state space. The boundary conditions of barrier island dunes in this state space ranged from a high elevation site on Cape Canaveral in Florida to a low elevation site on Ship Shoal in Virginia. The FRAGSTATS indices that contributed to the separation of sites along the first axis were dominantly patch configuration metrics (AI, LPI, SHAPE\_AM) and to a lesser extent, compositional metrics (SIDI). Along this axis, the aggregation and size of patches increased toward more positive axis values. Elevation patches were also lower, more convoluted, and less diverse in this axis direction. Toward negative axis values, there were more elevational patch types and more evenness in their number across the dune landscape. Patch types were more uniformly represented and no

single patch type dominated. Response surface  $xR^2$  values were generally strong for all of these variables (Figure 4. 6).

The distribution of sites along the second axis was associated with changes in kurtosis, skewness, spatial autocorrelation structure, and size. Response surface  $xR^2$  values were weaker for these higher dimensional variables (Figure 4. 7). Variability in these topographic metrics along the second axis was greatest around intermediate elevations on the first axis. These intermediate elevations are approximately 0.45 to 0.55 in Z-score value or between 1.39 and 1.44 meters in absolute value. Dune topographies falling within these intermediate elevations differed strongly in these continuous surface metrics. For example, the wave-dominated islands of Assateague (Virginia and Maryland) and South Core Banks (North Carolina) tended to have mean elevations close to those of the tide-dominated sea islands of Sapelo (Georgia) and Kiawah (South Carolina). However, these two sets of islands differed in the kurtosis, skewness, size, and spatial autocorrelation structure of topography and elevation. Similarly, topographies on Hog and Parramore islands occupy a similar elevational range along the first axis, but they too differ in these higher dimension spatial properties along the second axis.

For Sapelo, Kiawah, and Parramore islands, dune topographies tended to have a platykurtic (less peaked) distribution of elevations that are skewed toward larger positive elevation values (the long tail is in the direction of a few low elevations). Their dune topographies were also expressed across a relatively small plot size or habitat extent. On Assateague Island, South Core Banks, and Hog Island, dune elevations are more leptokurtic (peaked) and skewed toward small elevations (the long tail is in the direction of a few high elevations). Topography was also expressed across larger habitat extents. PCoA extracted

a single dominant axis of variability in the directional correlograms (Figure 4. 8). In the PCoA scatterplot, elevation correlations changed from strongly positive to negative with increasing distance lags at smaller, more negative axis values. Elevation correlations remained zero or slightly negative with increasing distance lags toward more positive values. In the final state space, this trend in autocorrelation along the second NMDS axis corresponded to islands with zero to slightly negative autocorrelations at increasing distance lag toward the bottom of state space and islands with more strongly negative correlations at the top of the state space (Figure 4. 9).

CONTAG, LSI, and maximum elevation were correlated with both NMDS axes of topographic state space. This implies that they were collinear with elevational properties along the first axis and with the higher dimensional spatial metrics along the second axis. Response curves (Figure 4. 10) indicated that the equivalent values for these topographic metrics could develop at different elevations. For example, the contour lines for CONTAG indicate that topographic contagion decreases from bottom right to the upper left of state space. Based on island centroid position, the higher wave-dominated islands of South Core Banks and Assateague have CONTAG values like lower-lying Parramore Island. Contagion on a higher island may be equivalent to contagion on a low-lying island that is more frequently overwashed and erosional because of greater biogeomorphic modulation and reinforcement of overwash exposure on the higher island. Conversely, higher elevation islands Sapelo and Kiawah have lower contagion values, but these are similar to those of a higher island, Cape Canaveral in Florida. In this case, the lower island has a contagion value like a higher island. This may also be due to the increased resistance to overwash

promoted by biogeomorphic properties on Sapelo and Kiawah despite an overall lower mean elevation.

Contours for LSI ran from the upper left to the lower right. In this direction, topography becomes more regular. Landscape regularity was also similar at different elevations. For example, Sapelo was higher in elevation than Metompkin, but they have the same LSI values for topographic regularity. Convergence in this property developed even though Metompkin is much more erosional and storm-exposed than Sapelo. Similarly, Kiawah was higher than Hog Island, but these two islands also had the propensity for regularity in topography. The differences in elevation given similar values for regularity can also be explained through changes in the relative importance of geomorphic and biogeomorphic interactions. Regularity in landscape shape is a consequence of homogenizing geomorphic processes associated with storm exposure and erosion on Metompkin and Hog Island. On Sapelo and Kiawah, regularity in topography may be more related to biogeomorphic interactions that also create regularity. Higher elevations and less frequent overwash disturbance may promote more regular shore-parallel dune features on these two islands.

Maximum elevation was also collinear with both axes. Similar maximum elevations can occur in different mean elevational conditions. Lower-lying islands may have equivalent maximum elevations due to erosional remnants. On higher islands these maximums may occur through biogeomorphic processes of dune-building.

## 4.5 Discussion

The first axis defined the geomorphic boundary conditions of state space, from high islands (Cape Canaveral, Florida) to low erosional islands (Ship Shoal, Virginia). However, the correspondence of mean island elevation and position along this resistance axis in topographic state space masked the considerable variability within each individual island. The variability in site position in state space for each island suggests that resistance and consequently resilience may vary significantly within an individual island. That island centroids versus site positions were more reflective of resilience properties follows Sankaran et al. (2018). They argue that this coarsening is necessary to detect resilience properties when spatial properties of resilience are assessed.

Elevation, as a resistance variable, was strongly correlated with the first axis. The dominance of configuration or shape-oriented FRAGSTATS indices as correlates of the first axis also suggests a greater importance of geomorphic processes for the first axis, which was essentially an elevational continuum in state space. However, this low dimension also marks a transition in process-form states, from aggradation and positive relief at high elevations to erosion and inverted (or negative) relief that can develop at low elevations. Switching between aggradational and erosional conditions may not necessarily be threshold-driven but more gradual in nature given that aggradational and erosional conditions can change over relatively small geographic distances along an island. This first axis may represent the resistance-associated states postulated by Durán and Moore (2015) for the generally low barrier islands of Virginia. Using only basic elevational measures, they presented model and observational evidence for transitions between a high dune state to a low dune state along barrier islands of the Virginia coast. Once elevations go below a

certain minimum threshold of elevation, a site may become locked into a low resistance state. Once above this elevation, deposition and constructive dune-building processes can augment coastal resistance. Vegetation plays a role in this transition, but may be mainly as an anchoring mechanism rather than any landscape integration of biogeomorphic feedbacks.

As expected, the second axis of state space was correlated with higher dimensional topographic metrics reflective of landscape-scale biogeomorphic structure and higher resilience. These metrics (plot size, spatial autocorrelation, skewness and kurtosis) were weaker and contributed less to the overall variability of topography in state space. As also postulated, islands with the same mean elevations along the middle of the first axis (i.e., intermediate elevations) differed the most in these spatial landscape-extent topographic properties and were more representative of stability domain models of barrier dune resilience. Within the Georgia Bight region of state space, South Core Banks and Sapelo, islands that have been affiliated with stability domain dynamics (Stallins 2005) were positioned at opposite ends of the second axis. Even though they have the same mean elevations, they have very different measures of spatial autocorrelation structure, skewness, and kurtosis. Changes in these properties may be associated with more abrupt threshold transitions given that these properties develop across the entire landscape.

Based on their position in state space, Hog and Parramore islands can be validated as approximations of the stability domain dynamics associated with Sapelo and South Core Banks. Parramore has been described as a low island with frequent overwash. Hog is often defined as having more properties that resist disturbance (Wolner et al. 2013; Brantley et al. 2014). These two Virginia Barrier Islands had a similar mean elevational position along



the first axis. Island centroids also separated along the second axis as a function of their more spatially-explicit, landscape-scale properties. However, given that the distance separating them along the second axis is small compared to the distance between Sapelo and South Core Banks, transitions states represented by Hog and Parramore may not be threshold-driven.

Based on these interpretations of the state space structure, two types of transitions may develop on barrier islands. Gradual transitions may manifest where elevation determines resistance and the propensity for the persistence of a high, aggradational state or a low, erosional state. When resilience is more spatially structured at intermediate elevations, threshold changes between biogeomorphic stability domains may develop. This suggests that depending upon what types of spatial patterns are assessed and how they are measured, different kinds of transitions will be evident. It also suggests that it may be more difficult to anticipate the nature of transitions along barrier coasts. Greater attention to landscape attributes of topography and adoption of a cross-scaling approach may provide more evidence for what kinds of transitions to anticipate. However, the state space approach employed in this study showed how to distinguish the relative importance of geomorphic and biogeomorphic contribution to resilience properties. Where different elevations expressed similar values for elevational patch shape and size in state space, it was possible to infer the extent they were derived from geomorphic or biogeomorphic processes. Equivalent levels of topographic contagion or regularity can be produced as a consequence of geomorphic processes at high and low elevations and through biogeomorphic interactions at more intermediate elevations.

A region of bistability or dynamical instability may develop in the center of topographic state space, based on two-dimensional solution derived in this study. Here, elevation is not sufficient to be either a high or low state in the sense of Duran and Moore (2015). Nor are the landscape spatial properties reinforced through biogeomorphic feedbacks characteristic of the stability domain model of barrier dune resilience (Stallins 2005). More formal probabilistic measures of occupancy in region of state space could provide more evidence for regions that are dynamically resilient or unfavorable (Figure 4.11). Field observations could verify if these sites have more variability in vegetation and topography over time.

#### **4.6 Conclusion**

The cross-scale data modeling approach used to construct topographic state space distinguished geomorphic and biogeomorphic properties of barrier island dunes. Geomorphic boundary conditions were expressed along the first axis. These conditions mark the extremes of elevation and the contrasts in resistance of sandy barrier shores. As conditions along this elevational continuum switch from aggradational to erosional, elevation may be associated with gradual transitions in state. Spatial variables are less important for this expression of resistance. At intermediate elevations, where resistance was neither at its highest or lowest, island topographies were the most differentiated in landscape-scale metrics. Regions of state space were identified along this second axis that potentially correspond to high resilience disturbance-resisting and disturbance-reinforcing stability domains. These domains are more organized around biogeomorphic interactions of dune landforms and vegetation across the continuous surface of the landscape. The methodology from this study offers a theoretical base to discuss the similar transition from

reflective to dissipative beach states (Short and Hesp 1982; Sherman and Bauer 1993). Changes in state along the second axis may be more threshold-driven. However, the state space constructed in this study reflected the central tendency of island topographies. Thus, these resilience properties and the relative dominance of geomorphic and biogeomorphic processes associated with transitions in resistance and resilience should not be considered applicable to an entire island. For a given island, propensities exist for certain kinds of transitions and resilience properties to predominate over others.

In sum, the major contribution of this study is that it highlights the importance of using different representations of topography if the goal is to compare their dynamical properties or resistance and resilience. What variables are used to define topography will shape what resilience properties are detectable and what kinds of transitions may occur. Using a cross-scale state space approach created regions of state space in which the distinction between the geomorphic and biogeomorphic contributions to resistance and resilience could be made. Future studies may find it useful to apply these kinds of state space approaches, as they could promote more judicious field site selections for conducting experiments to elucidate ecological mechanisms (Dilts et al. 2010). For example, it would be expected that the biogeomorphic mechanisms leading to domain states would be more visible by comparing the topographies among certain pairs of islands, like Assateague and Kiawah or Sapelo and South Core Banks, than others such as Hog and Metompkin. These two Virginia Barrier Islands likely exhibit geomorphic transitions with more passive roles for vegetation and less landscape-scale integration of biogeomorphic feedbacks.

The approach in this study has been exploratory in that it raises questions as much as it tests and comments upon older ones. Exploratory, data-driven abductive approaches

like this study are increasingly used in tandem with the traditional inductive and deductive frameworks of ecology (Kell and Oliver 2004; Sagarin and Pauchard 2010).

**Table 4. 1** Cross-scale data ontologies and levels of measurement.

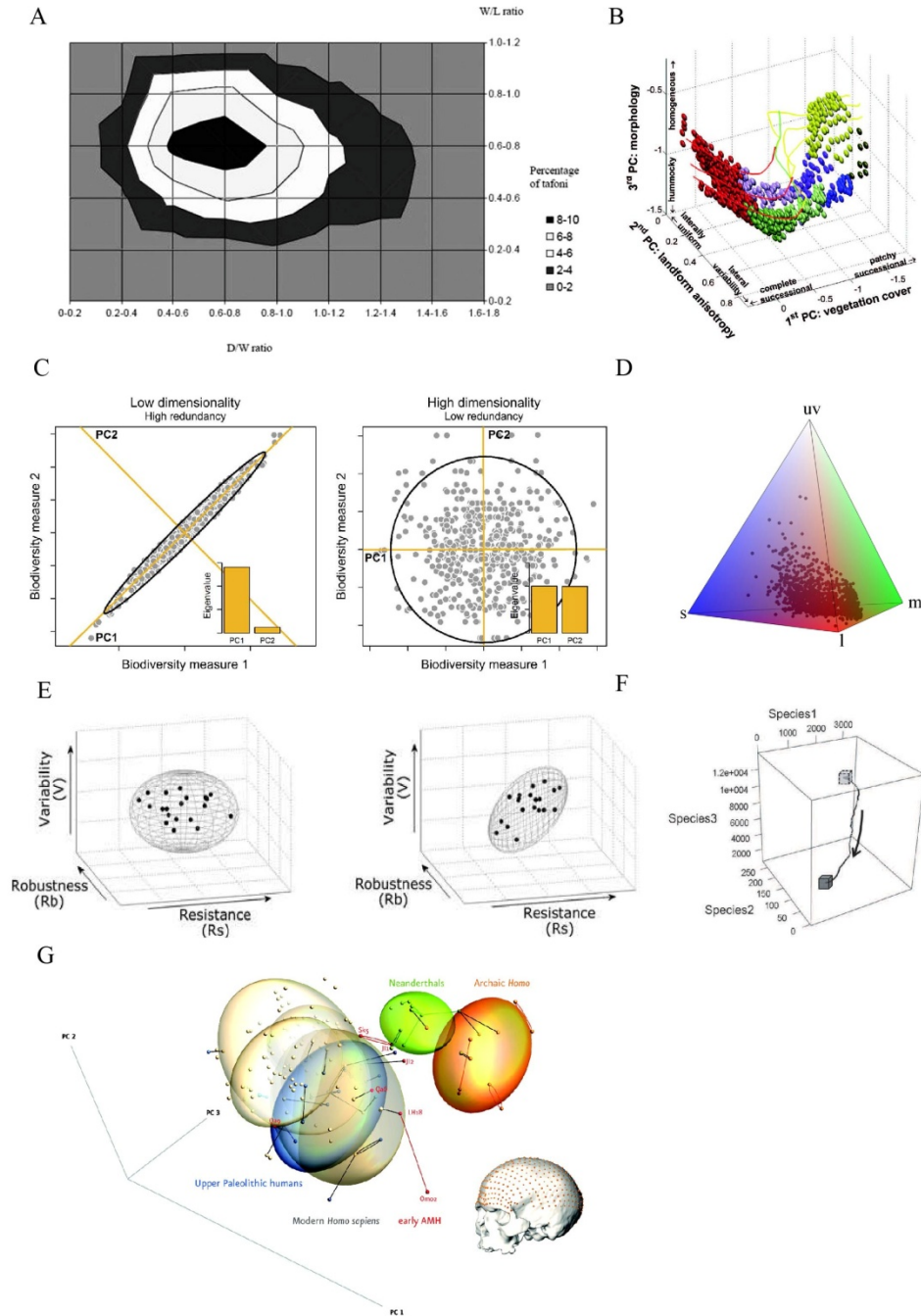
| Topographic variable   | Geomorphic relevance                       | Geometry                                      | Variables (Software)  |
|------------------------|--|---|---|
| Descriptive statistics | Position of land relative to marine inputs | Global summary; aggregate mean field measures | Absolute values for mean, maximum elevation, 25 <sup>th</sup> , 50 <sup>th</sup> , 75 <sup>th</sup> percentiles (GS+) |
| Patch metrics          | Formation of dune landforms                | Polygons of elevation intervals               | Relativized indices of patch shape, area, diversity (FRAGSTATS)   |
| Continuum metrics      | Spatial landscape structure                | Gradients                                     | Moran's <i>I</i> in directional correlograms; plot size; skewness and kurtosis of elevation (GS+)                     |

**Table 4. 2** Summary of FRAGSTATS landscape indices utilized in the study.

| Index    | Description  | Interpretation   |
|----------|--|--|
| AI       | Aggregation of patches   | Higher AI implies more aggregated patch distribution within the plot   |
| CONTAG   | Aggregation based on pixel adjacencies                         | Higher CONTAG implies more aggregated patch distribution within the plot   |
| IJI      | Aggregation of patches   | Higher IJI implies more equal adjacency of all other patch types within the plot (i.e., maximum interspersion and juxtaposition) |
| LPI      | Area percentage of the largest patch within the plot           | Higher LPI implies higher dominance of a single patch within the plot  |
| LSI      | Shape regularity of patches based on perimeter                 | Higher LSI implies increasing landscape shape irregularity   |
| PAFRAC   | Shape regularity based on fractal perimeter-area relationships | Higher PAFRAC implies that all patch shapes within a plot tend to be convoluted  |
| SHAPE_AM | Shape regularity of patches based on perimeter                 | Higher SHAPE_AM implies more irregular patch shape   |
| SIDI     | Landscape patch diversity                                      | Higher SIDI implied higher patch richness and more equitable patch distribution with the plot                                    |

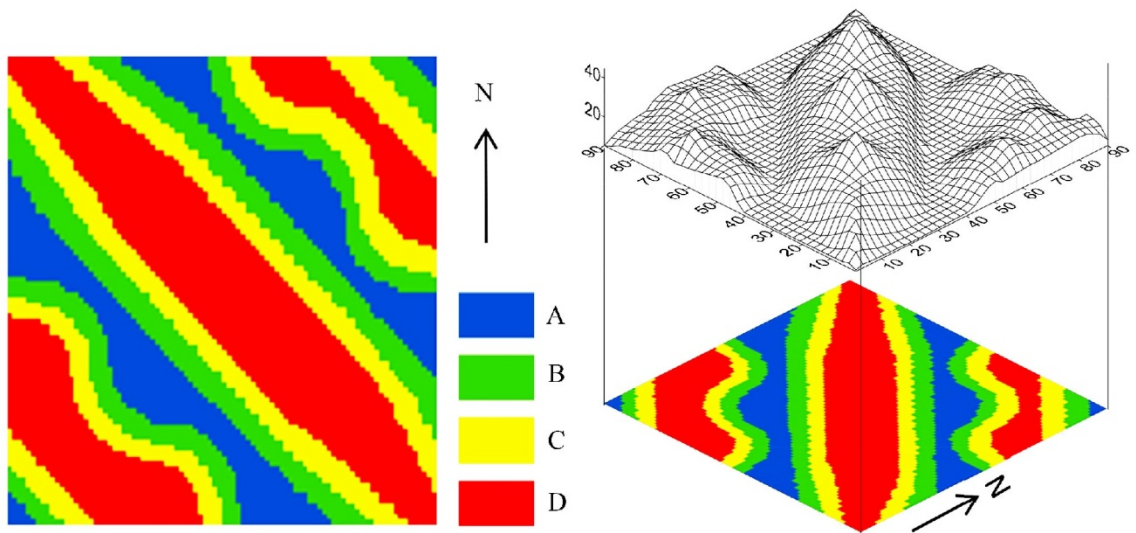
**Table 4. 3** Pearson's correlation coefficients for NMDS axis position and original variables.

| Variable        | Axis 1       | Axis 2       |
|-----------------|--------------|--------------|
| Low dimension   |              |              |
| Mean            | <b>-0.89</b> | -0.27        |
| 25th percentile | <b>-0.70</b> | -0.40        |
| 50th percentile | <b>-0.86</b> | -0.19        |
| 75th percentile | <b>-0.92</b> | -0.14        |
| AI              | <b>0.87</b>  | 0.07         |
| LPI             | <b>0.73</b>  | 0.10         |
| SHAPE_AM        | <b>0.78</b>  | -0.25        |
| SIDI            | <b>-0.85</b> | -0.01        |
| IJI             | <b>-0.71</b> | 0.37         |
| PAFRAC          | <b>-0.68</b> | -0.16        |
| High dimension  |              |              |
| Skewness        | 0.15         | <b>-0.54</b> |
| Kurtosis        | 0.40         | <b>-0.72</b> |
| Autocorrelation | 0.12         | <b>-0.61</b> |
| Plot size       | 0.32         | <b>-0.74</b> |
| Both dimensions |              |              |
| CONTAG          | <b>0.80</b>  | <b>-0.50</b> |
| LSI             | <b>-0.49</b> | <b>-0.70</b> |
| Maximum         | <b>-0.67</b> | <b>-0.58</b> |



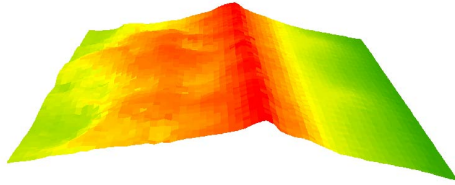
**Figure 4. 1** Examples of state space in other studies. (A) Morphospace of tafoni occurrence (Inkpen and Hall 2016); (B) 3D phase-space of dune landscapes (Baas and Nield 2010); (C) Dimensionality of biodiversity measure (Stevens and Tello 2018); (D) Avian sensory color space (Chartier et al. 2014); (E) Dimensionality of ecological stability (Donohue et al. 2013); (F) Three dimensional phase of stability (Barros et al. 2016); (G) Anatomically modern humans and archaic forms of *Homo* in shape space (Gunz 2009).





**Figure 4. 2** How patch structure is derived from a more continuous elevational surface from Wu et al. (2017). Elevation intervals in this study were reclassified from centimeter interval to decimeter intervals.

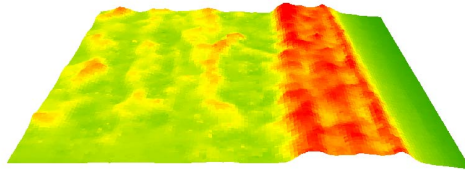
AI=34.50 (-2.26)  
Canaveral B



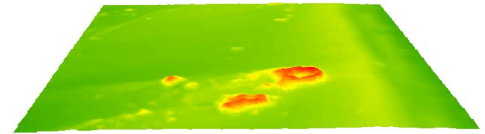
AI=91.84 (1.64)  
Cedar A



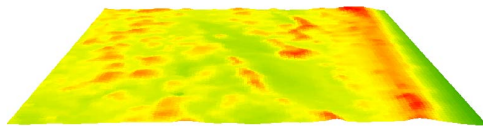
CONTAG=35.07 (-1.28)  
Bull D



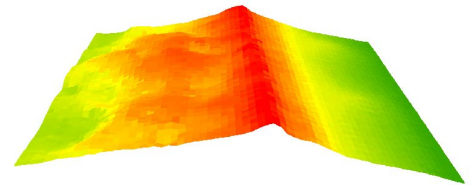
CONTAG=59.14 (2.78)  
Cedar E



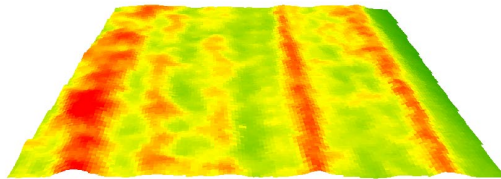
IJI=47.76 (-2.21)  
Ship Shoal C



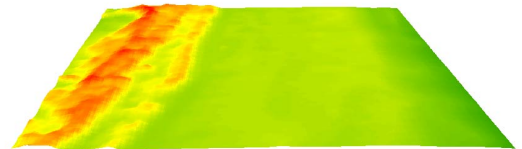
IJI=66.79 (2.47)  
Canaveral B



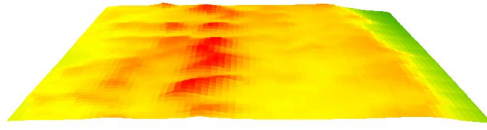
LPI=0.85 (-1.36)  
Sapelo A



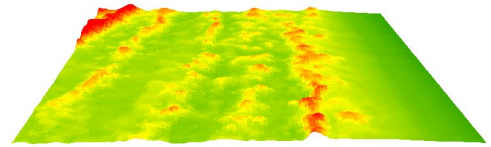
LPI=28.09 (3.00)  
Metompkin D



LSI=92.30 (-1.24)  
Ship Shoal D



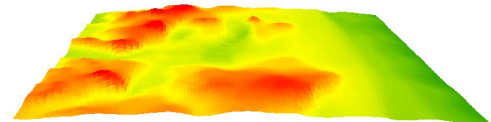
LSI=42.94 (1.53)  
Kiawah D



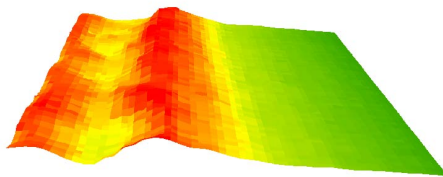
PAFRAC=1.43 (-3.02)  
Cedar A



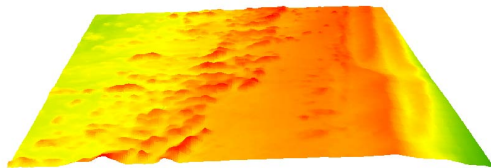
PAFRAC=1.58 (1.43)  
Assateague B



SHAPE\_AM=2.21 (-1.44)  
Sapelo B



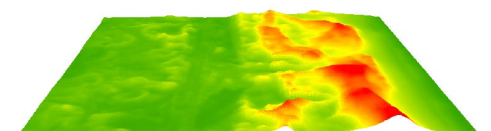
SHAPE\_AM=5.53 (1.69)  
Cedar D



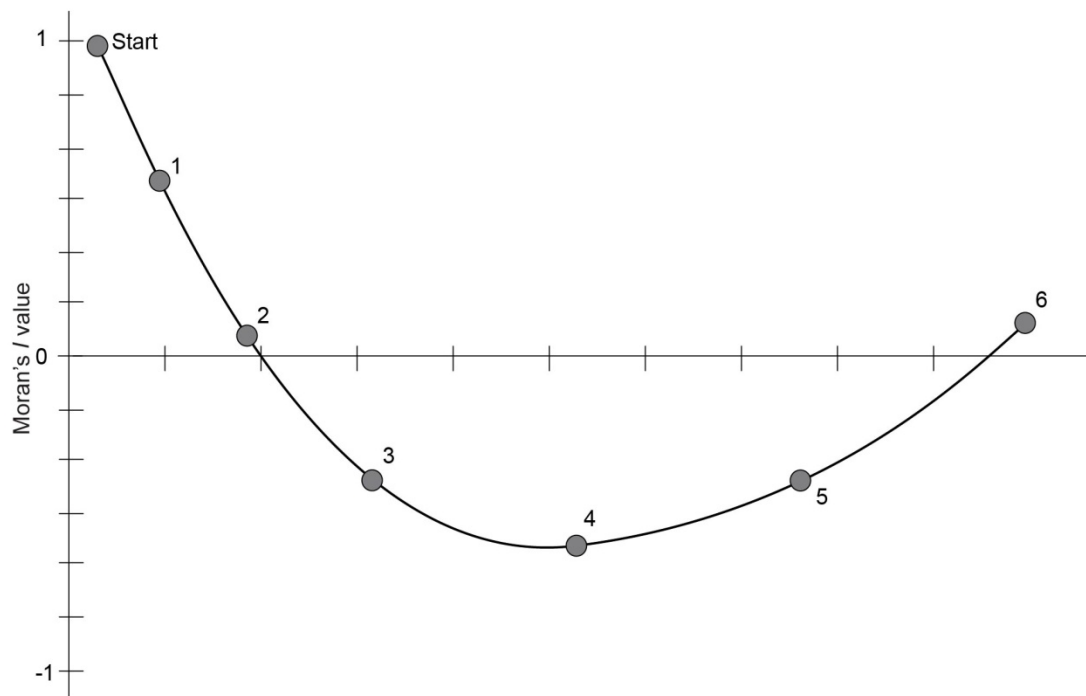
SIDI=0.87 (-1.36)  
Metompkin D



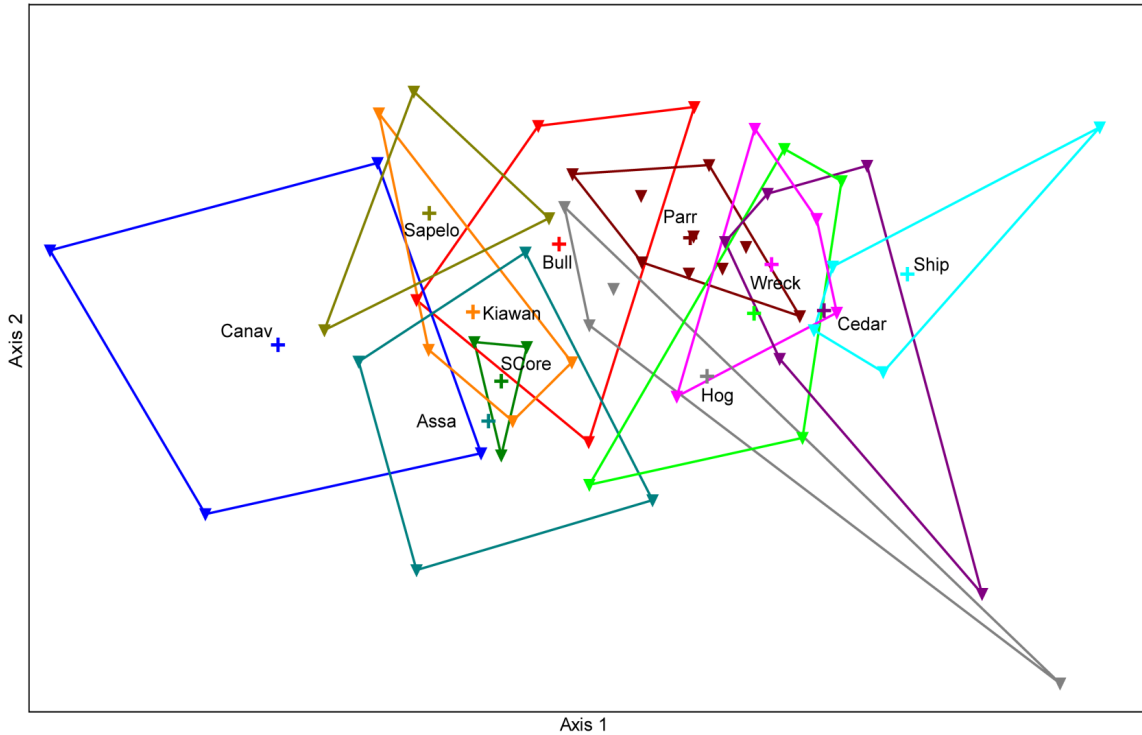
SIDI=0.96 (1.13)  
Assateague C



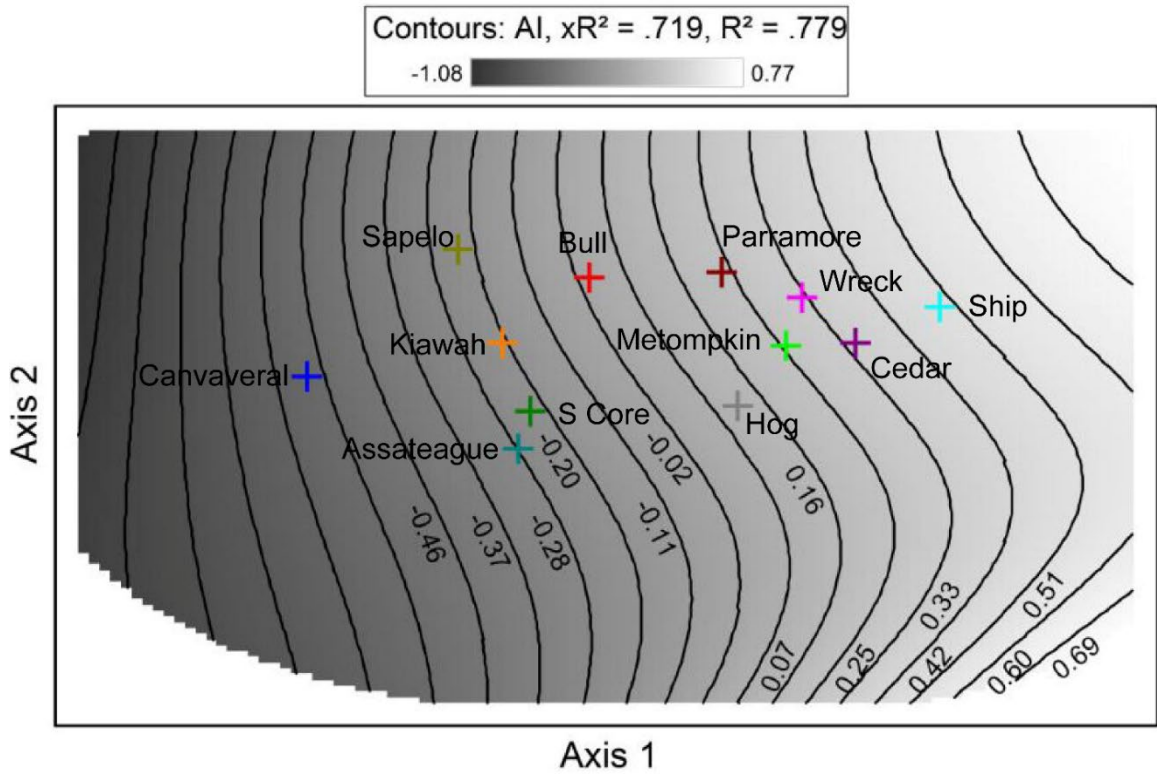
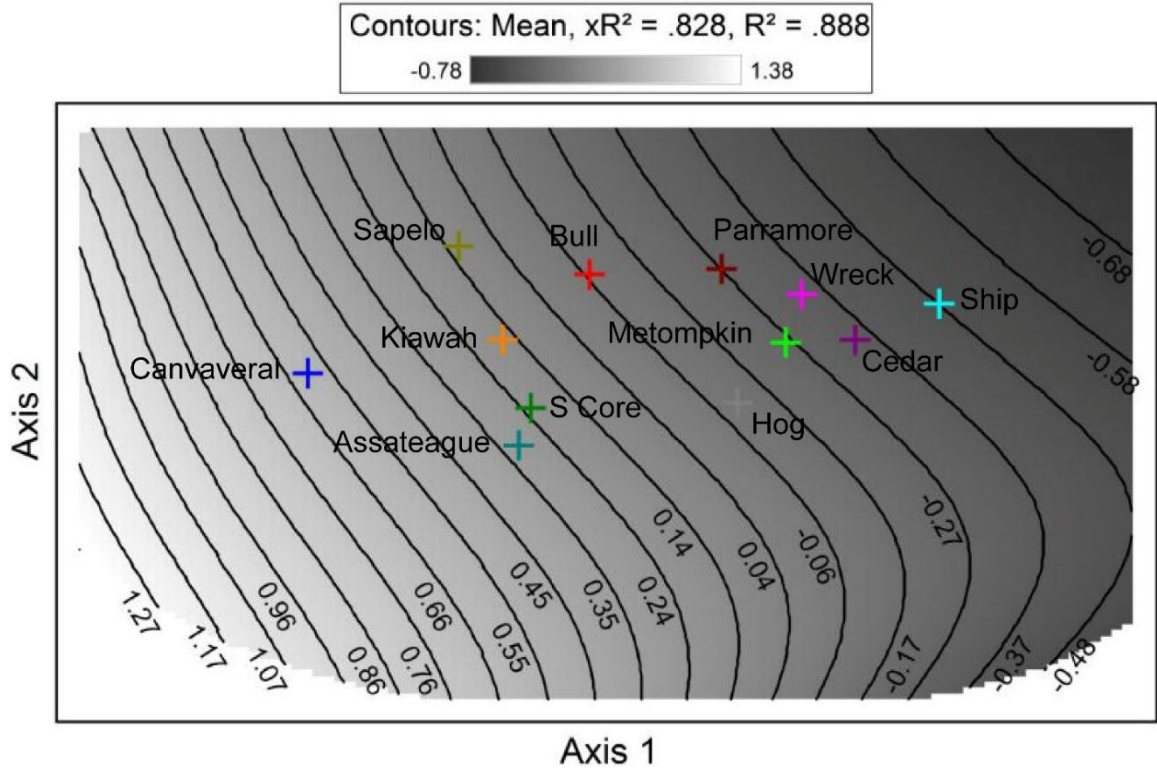
**Figure 4. 3** DEMs illustrating the contrasts in landscape indices of patch elevational structure among island sites. The first value is the original FRAGSTATS index value and the second is its equivalent Z-score value.

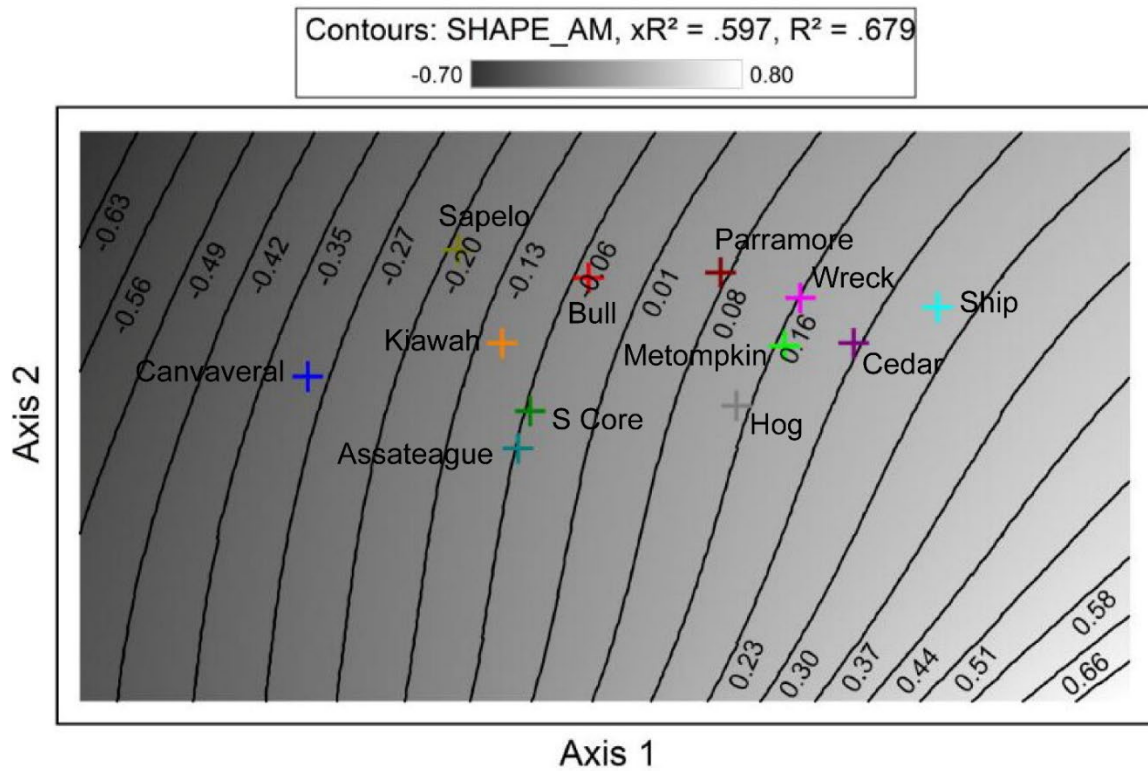
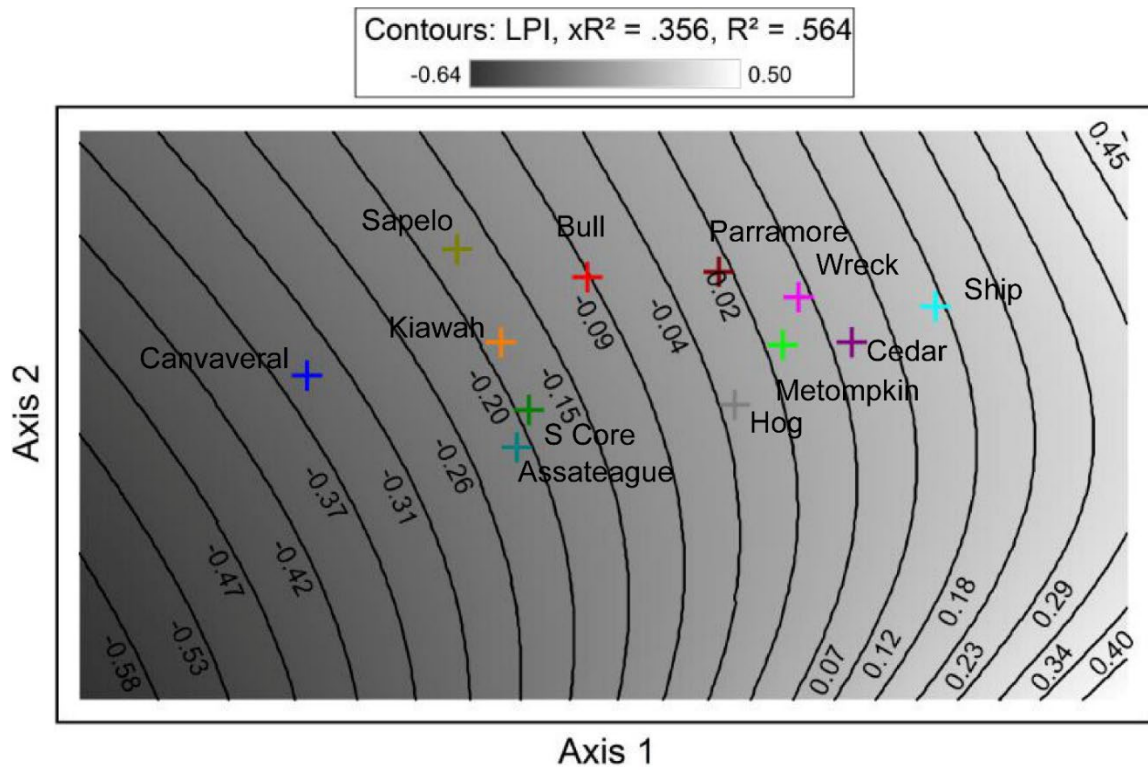


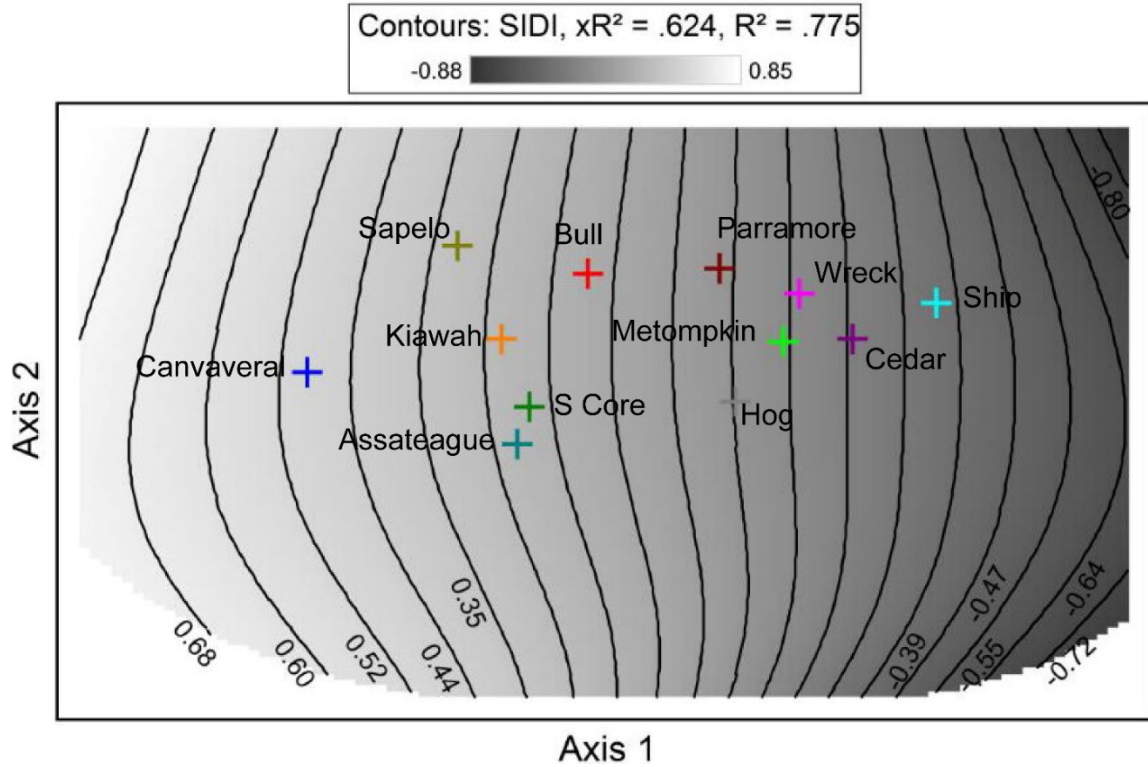
**Figure 4. 4** Six Moran's  $I$  values were sampled from the directional correlograms and ordinated using PCoA to distill spatial autocorrelation structure into individual metrics. Sampling to obtain these six observations follows these instructions: (a) Find first non-zero Moran's  $I$  value (Point 2), (b) Find halfway point between Point 2 and Start (Point 1). (c) Find last value (Point 6), (d) Find midpoint between Point 2 and Point 6 (Point 4), (e) Find midpoint between Point 2 and Point 4 (Point 3), (f) Find halfway point between Point 4 and Point 6 (Point 5).



**Figure 4. 5** Topographic state space. Cross symbols represent centroids for all the plots of an individual island. Lines are convex hulls connecting the plots of the island. Abbreviation list: Assa: Assateague Island, Cedar: Cedar Island; Hog: Hog Island; Meto: Metompkin Island; Par: Parramore Island, Ship: Ship Shoal Island; Wreck: Wreck Island; Bull: Bull Island; Canav: Canaveral Island; Kiawah: Kiawah Island; Sapelo: Sapelo Island; Score: South Core Banks.



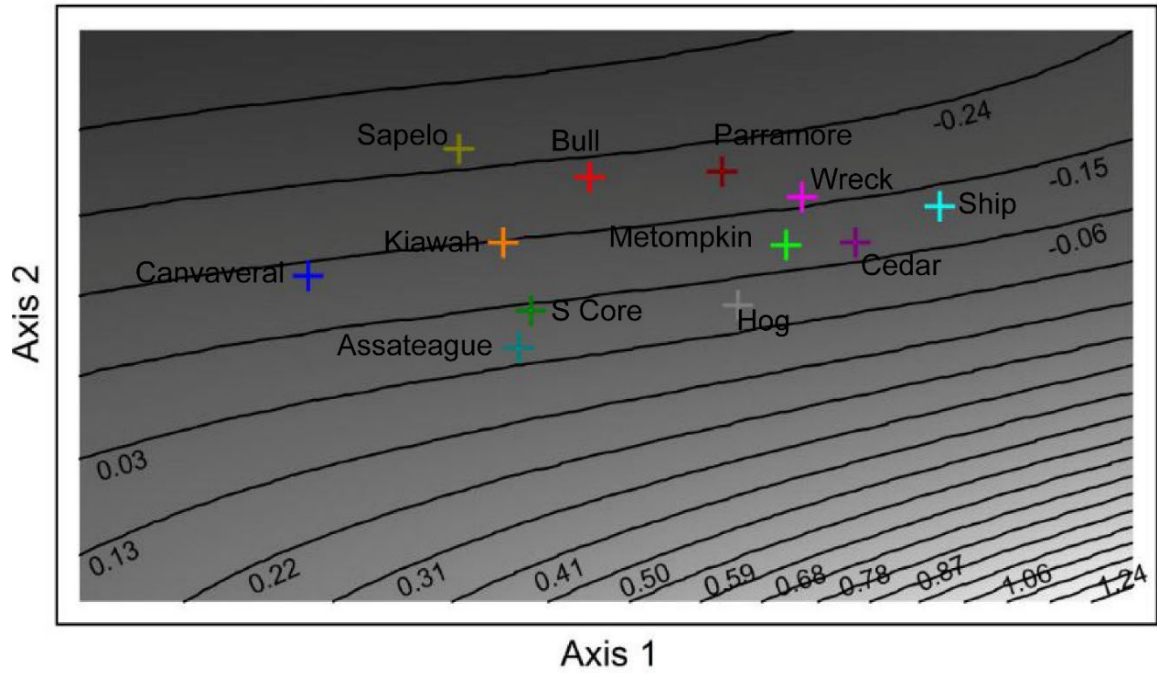





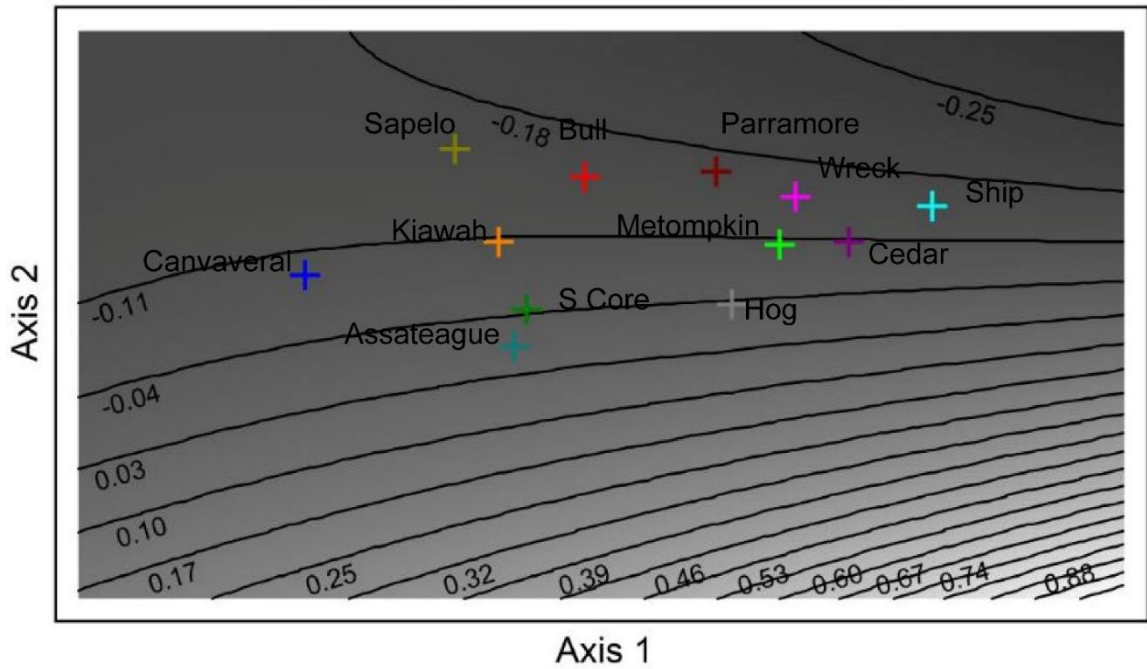
**Figure 4. 6** Island centroids and response surfaces for mean elevation, AI, LPI, SHAPE\_AM, and SIDI. AI is often correlated with IJI. SHAPE\_AM and PAFRAC also measure similar properties. These two variables are not shown. Mean site mean elevations: Assateague Island, 1.64 m; Metompkin Island, 0.99 m; Cedar Island, 0.75 m; Parramore Island, 0.90 m; Hog Island, 1.03 m; Wreck Island, 0.74 m; and Ship Shoal Island, 0.74 m; South Core Banks, 1.65 m; Bull Island, 1.03 m; Kiawah Island, 1.45 m; Sapelo Island, 1.44 m, and Canaveral Island, 2.22 m.

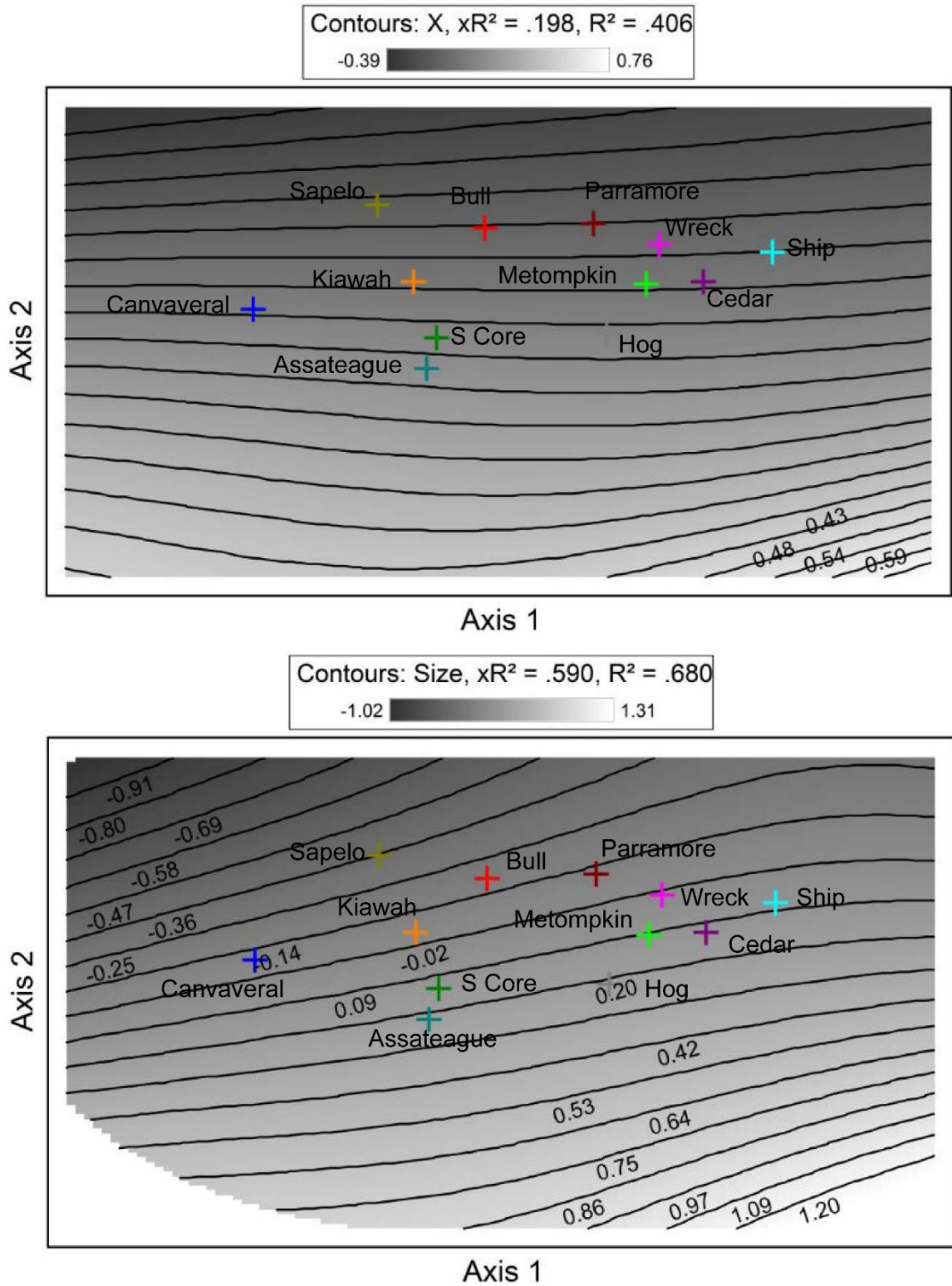


Contours: Kurtosis,  $xR^2 = .674$ ,  $R^2 = .769$   
 -0.43  1.52

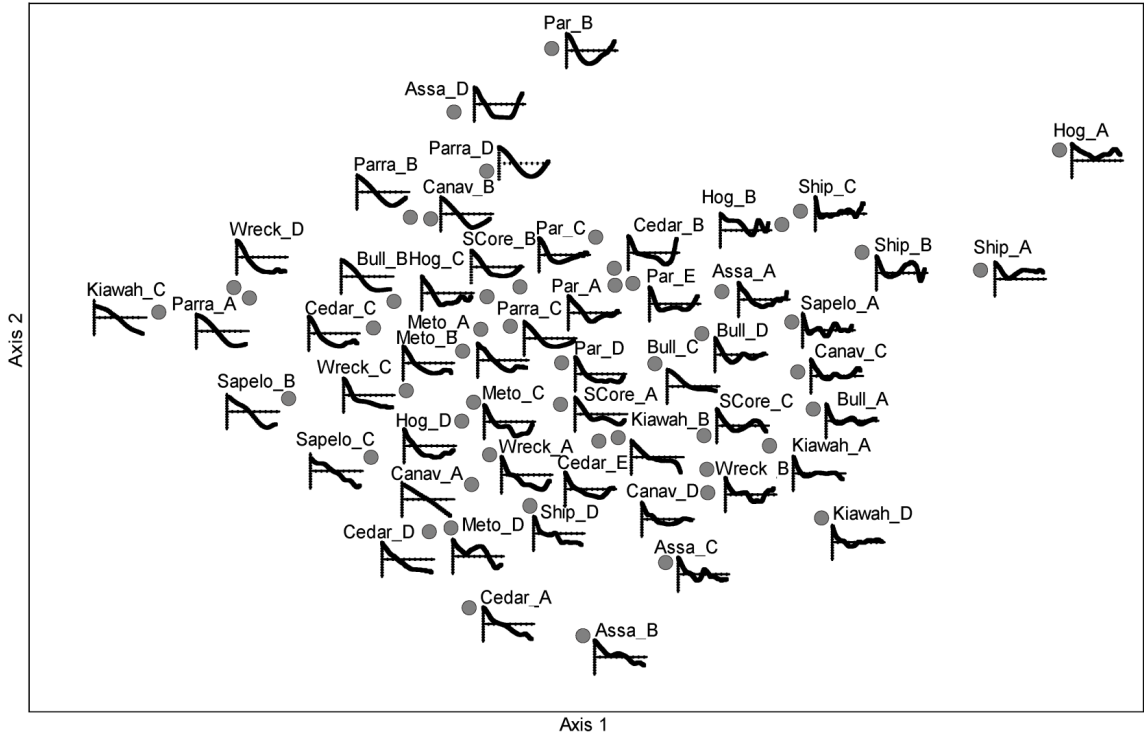


Contours: Skewness,  $xR^2 = .331$ ,  $R^2 = .482$   
 -0.32  1.17

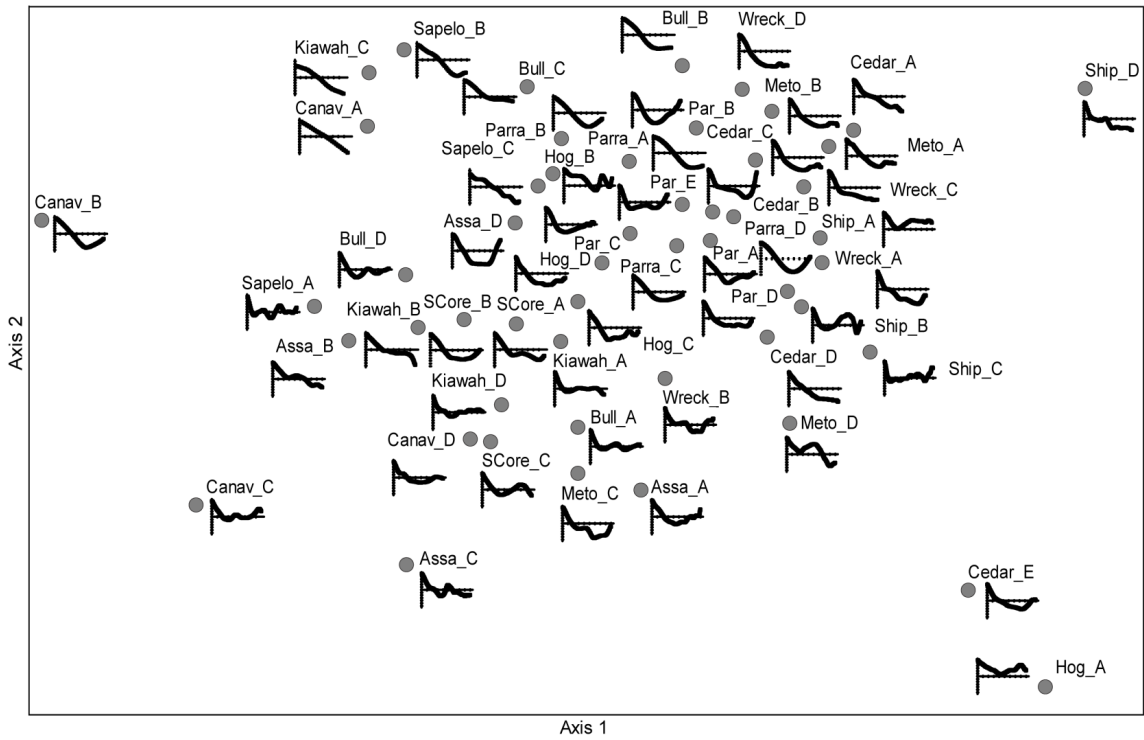




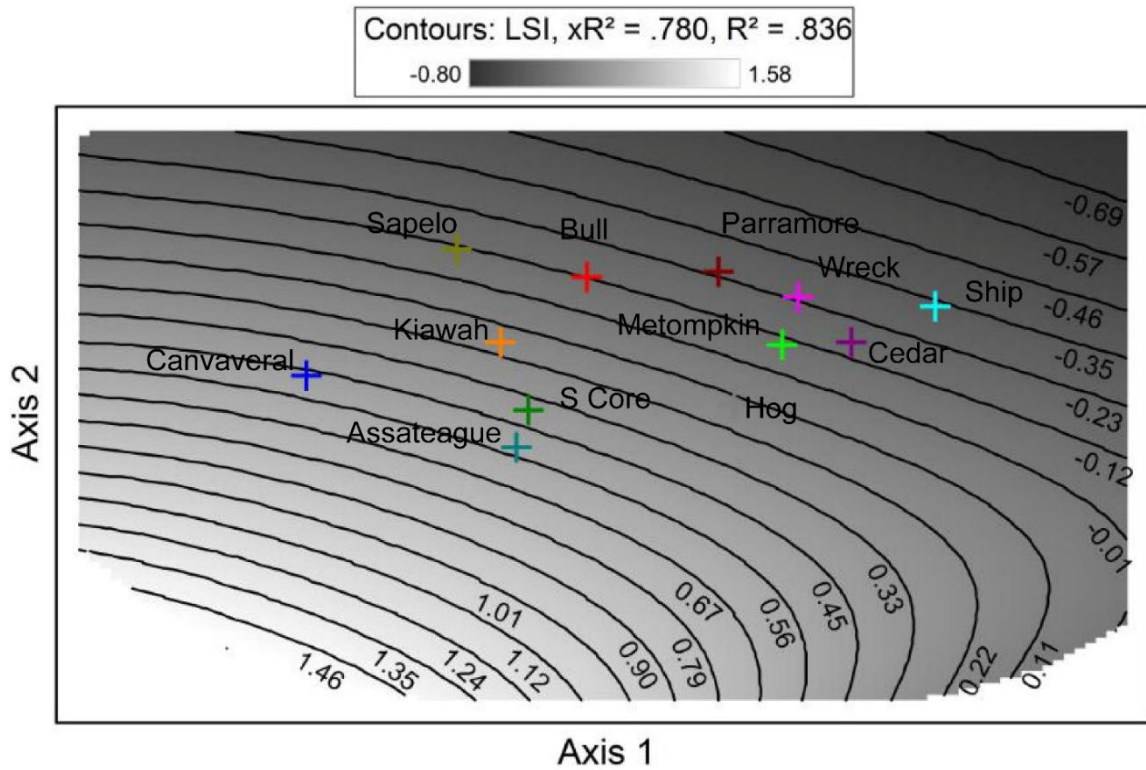
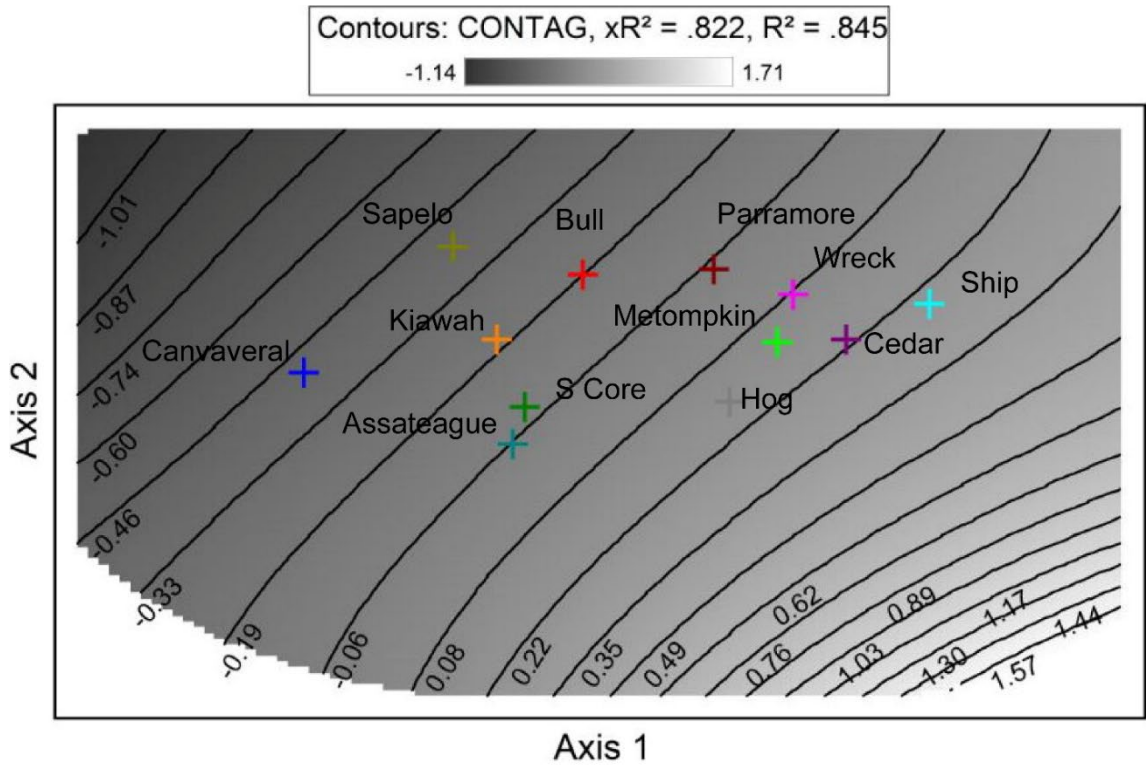
**Figure 4. 7** Island centroids and response surfaces for kurtosis, skewness, spatial autocorrelation structure, and size.

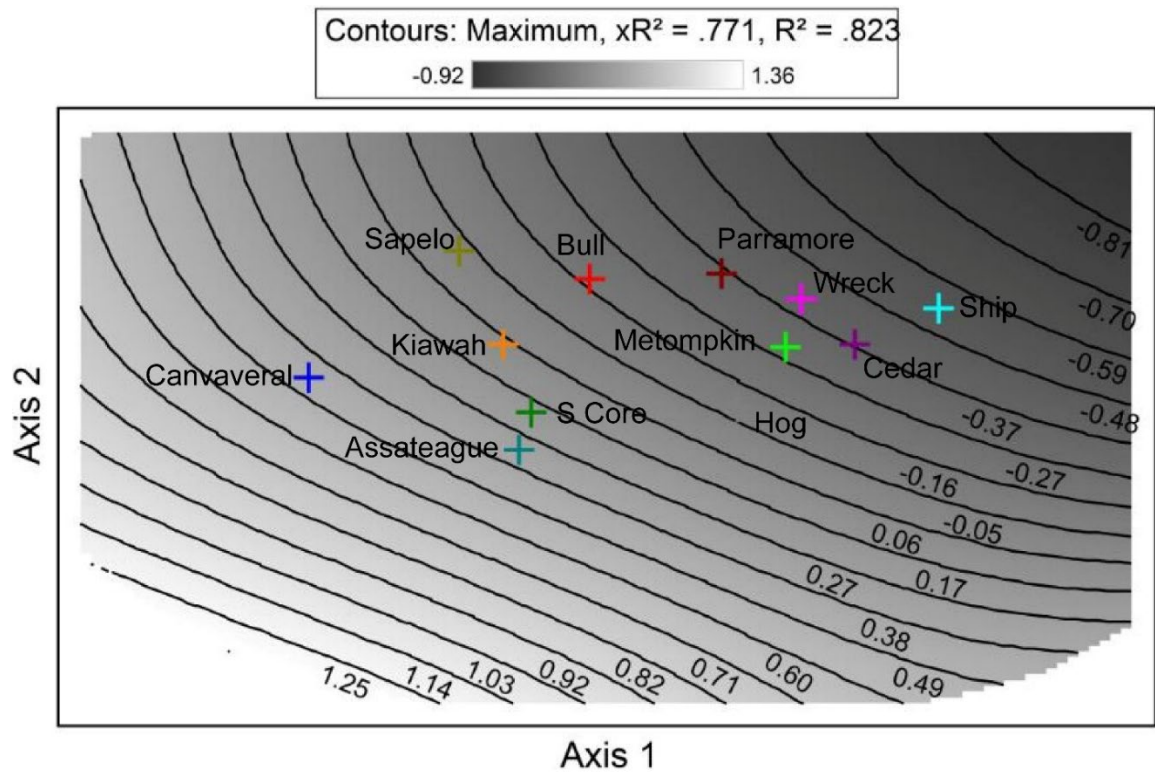


**Figure 4. 8** PCoA scatterplot for the combined dataset, showing variability in the directional spatial autocorrelation structure among island plots.

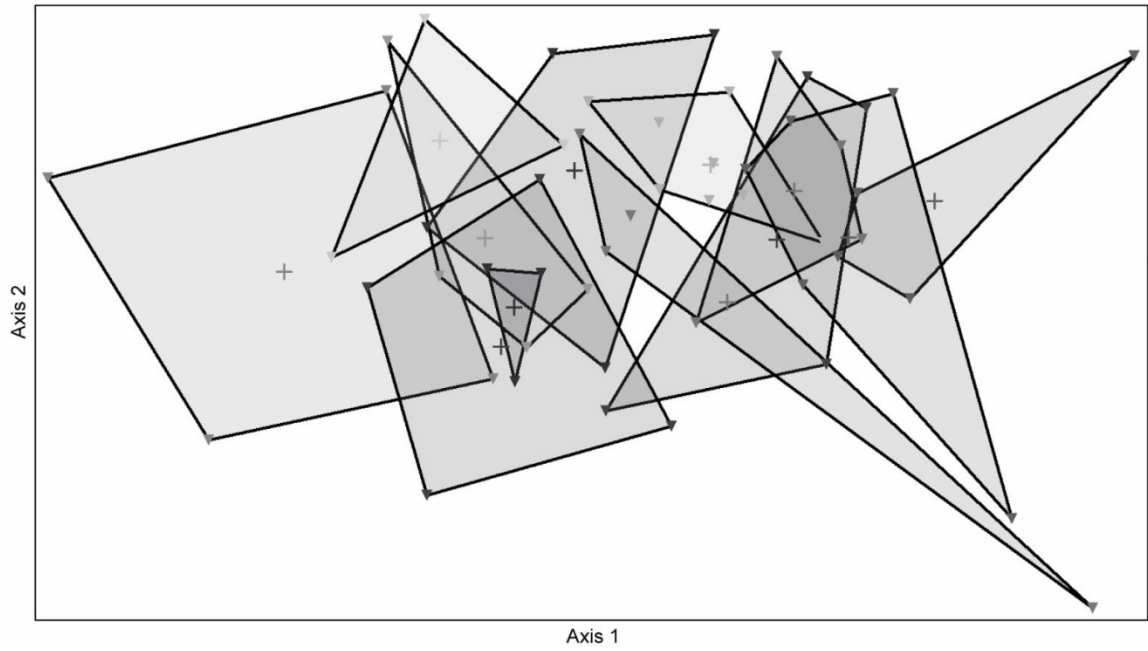


**Figure 4. 9** Directional correlograms for each site plotted in NMDS state space.





**Figure 4. 10** Island centroids and response surfaces for CONTAG, LSI, and maximum elevation.



**Figure 4. 11** Gray scale convex hulls. Darker shades indicate more frequently observed topographies. Light areas indicate infrequently observed topographies.

## Chapter 5. Conclusion

The studies of barrier island dune biogeomorphic recovery and response dynamical states (Stallins, 2005; Wolner et al. 2013; Brantley et al. 2014; Durán and Moore 2015; Goldstein and Moore 2016) have relied on numerical simulations and field observations. These studies were also developed in two different regions, the Georgia Bight and the Virginia coast. A relatively small number of islands were used to advance the concept of dune stability domains of Stallins (2005) in the Georgia Bight and high and low island dune states (Durán and Moore 2015) in Virginia. These models of biogeomorphic processes describe organizational states of barrier dunes that exhibit resistance and resilience. Even though dune topography plays a large role in these models of dune response and recovery, topographic characterization has been based on a few elevational variables. Levels of resistance and resilience are assigned to topographies, but the basis for ascribing these two properties to stretches of coast lacks a firm theoretical and methodological basis. In addition, stability domain dynamics were associated with island morphologies. High and low island states, by contrast, rely only on elevational properties. More rigorous comparisons of the topography across these regions and among the islands that comprise them would provide information about the validity of generalizations that have been made about resilience properties, especially if resilience properties could be quantified and linked to topography in a robust manner. I have anchored my approach in resilience theory to compare topographies and resilience properties. Through the modeling of cross-scale resilience, multiple representations of dune topography were systematically compared, and these topographies were linked to their resilience properties. State space, and the structure of this cross-scaled data, provided a means to articulate and test hypotheses regarding

differences in topography and their resilience properties among selected barrier islands of the Georgia Bight and Virginia.

Three sets of questions were posed in three analytical chapters. In my first analytical chapter, I examined how dune topography varies according to island morphologies of the Virginia coast and found that local controls also important in shaping the dune topography. In my second analytical chapter, I documented how two different barrier coast regions, the Georgia Bight and the Virginia coast, differ in topography and in their resilience properties. Dimensionality and the loading of topographic metrics on these axes in state space were utilized to assess resilience prosperities. Dimensionality and the loading of topographic metrics on these axes in state space were utilized to assess resilience prosperities. Compared with the Virginia barrier dune system, the Georgia Bight one is more resilient and has well-developed spatial structuring in dune topography. In my third analytical chapter, I discussed the structure of the topographic state space to provide more evidence that these axes represent biogeomorphic processes affiliated with resistance and resilience. Similar dune topographic features of contagion or regularity were not necessarily shaped by the same processes; it is matter in the difference in resistance and resilience.

## **5.1 Dune topography and island morphologies along the Virginia coast**

Along the Virginia coast, dune topography was shown to be associated with island morphology. Classification of morphological compartments of the Virginia Barrier Islands by Leatherman (1982), Rice and Leatherman (1983), Deaton et al. (2017) and Haluska (2017) paralleled the way in which dune topography varied, as inferred from the position



of island topographies in state space. However, local within-island variability of erosion and deposition does play a role in where topographies for an island plotted in state space. Human engineering of the coast on two islands, Assateague Island and Wallops Island, altered the topography of study sites on Metompkin and Cedar islands. Sites from Metompkin and Cedar plotted among sites from the lowest elevational islands in state space (Wreck and Ship Shoal) and farther from the morphological compartment adjacent to them along the coast (Assateague). Data from Haluska (2017) validated that the variability in topography along an individual island could be attributed to shifts in shoreline accretion and erosion alongshore. Although dune topography has a propensity to track with island morphology, within-island variability in erosion and accretion can override some of the affinities of topography with island morphological context. In general, the tide-dominated barrier islands, even with their smaller size, had a greater divergence of topography than the only wave-dominated island morphology in the study (Assateague Island). This finding is in agreement with Mulhern et al. (2017). They observed that the morphology of tide-dominated islands tends to be more variable than that of wave-dominated islands. In part, the smaller size of the tide-dominated barrier islands of the Virginia coast may make them more sensitive to changes in erosion and accretion along their length. The closer proximity to tidal inlets, which serve as sinks and sources of sediment, may create more frequent changes in adjacent topographies.

## **5.2 Comparing topography and resilience across two barrier coast regions**

This chapter aimed to compare topographies of the Virginia coast with those from the Georgia Bight, and to examine the two existing biogeomorphic models of barrier island resilience properties. These models do not quantify resilience properties nor link them to

topographic variability along a large geographic stretch of coast. Cross-scale data modeling of resilience and topography in state space provided the means to compare topographies and associate them with resilience properties in a systematic, quantitative manner. A common critique of exploratory, descriptive studies in geography is the lack of controls. However, a replicate sampling, one in each regional data set, confirmed that the sampling strategy employed was not overly sensitive to sample bias or to the point in time in which the LiDAR data was collected. Parramore Island was sampled twice, each time by different investigators independently, each using a different LiDAR data set (2012 and 2014). The topographies produced in these separate samplings fell near each other in state space. In general, the cross-scale modeling of dune topographic state space and its visualization as topographic state space was in agreement with the known contrasts in nearshore conditions that define the Georgia Bight and the Virginia coast. The dimensionality of data and the trends in how low-dimensional resistance metrics and high dimensional resilience metrics loaded on the axes of the state space provided the quantitative evidence for my findings.

### 5.2.1 Topographic differences between Virginia and the Georgia Bight

Only two dimensions were needed to define the state space of the predominantly erosional, low-relief Virginia islands. Elevation was a major influence on topography, but the correlations of all the topographic metrics with state space axis positions were weaker and exhibited greater multicollinearity. This suggested that topography across all scales appears to be more directly coupled to exogenous events such as overwash. In contrast, the Georgia Bight state space had three dimensions and less multicollinearity. Axis correlations were stronger and tended to be distributed across all three axes. Spatial structuring was more strongly developed. Patch and gradient metrics loaded more strongly on higher

dimensional axes and were less collinear with elevation. This suggested a greater role for endogenous biogeomorphic development. Topography is certainly subject to storm inputs in the Georgia Bight, but because these islands are not as low and erosional as the Virginia coast, dune vegetation may contribute more to landscape-extent topography. In Virginia, dune vegetation may be limited to more of an anchoring function, with less propensity for biogeomorphic feedbacks to be integrated into landscape-extent topographic structure.

The Virginia island sites occupied a mostly separate area from the Georgia Bight in the combined state space. Dunes on the Virginia Barrier Islands are lower and vary less in elevation over large horizontal distances. Landforms are more curvilinear in shape. The Georgia Bight topographies exhibited more rectilinear shore-parallel landforms. Topography was higher and more variable over shorter horizontal distances. The two regions are largely defined by elevational differences expressed along the first axis of the combined state space. Islands from the Georgia Bight were more strongly differentiated along the second axis of combined state space. Topographic differences along the second axis tracked contrasts in the kurtosis or peakedness of elevation observations across their surface, the size of each site, and in the variability of elevation within sites. Because the Georgia Bight islands occurred along a broader length of the second axis, they can be considered more strongly structured by these spatially explicit higher-dimension properties than the Virginia Barrier Islands.

The distinctiveness of the Virginia Barrier Islands in state space was attributed to the rapid rates of relative sea level rise along the Virginia coast (Leatherman 1982; Sallenger et al. 2012; Haluska 2017; Deaton et al. 2017), which may in part also reflect the differences between regions in sediment availability. Their distinctiveness may also be a

consequence of the impacts of Hurricane Sandy in 2012. However, Hapke et al. (2016) found that the response to Sandy at Fire Island, New York was not notable or distinguishable from several other large storms of the prior decade. Island morphology, as shaped by complex nearshore patterns of wave and tidal energy. Island morphology, as shaped by complex nearshore patterns of wave and tidal energy (Hayes 1979; Davis and Hayes 1984; Hayes 1994; Mulhern et al. 2017), was not the dominant influence on dune topography in the combined state space, was not the dominant influence on dune topography in the combined state space. Tide-dominated island morphologies from Virginia and the Georgia Bight had topographies that fell all along the first axis. By contrast, well-structured topographic trends based on island morphology developed for the second axis and mostly for the islands in the Georgia Bight.

### 5.2.2 Resilience properties and the compatibility of existing dune dynamical models

The greater length of the first axis and its affinity with elevation suggests that resistance is a dominant influence on the structure of the combined state space. Resistance along the first and major axis of topographic state space may be more a consequence of the direct anchoring effects of vegetation, and less from the biogeomorphic feedbacks that can develop and integrate spatially across landscape extents described in Stallins (2005). These anchoring effects likely confer some resilience along the first axis of state space. We posited that the first axis of the state space derived in this study captures aspects of Durán and Moore's (2015) model of low and high island states developed for the low relief Virginia Barrier Islands.

Metrics indicative of landscape-extent biogeomorphic resilience were correlated with the second axis, which explained less variance in the data set than the first axis. Thus, resilience can be considered a less dominant dimension of topographic state space than resistance. Topographies distributed along the second axis spanned mixed-energy, tide-dominated barrier island morphologies to those that were more wave-dominated. Thus, the second axis may better represent the potentially resilience-maximizing stability domains affiliated with island morphology described by Stallins (2005). Resilience is higher at either end of the second axis, and can be attributed to the landscape-extent biogeomorphic feedbacks postulated for the stability domain dynamics. The resilience associated with island morphology along the second axis developed only at intermediate elevations along the middle of this first axis.

In short, based on the elevation variable only, Duran and Moore's (2015) model presented the resistance variation from high islands to low islands in Virginia. Within the intermediate elevations, bistability occurred; however, landscape-extent biogeomorphic resilience proposed by Stallins (2005) based on field observations in the Georgia Bight was not considered. My findings from state space integrate these two models to fully consider resilience properties across a large geographic area from Virginia to Florida and link the biogeomorphic resilience to dune topographic features by the cross-scale data modeling of dune topography. Through this dissertation, I have identified common ground between the two existing models of barrier island dune states. They illuminate different, but complementary, properties of resilience.

### 5.3 Using response curves to delineate resistance and resilience

The goal in this chapter was to use differences in how dune topographic metrics correlated with the axes of state space to convey that these axes capture geomorphic and biogeomorphic processes related to resilience. Dune topographic metrics correlated with the first axis demarcated the geomorphic boundary conditions for barrier dunes. These conditions define the extremes of elevation and the range of resistance for the barrier island sites included in this study. Conditions along this elevational continuum switch, likely gradually, from aggradational to erosional. Dune topographic metrics correlated the second axis demarcated resilience organized around biogeomorphic interactions of dune landforms and vegetation across the continuous surface of the landscape.

The dune topographic metrics that were correlated with both axes that were more useful to validate the interpretation of the first axis as geomorphic and the second axis as biogeomorphic. The generally higher elevation islands of South Core Banks and Assateague had topographic contagion indices like lower-lying Parramore Island in Virginia. Contagion on these higher islands equivalent to contagion on a low-lying, more frequently overwashed erosional island may be due to greater biogeomorphic modification and reinforcement of overwash exposure on the higher islands. In other words, dune plants on South Core and Assateague augment exposure to overwash to the extent the topography has a contagion value like a lower island. Conversely, the islands of Sapelo and Kiawah had contagion values like those on a higher island, Cape Canaveral in Florida. In this case, the lower islands of Sapelo and Kiawah may have a contagion value like a higher island due to the increased resistance to overwash promoted by biogeomorphic processes on Sapelo and Kiawah. Vegetation-mediated dune and swale topographies may confer

resistance such that a lower, potentially more exposed island has reduced contagion values as on a higher island.

Topographic regularity was another variable that permits inference of the geomorphic and biogeomorphic components of state space. Sapelo had the same level of topographic regularity as a lower, frequently overwash island, Metompkin Island in Virginia. Similarly, Kiawah Island in South Carolina was higher than Hog Island, but these two islands also had the same levels of topographic regularity. Regularity in topography is a consequence of homogenizing geomorphic processes associated with storm exposure and erosion on Metompkin and Hog Island. On Sapelo and Kiawah, regularity in topography may be more related to biogeomorphic interactions that create regularity. Higher elevations and less frequent overwash disturbance on Sapelo and Kiawah may promote more regular shore-parallel landforms.

Like contagion and topographic regularity, maximum elevation was also correlated with both axes and could also be used to confirm the geomorphic and biogeomorphic components of state space. Similar maximum elevations developed on islands with different mean elevations. Lower-lying islands may have had equivalent maximum elevations to high islands because of erosional dune remnants. Due to pervasive erosion and frequent overwash on low islands, an erosional high may remain in the landscape. A negative or inverted topography may develop, in which vegetation plays mostly an anchoring role, particularly at high elevations. On higher islands these maximums may occur through more aggradational biogeomorphic feedbacks that result in high positive relief.

#### **5.4 Broader implications**

Several findings of this dissertation have broader implications. First, resistance, rather than resilience, is the more dominant property structuring the dynamic responses of barrier dunes to high water events. Yet quantifying resilience properties for coastal dunes may be best inferred through comparison and contrast rather than by attempting to attach a level of resistance or resilience to a local site. Considerable topographic variability, and thus variability in resilience properties, were expressed alongshore of all the islands. Resistance and resilience is an emergent property, a propensity rather than an at a point property.

Another broader implication is that it is important to use different representations of topography if the goal is to compare topographies and infer resistance and resilience from them. What variables are used to define topography will shape what resilience properties are observed. By making comparisons of topography from metrics derived from these representations that associate with resistance and resilience, I posited that the two models of barrier island dune dynamical states (Stallins 2005; Durán and Moore 2015) capture different but complementary resilience properties. Both incorporate resistance, but they differ in how they ascribe resilience. Stability domains represent more of the landscape spatial processes, which are difficult to model in detail. In high and low state models, resilience is more correlated with resistance. The anchoring effects of vegetation and dune height is the primary topographic criteria.

The findings of this study are limited in that only topography was sampled, and vegetation was not, even though topography and vegetation are tightly coupled on coastal dunes. More experimentation is necessary to distill the topographic metrics that would



optimize the modeling of topographic state space to infer its resilience properties. Space was emphasized over time, an important dimension for understanding the combined effects of sea-level rise and storm exposures. Stutz and Pilkey (2011) identified approximately 2100 barrier islands in their global inventory. The addition of more dune topographies from other islands, particularly those from Texas and the northern Gulf of Mexico, or those of the German Bight, would be the next step in the development of topographic state space. Using LiDAR data from different years for the same location would also contribute detail to state space. Nonetheless, the Virginia coast and especially the Georgia Bight exhibit a wide range of island morphologies. This study has provided some initial boundaries for barrier dune topographic state space. However, as a result of rising sea levels, coastal barrier dune topographies may already be converging upon a smaller region of state space, as has been recently observed for the Virginia islands (Zinnert et al. 2019). Tracking a large number of islands over time would provide a unified record of dune pattern and process and the responses that occur in response to rising sea levels and more frequent incursions of storm surge.

## Bibliography

- Allen CR, Gunderson L, Johnson AR (2005) The use of discontinuities and functional groups to assess relative resilience in complex systems. *Ecosystems* 8:958-966.
- Allen CR, Holling C (2010) Novelty, adaptive capacity, and resilience. *Ecology and society* 15(3)
- Allen CR, Angeler DG, Cumming GS, Folke C, Twidwell D, Uden DR (2016) Quantifying spatial resilience. *Journal of Applied Ecology* 53(3):625-635
- Anthony EJ, Orford JD (2002) Between wave- and tide-dominated coasts: the middle ground revisited. *Journal of Coastal Research* SI 36:8-15
- Baas AC, Nield JM (2010) Ecogeomorphic state variables and phase-space construction for quantifying the evolution of vegetated aeolian landscapes. *Earth Surface Processes and Landforms* 35(6):717-731
- Barros C, Thuiller W, Georges D, Boulangeat I, Münkemüller T (2016) N-dimensional hypervolumes to study stability of complex ecosystems. *Ecology letters* 19(7):729-742
- Bauer BO, Veblen TT, Winkler JA (1999) Old methodological sneakers: fashion and function in a cross-training era. *Annals of the Association of American Geographers* 89 (4):679-687
- Bel G, Hagberg A, Meron E (2012) Gradual regime shifts in spatially extended ecosystems. *Theoretical Ecology* 5:591-604
- Bissonette JA (2017) Avoiding the scale sampling problem: a consistent solution. *Journal of Wildlife Management* 81(2):192-205
- Brantley ST, Bissett SN, Young DR, Wolner CW, Moore LJ (2014) Barrier island morphology and sediment characteristics affect the recovery of dune building grasses following storm-induced overwash. *PLOS ONE* 9(8):e104747
- Brown JK, Zinnert JC (2018) Mechanisms of surviving burial: dune grass interspecific differences drive resource allocation after sand deposition. *Ecosphere* 9(3):e02162
- Brunsdon D, Thornes J (1979) Landscape sensitivity and change. *Transactions of the Institute of British Geographers* 4(4): 463-484
- Brunsdon D (2001) A critical assessment of the sensitivity concept in geomorphology. *Catena* 42(2): 99-123
- Carter R (1991) Near-future sea level impacts on coastal dune landscapes. *Landscape Ecology* 6(1-2):29-39
- Chartier M, Jabbour F, Gerber S, Mitteroecker P, Sauquet H, Balthazar M, Staedler Y, Crane PR, Schönenberger J (2014) The floral morphospace—a modern comparative approach to study angiosperm evolution. *New Phytologist* 204(4):841-853

- Collins SL, Avolio ML, Gries C, Hallett LM, Koerner SE, La Pierre KJ, Rypel AL, Sokol ER, Fey SB, Flynn DFB, Jones SK, Ladwig LM, Ripplinger J, Jones M.B (2018) Temporal heterogeneity increases with spatial heterogeneity in ecological communities. *Ecology* 99:858-865
- Corenblit D, Tabacchi E, Steiger J, Gurnell AM (2007) Reciprocal interactions and adjustments between fluvial landforms and vegetation dynamics in river corridors: A review of complementary approaches. *Earth-Science Reviews* 84(1):56-86
- Corenblit D, Steiger J, Gurnell AM, Naiman RJ (2009) Plants intertwine fluvial landform dynamics with ecological succession and natural selection: a niche construction perspective for riparian systems. *Global Ecology and Biogeography* 18(4):507-520
- Corenblit D, Baas AC, Balke T, Bouma T, Fromard F, Garófano-Gómez V, González E, Gurnell AM, Hortobágyi B, Julien F, Kim D, Lambs L, Stallins JA, Steiger J, Tabacchi E, Walcker R (2015) Engineer pioneer plants respond to and affect geomorphic constraints similarly along water-terrestrial interfaces world-wide. *Global Ecology and Biogeography* 24(12):1363-1376
- Cumming GS (2011) Spatial resilience: integrating landscape ecology, resilience, and sustainability. *Landscape Ecology* 26(7):899-909
- Cumming GS, Morrison TH, Hughes TP (2017) New directions for understanding the spatial resilience of social-ecological systems. *Ecosystems* 20(4):649-664
- Cushman SA, McGarigal K, Neel MC (2008) Parsimony in landscape metrics: strength, universality, and consistency. *Ecological Indicators* 8(5):691-703
- Davis RA, Hayes MO (1984) What is a wave-dominated coast?. *Marine Geology* 60(1):313-329
- Davis RA (1994) Chapter 1 Barrier island systems-a geologic overview. In: Davis RA (ed) *Geology of Holocene barrier island systems*. Springer-Verlag, Berlin Heidelberg, pp 1-46
- Davidson-Arnott R, Hesp P, Ollerhead J, Walker I, Bauer B, Delgado-Fernandez I, Smyth T (2018) Sediment budget controls on foredune height: comparing simulation model results with field data. *Earth Surface Processes and Landforms* 43 (9):1798-1810
- Deaton CD, Hein CJ, Kirwan ML (2017) Barrier island migration dominates ecogeomorphic feedbacks and drives salt marsh loss along the Virginia Atlantic Coast, USA. *Geology* 45(2):123-126
- Dilts TE, Yang J, Weisberg PJ (2010) The landscape similarity toolbox: new tools for optimizing the location of control sites in experimental studies. *Ecography* 33(6):1097-1101

- Donohue I, Petchey OL, Montoya JM, Jackson AL, McNally L, Viana M, Healy K, Lurgi M, O'Connor NE, Emerson MC (2013) On the dimensionality of ecological stability. *Ecology letters* 16(4):421-429
- Donohue I, Hillebrand H, Montoya JM, Petchey OL, Pimm SL, Fowler MS, Healy K, Jackson AL, Lurgi M, McClean D, O'Connor NE, O'Gorman EJ, Yang Q (2016) Navigating the complexity of ecological stability. *Ecology letters* 19(9):1172-1185
- Downs PW, Gregory KJ (1995) Approaches to river channel sensitivity. *The Professional Geographer* 47(2):168-175
- Durán O, Moore LJ (2013) Vegetation controls on the maximum size of coastal dunes. *Proceedings of the National Academy of Sciences* 110(43):17217-17222
- Durán O, Moore LJ (2015) Barrier island bistability induced by biophysical interactions. *Nature Climate Change* 5(2):158-162
- Everard M, Jones L, Watts B (2010) Have we neglected the societal importance of sand dunes? An ecosystem services perspective. *Aquatic Conservation: Marine and Freshwater Ecosystems* 20(4):476-487
- Feagin R, Wu X, Smeins F, Whisenant S, Grant W (2005) Individual versus community level processes and pattern formation in a model of sand dune plant succession. *Ecological Modelling* 183 (4):435-449
- Feagin RA, Wu XB (2007) The spatial patterns of functional groups and successional direction in a coastal dune community. *Rangeland Ecology & Management* 60(4):417-425
- Feagin RA, Smith WK, Psuty NP, Young DR, Martínez ML, Carter GA, Lucas KL, Gibeaut JC, Gemma JN, Koske RE (2010) Barrier islands: coupling anthropogenic stability with ecological sustainability. *Journal of Coastal Research* 26(6):987-992.
- Feagin RA, Figlus J, Zinnert JC, Sigren J, Martínez ML, Silva R, Smith WK, Cox D, Young DR, Carter G (2015) Going with the flow or against the grain? The promise of vegetation for protecting beaches, dunes, and barrier islands from erosion. *Frontiers in Ecology and the Environment* 13(4):203-210
- Feagin R, Furman M, Salgado K, Martinez M, Innocenti R, Eubanks K, Figlus J, Huff T, Sigren J, Silva R (2019) The role of beach and sand dune vegetation in mediating wave run up erosion. *Estuarine, Coastal and Shelf Science* 219:97-106
- Fenster MS, Dolan R, Smith JJ (2016) Grain-size distributions and coastal morphodynamics along the southern Maryland and Virginia Barrier Islands. *Sedimentology* 63(4):809-823
- Fonstad MA, Marcus WA (2010) High resolution, basin extent observations and implications for understanding river form and process. *Earth Surface Processes and Landforms* 35(6):680-698

- Fryirs KA (2017) River sensitivity: a lost foundation concept in fluvial geomorphology. *Earth Surface Processes and Landforms* 42(1):55-70
- Génin A, Majumder S, Sankaran S, Schneider FD, Danet A, Berdugo M, Guttal V, Kéfi S (2018) Spatially heterogeneous stressors can alter the performance of indicators of regime shifts. *Ecological Indicators* 94 (1):520-533
- Godfrey PJ, Godfrey MM (1976) Barrier island ecology of Cape Lookout National Seashore and vicinity, North Carolina. U.S. Government Printing Office, Washington, DC
- Godfrey PJ (1977) Climate, plant response and development of dunes on barrier beaches along the U.S. east coast. *International Journal of Biometeorology* 21(3):203-216.
- Godfrey PJ, Leatherman SP, Zaremba R (1979) A geobotanical approach to classification of barrier beach systems. In: Leatherman SP (ed) *Barrier Islands*. Academic Press, New York, pp 99-126
- Goldstein EB, Moore LJ (2016) Stability and bistability in a one-dimensional model of coastal foredune height. *Journal of Geophysical Research: Earth Surface* 121(5):964-977
- Goldstein EB, Moore LJ, Durán Vinent O (2017) Lateral vegetation growth rates exert control on coastal foredune hummockiness and coalescing time. *Earth Surface Dynamics* 5(3):417-427
- Goldstein EB, Mullins EV, Moore LJ, Biel RG, Brown JK, Hacker SD, Jay KR, Mostow RS, Ruggiero P, Zinnert JC (2018) Literature-based latitudinal distribution and possible range shifts of two US east coast dune grass species (*Uniola paniculata* and *Ammophila breviligulata*). *PeerJ* 6:e4932
- Grimm V, Wissel C (1997) Babel, or the ecological stability discussions: an inventory and analysis of terminology and a guide for avoiding confusion. *Oecologia* 109 (3):323-334.
- Gunderson LH (2000) Ecological Resilience—in theory and application. *Annual Review of Ecology and Systematics* 31(1):425-439
- Gunz P, Bookstein FL, Mitteroecker P, Stadlmayr A, Seidler H, Weber GW (2009) Early modern human diversity suggests subdivided population structure and a complex out-of-Africa scenario. *Proceedings of the National Academy of Sciences* 106 (15):6094-6098
- Gutierrez BT, Williams SJ, Thieler ER (2007) Potential for shoreline change due to sea-level rise along the US Mid-Atlantic region. U.S. Geological Survey, Reston, VA
- Gutierrez BT, Plant NG, Thieler ER, Turecek A (2015) Using a Bayesian network to predict barrier island geomorphologic characteristics. *Journal of Geophysical Research: Earth Surface* 120 (12):2452-2475
- Guttal V, Jayaprakash C (2008) Changing skewness: an early warning signal of regime shifts in ecosystems. *Ecology Letters* 11(5):450-460

- Guttal V, Jayaprakash C (2009) Spatial variance and spatial skewness: leading indicators of regime shifts in spatial ecological systems. *Theoretical Ecology* 2(1):3-12
- Haluska JD (2017) Analysis of Virginia Barrier Island shoreline movement and correlations to sea level and wave height changes and teleconnection patterns. Dissertation, Old Dominion University
- Hapke CJ, Plant NG, Henderson RE, Schwab WC, Nelson TR (2016) Decoupling processes and scales of shoreline morphodynamics. *Marine Geology* 381:42-53.
- Harrison S (2001) On reductionism and emergence in geomorphology. *Transactions of the Institute of British Geographers* 26 (3):327-339.
- Harris AL, Zinnert JC, Young DR (2017) Differential response of barrier island dune grasses to species interactions and burial. *Plant Ecology* 218 (5):609-619.
- Hayden BP, Santos MCFV, Shao G, Kochel RC (1995) Geomorphological controls on coastal vegetation at the Virginia Coast Reserve. *Geomorphology* 13(1):283-300
- Hayes M (1979) Barrier island morphology as a function of tidal and wave regime. In: Leatherman SP (ed) *Barrier Islands from the Gulf of Mexico to the Gulf of St. Lawrence*. Academic Press, New York, pp 1-28
- Hayes M (1994) Chapter 7 The Georgia Bight barrier system. In: Davis RA (ed) *Geology of Holocene barrier island systems*. Springer-Verlag, Berlin Heidelberg, pp 233-304
- Hesp PA, Davidson-Arnott R, Walker IJ, Ollerhead J (2005) Flow dynamics over a foredune at Prince Edward Island, Canada. *Geomorphology* 65 (1-2):71-84.
- Heisler LM, Poulin RG, Somers CM (2017) Stop using dichotomous terms to reference observations of scale-dependent habitat selection. *Landscape Ecology* 32(8):1531-1542
- Holling CS (1973) Resilience and stability of ecological systems. *Annual review of ecology and systematics* 4(1):1-23
- Holling CS (1992) Cross-scale morphology, geometry, and dynamics of ecosystems. *Ecological monographs* 62(4):447-502
- Holling CS (1996) Engineering resilience versus ecological resilience. In: Schulze PE (ed) *Engineering within ecological constraints*. National Academy Press, Washington DC, pp 31-43
- Hosier PE, Cleary WJ (1977) Cyclic geomorphic patterns of washover on a barrier Island in southeastern North Carolina. *Environmental Geology* 2(1):23-31
- Houser C (2013) Alongshore variation in the morphology of coastal dunes: Implications for storm response. *Geomorphology* 199:48-61
- Houser C, Wernette P, Rentschlar E, Jones H, Hammond B, Trimble S (2015) Post-storm beach and dune recovery: implications for barrier island resilience. *Geomorphology* 234:54-63

- Houser C, Wernette P, Weymer BA (2018) Scale-dependent behavior of the foredune: implications for barrier island response to storms and sea-level rise. *Geomorphology* 303:362-374
- Inkpen R, Petley D (2001) Fitness spaces and their potential for visualizing change in the physical landscape. *Area* 33(3):242-251
- Inkpen R, Hall K (2016) Using morphospaces to understand tafoni development. *Geomorphology* 261:193-199
- Isenburg M (2014) LAStools - efficient LiDAR processing software (version 141017, unlicensed). <http://rapidlasso.com/LAStools> Accessed 26 June 2018
- Jackson HB, Fahrig L (2015) Are ecologists conducting research at the optimal scale? *Global Ecology and Biogeography* 24(1):52-63
- Jasiewicz J, Netzel P, Stepinski TF (2014) Landscape similarity, retrieval, and machine mapping of physiographic units. *Geomorphology* 221:104-112
- Kedron PJ, Frazier AE, Ovando-Montejo GA, Wang J (2018) Surface metrics for landscape ecology: a comparison of landscape models across ecoregions and scales. *Landscape Ecology* 33 (9):1489-1504.
- Kell DB, Oliver SG (2004) Here is the evidence, now what is the hypothesis? The complementary roles of inductive and hypothesis-driven science in the post-genomic era. *Bioessays* 26(1):99-105
- Kim D, Zheng Y (2011) Scale-dependent predictability of DEM-based landform attributes for soil spatial variability in a coastal dune system. *Geoderma* 164(3-4):181-194
- Kim D, Cairns DM, Bartholdy J, Morgan CL (2012) Scale-dependent correspondence of floristic and edaphic gradients across salt marsh creeks. *Annals of the Association of American Geographers* 102(2):276-294
- Kochel RC, Kahn JH, Dolan R, Hayden BP, May PF (1983) Mid-Atlantic barrier coast classification. Office of Naval Research, Arlington, VA
- Kupfer JA (2012) Landscape ecology and biogeography: rethinking landscape metrics in a post-FRAGSTATS landscape. *Progress in Physical Geography* 36(3):400-420
- Laland KN, Sterelny K, Odling-Smee J, Hoppitt W, Uller T (2011) Cause and effect in biology revisited: is Mayr's proximate-ultimate dichotomy still useful?. *Science* 334:1512-1516
- Lane BA, Pasternack GB, Dahlke HE, Sandoval-Solis S (2017) The role of topographic variability in river channel classification. *Progress in Physical Geography* 41(5):570-600
- Lastochkin AN, Zhironov AI, Boltramovich SF (2018) System-morphological approach: another look at morphology research and geomorphological mapping. *Geomorphology* 303:486-503

- Laughlin DC (2014) The intrinsic dimensionality of plant traits and its relevance to community assembly. *Journal of Ecology* 102(1):186-193
- Lausch A, Blaschke T, Haase D, Herzog F, Syrbe R, Tischendorf L, Walz U (2015) Understanding and quantifying landscape structure—a review on relevant process characteristics, data models and landscape metrics. *Ecological Modelling* 295:31-41
- Leatherman SP (1982) *Barrier island handbook*. Coastal Publications, Charlotte, NC
- Long J, Robertson C (2018) Comparing spatial patterns. *Geography Compass* 12(2):e12356
- Long JW, de Bakker A, Plant NG (2014) Scaling coastal dune elevation changes across storm-impact regimes. *Geophysical Research Letters* 41(8):2899-2906
- Lorenzo-Trueba J, Ashton AD (2014) Rollover, drowning, and discontinuous retreat: distinct modes of barrier response to sea-level rise arising from a simple morphodynamic model. *Journal of Geophysical Research: Earth Surface* 119(4):779-801
- MacArthur R (1955) Fluctuations of animal populations and a measure of community stability. *Ecology* 36(3):533-536
- McCune B, Grace JB (2002) *Analysis of ecological communities*. MjM Software Design, Gleneden Beach, OR
- McCune B (2006) Non-parametric habitat models with automatic interactions. *Journal of Vegetation Science* 17(6):819-830
- McCune B, Mefford MJ (2016) *PC-ORD. Multivariate analysis of ecological data Version 7*. MjM Software Design, Gleneden Beach, OR
- McGarigal K, Cushman SA (2002) The gradient concept of landscape structure: or, why are there so many patches. <http://www.umass.edu/landeco/pubs/pubs> Accessed 26 June 2018
- McGarigal K, Tagil S, Cushman SA (2009) Surface metrics: an alternative to patch metrics for the quantification of landscape structure. *Landscape Ecology* 24(3):433-450
- McGarigal K, Cushman SA, Ene E (2012) *FRAGSTATS: Spatial pattern analysis program for categorical and continuous maps. Version 4.2*, University of Massachusetts, Amherst, MA
- McGarigal K (2015) *FRAGSTATS help. Documentation for FRAGSTATS 4*, University of Massachusetts, Amherst, MA
- Miller TE, Gornish ES, Buckley HL (2010) Climate and coastal dune vegetation: disturbance, recovery, and succession. *Plant Ecology* 206:97-104
- Mitasova H, Harmon RS, Weaver KJ, Lyons NJ, Overton MF (2012) Scientific visualization of landscapes and landforms. *Geomorphology* 137(1):122-137



- Monge JA (2014) Convergence of dune topography among multiple barrier island morphologies. Master Thesis, University of Kentucky
- Monge JA, Stallins JA (2016) Properties of dune topographic state space for six barrier islands of the U.S. southeastern Atlantic coast. *Physical Geography* 37(6):452-475
- Moore LJ, Durán O, Ruggiero P (2016) Vegetation control allows autocyclic formation of multiple dunes on prograding coasts. *Geology* 44 (7):559-562
- Morozov A, Poggiale JC (2012) From spatially explicit ecological models to mean-field dynamics: the state of the art and perspectives. *Ecological Complexity* 10:1-11
- Mulhern JS, Johnson CL, Martin JM (2017) Is barrier island morphology a function of tidal and wave regime?. *Marine Geology* 387:74-84
- Nash KL, Allen CR, Angeler DG, Barichievy C, Eason T, Garmestani AS, Graham NAJ, Granholm D, Knutson M, Nelson RJ, Nyström M, Stow CA, Sundstrom SM (2014) Discontinuities, cross-scale patterns, and the organization of ecosystems. *Ecology* 95(3):654-667
- National Oceanic and Atmospheric Administration and National Ocean Service (2012) VDatum User Guide. Vertical Datum Transformation. <https://vdatum.noaa.gov/docs/userguide.html>. Accessed 26 June 2018
- Nebel SH, Trembanis AC, Barber DC (2012) Shoreline analysis and barrier island dynamics: decadal scale patterns from Cedar Island, Virginia. *Journal of Coastal Research* 28(2):332-341
- Niesterowicz J, Stepinski TF (2016) On using landscape metrics for landscape similarity search. *Ecological indicators* 64:20-30
- Odum WE, Smith TJ, Dolan R (1987) Suppression of natural disturbance: long-term ecological change on the Outer Banks of North Carolina. In: Turner MG (Ed) *Landscape Heterogeneity and Disturbance*. Springer, New York, pp 123-135
- Oertel G, Kraft J (1994) Chapter 6 New Jersey and Delmarva barrier islands. In: Davis RA (ed) *Geology of Holocene barrier island systems*. Springer-Verlag, Berlin Heidelberg, pp 207-232
- Parker KC, Bendix J (1996) Landscape-scale geomorphic influences on vegetation patterns in four environments. *Physical Geography* 17:113-141
- Peck, J.E. (2010) *Multivariate analysis for community ecologists: step-by-step using PC-ORD*. MjM Software Design, Glenden Beach, OR
- Peterson G, Allen CR, Holling CS (1998) Ecological resilience, biodiversity, and scale. *Ecosystems* 1(1):6-18
- Phillips JD (1999) Divergence, convergence, and self-organization in landscapes. *Annals of the Association of American Geographers* 89(3):466-488

- Phillips JD (2006) Evolutionary geomorphology: thresholds and nonlinearity in landform response to environmental change. *Hydrology and Earth System Sciences* 10(5):731-742
- Phillips JD (2009a) Changes, perturbations, and responses in geomorphic systems. *Progress in Physical Geography* 33(1):17-30
- Phillips JD (2009b) Landscape evolution space and the relative importance of geomorphic processes and controls. *Geomorphology* 109(3-4):79-85
- Phillips JD, Van Dyke C (2016) Principles of geomorphic disturbance and recovery in response to storms. *Earth Surface Processes and Landforms* 41(7):971-979
- Phillips JD (2018) Coastal wetlands, sea level, and the dimensions of geomorphic resilience. *Geomorphology* 305:173-184
- Piecuch CG, Huybers P, Hay CC, Kemp AC, Little CM, Mitrovica JX, Ponte RM, Tingley MP (2018) Origin of spatial variation in US East Coast sea-level trends during 1900-2017. *Nature* 564 (7736):400-404
- Plant NG, Flocks J, Stockdon HF, Long JW, Guy K, Thompson DM, Cormier JM, Smith CG, Miselis JL, Dalyander PS (2014) Predictions of barrier island berm evolution in a time-varying storm climatology. *Journal of Geophysical Research: Earth Surface* 119(2):300-316
- Prager SD, Reiners WA (2009) Historical and emerging practices in ecological topology. *Ecological Complexity* 6(2):160-171
- Praskievicz S (2018) River Classification as a geographic tool in the age of big data and Global Change. *Geographical Review* 108 (1):120-137
- Psuty N, Silveira T (2010) Global climate change: an opportunity for coastal dunes?. *Journal of Coastal Conservation* 14 (2):153-160
- Psuty N, Silveira T (2011) Monitoring shoreline change along Assateague barrier island: the first trend report. *Journal of Coastal Research* SI 64:800-804
- Radchuk V, Laender FD, Cabral JS, Boulangeat I, Crawford M, Bohn F, Raedt JD, Scherer C, Svenning JC, Thonicke K (2019) The dimensionality of stability depends on disturbance type. *Ecology Letters* 22:674-684
- Rice T, Leatherman S (1983) Barrier island dynamics: the eastern shore of Virginia. *Southeastern Geology* 24(3):125-137
- Robertson G (2000) *GS+: geostatistics for the environmental sciences*. Gamma Design Software, Plainwell, MI
- Rogers LJ, Moore LJ, Goldstein EB, Hein CJ, Lorenzo-Trueba J, Ashton AD (2015) Anthropogenic controls on overwash deposition: evidence and consequences. *Journal of Geophysical Research: Earth Surface* 120(12):2609-2624
- Roman CT, Nordstrom KF (1988) The effect of erosion rate on vegetation patterns of an east coast barrier island. *Estuarine, Coastal and Shelf Science* 26(3):233-242

- Ryu W, Sherman DJ (2014) Foredune texture: landscape metrics and climate. *Annals of the Association of American Geographers* 104(5):903-921
- Sagarin R, Pauchard A (2010) Observational approaches in ecology open new ground in a changing world. *Frontiers in Ecology and the Environment* 8(7):379-386
- Sankaran S, Majumder S, Kéfi S, Guttal V (2018) Implications of being discrete and spatial for detecting early warning signals of regime shifts. *Ecological Indicators* 94:503-511.
- Sallenger Jr AH, Doran KS, Howd PA (2012) Hotspot of accelerated sea-level rise on the Atlantic coast of North America. *Nature Climate Change* 2(12):884-888
- Seminack CT, McBride RA (2015) Geomorphic history and diagnostic features of former tidal inlets along Assateague Island, Maryland-Virginia: a life-cycle model for inlets along a wave-dominated barrier islands. *Shore and Beach* 83:3-24
- Scheffer M, Carpenter SR, Dakos V, van Nes EH (2015) Generic indicators of ecological resilience: inferring the chance of a critical transition. *Annual Review of Ecology, Evolution, and Systematics* 46(1):145-167
- Schumm SA, Lichty RW (1965) Time, space, and causality in geomorphology. *American journal of science* 263(2):110-119
- Schumm SA (1979) Geomorphic thresholds: the concept and its applications. *Transactions of the Institute of British Geographers* 4(4):485-515
- Schwarz C, Gourgue O, van Belzen J, Zhu Z, Bouma TJ, van de Koppel J, Ruessink G, Claude N, Temmerman S (2018) Self-organization of a biogeomorphic landscape controlled by plant life-history traits. *Nature Geoscience* 11(9):672-677
- Sherman DJ, Bauer BO (1993) Dynamics of beach-dune systems. *Progress in Physical Geography* 17(4):413-447
- Sherman DJ, Hales BU, Potts MK, Ellis JT, Liu H, Houser C (2013) Impacts of Hurricane Ike on the beaches of the Bolivar Peninsula, TX, USA. *Geomorphology* 199:62-81
- Short A, Hesp P (1982) Wave, beach and dune interactions in southeastern Australia. *Marine Geology* 48(3-4):259-284
- Spalding MD, McIvor AL, Beck MW, Koch EW, Möller I, Reed DJ, Rubinoff P, Spencer T, Tolhurst TJ, Wamsley TV, Wesenbeeck BK, Wolanski E, Woodroffe CD (2014) Coastal ecosystems: a critical element of risk reduction. *Conservation Letters* 7(3):293-301
- Stallins JA, Parker AJ (2003) The influence of complex systems interactions on barrier island dune vegetation pattern and process. *Annals of the Association of American Geographers* 93(1):13-29
- Stallins JA (2005) Stability domains in barrier island dune systems. *Ecological Complexity* 2(4):410-430

- Stallins JA, Corenblit D (2018) Interdependence of geomorphic and ecologic resilience properties in a geographic context. *Geomorphology* 305:76-93
- Stevens RD, Tello JS (2014) On the measurement of dimensionality of biodiversity. *Global ecology and biogeography* 23(10):1115-1125
- Stevens RD, Tello JS (2018) A latitudinal gradient in dimensionality of biodiversity. *Ecography* 41 (12):2016-2026.
- Stutz ML, Pilkey OH (2011) Open-ocean barrier islands: global influence of climatic, oceanographic, and depositional settings. *Journal of Coastal Research* 27(2):207-222
- Sundstrom SM, Angeler DG, Garmestani AS, García JH, Allen CR (2014) Transdisciplinary application of cross-scale resilience. *Sustainability* 6(10):6925-6948
- Sundstrom SM, Allen CR, Gunderson LH (2016) Letter resisting resilience theory: a response to Connell and Ghedini. *Trends in Ecology & Evolution* 31(6):412-413
- Sundstrom SM, Angeler DG, Barichievy C, Eason T, Garmestani A, Gunderson L, Knutson M, Nash KL, Spanbauer T, Stow C (2018) The distribution and role of functional abundance in cross-scale resilience. *Ecology* 99 (11):2421-2432
- Temmerman S, Meire P, Bouma TJ, Herman PMJ, Ysebaert T, De Vriend HJ (2013) Ecosystem-based coastal defence in the face of global change. *Nature* 504 (7478):79-83
- Thomas MF (2001) Landscape sensitivity in time and space — an introduction. *Catena* 42(2):83-98
- Turner MG, Gardner RH (2015) *Landscape ecology in theory and practice: pattern and process*. Springer, New York
- Walker IJ, Davidson-Arnott RG, Bauer BO, Hesp PA, Delgado-Fernandez I, Ollerhead J, Smyth TAG (2017) Scale-dependent perspectives on the geomorphology and evolution of beach-dune systems. *Earth-Science Reviews* 171:220-253
- Wernette P, Houser C, Weymer BA, Everett ME, Bishop MP, Reece B (2018a) Influence of a spatially complex framework geology on barrier island geomorphology. *Marine Geology* 398:151-162
- Wernette P, Thompson S, Eyler R, Taylor H, Taube C, Medlin A, Decuir C, Houser C (2018b) Defining dunes: evaluating how dune feature definitions affect dune interpretations from remote sensing. *Journal of Coastal Research* 346:1460-1470
- Williams A, Leatherman S (1993) Process form relationships of USA east coast barrier islands. *Zeitschrift für Geomorphologie* 37(2):179-197
- Wohl E (2018) Geomorphic context in rivers. *Progress in Physical Geography* 42 (6):841-857

- Wolner CW, Moore LJ, Young DR, Brantley ST, Bissett SN, McBride RA (2013) Ecomorphodynamic feedbacks and barrier island response to disturbance: insights from the Virginia Barrier Islands, Mid-Atlantic Bight, USA. *Geomorphology* 199:115-128
- Wu J, Jelinski DE, Luck M, Tueller PT (2000) Multiscale analysis of landscape heterogeneity: scale variance and pattern metrics. *Geographic Information Sciences* 6(1):6-19
- Wu Q, Guo F, Li H, Kang J (2017) Measuring landscape pattern in three dimensional space. *Landscape and Urban Planning* 167:49-59
- Yousefi Lalimi F, Silvestri S, Moore L, Marani M (2017) Coupled topographic and vegetation patterns in coastal dunes: remote sensing observations and ecomorphodynamic implications. *Journal of Geophysical Research: Biogeosciences* 122(1):119-130
- Zaremba RE, Leatherman SP (1986) Vegetative physiographic analysis of a U.S. northern barrier system. *Environmental Geology and Water Sciences* 8:193-207
- Zinnert JC, Brantley ST, Young DR (2016a) Bistability and the future of barrier islands. *Nature Climate Change* 6(1):5
- Zinnert JC, Shiflett SA, Via S, Bissett S, Dows B, Manley P, Young DR (2016b) Spatial-temporal dynamics in barrier island upland vegetation: the overlooked coastal landscape. *Ecosystems* 19(4):685-697
- Zinnert JC, Stallins JA, Brantley ST, Young DR (2017) Crossing scales: the complexity of barrier-island processes for predicting future change. *BioScience* 67(1):39-52
- Zinnert JC, Via S, Nettleton BP, Tuley PA, Moore LJ, Stallins JA (2019) Connectivity in coastal systems: barrier island vegetation influences upland migration in a changing climate. *Global Change Biology* 25(7):2419-2430

## VITA

### LI-CHIH HSU

#### EDUCATION

- 2010 National Taiwan University, Taipei, Taiwan: **M.Sc.** (Geography)  
2006 National Taiwan University, Taipei, Taiwan: **B.Sc.** (Geography)

#### PROFESSIONAL EXPERIENCE

- 2015-2018 Teaching Assistant, University of Kentucky  
2011-2013 Secondary school instructor, Rui-Fang Industrial High School, Taiwan  
2006-2010 Teaching Assistant, National Taiwan University

#### PUBLICATIONS

- Hsu, L. C.** and Lee, C. T. (2018) The current extent and historical expansion of mangroves in the Kuantu Nature Reserve, North Taiwan, *Journal of Coastal Research*, 34(2), 360–372.
- Hsu, L. C.** and Lee, C. T. (2013) Mangrove distribution change in Kuantu Nature Reserve from the perspective of biogeomorphology, *Quarterly Journal of Chinese Forestry*, 46(1):87-106. (in Chinese with English abstract)
- Hsu, L. C.** and Lee, C. T. (2010) Mangrove distribution change in Kuantu Nature Reserve from 1978 to 2006, *Hwa Kang Geographical Journal*, 26: 31-42. (in Chinese with English abstract)
- Shiao, C.R., Lee, C.T., **Hsu, L. C.**, Lin, J.C., Fang, Y.P. and Lee, L.L. (2010) A species inventory of terrestrial vascular plants on five islands located in southeastern Penghu Archipelago, *Bulletin of National Park Society*, 20(2): 69-85. (in Chinese with English abstract)

#### SCHOLASTIC AND PROFESSIONAL HONORS

- 2019 International Student Tuition Scholarship, University of Kentucky  
2019 Graduate School Travel Award, University of Kentucky  
2019 COMA Norbert Psuty Travel Incentive, Association of American Geographers  
2018 International Student Tuition Scholarship, University of Kentucky  
2018 Graduate School Travel Award, University of Kentucky  
2018 COMA Norbert Psuty Travel Incentive, Association of American Geographers  
2017 Graduate Student Congress Travel Funding, University of Kentucky  
2017 Graduate School Travel Award, University of Kentucky  
2017 COMA Norbert Psuty Travel Incentive, Association of American Geographers

2017 Geography Department's PhD student Travel Award, University of Kentucky  
2016 Graduate School Travel Award, University of Kentucky  
2015 Barnhart-Withington Research Award, University of Kentucky  
2013-2015 Government Scholarship for Studying Abroad, Ministry of Education, Taiwan  
2009 Master Thesis Fellowship, Chilin Foundation, Taiwan  
2006 College of Science Dean's Award, National Taiwan University  
2006 Presidential Award, National Taiwan University